INVESTIGATION OF TRACE URANIUM IN BIOLOGICAL MATRICES

A Dissertation

by

JAMES CHRISTOPHER MILLER

Submitted to the Office of Graduate Studies of
Texas A&M University
in partial fulfillment of the requirements for the degree of

DOCTOR OF PHILOSOPHY

Chair of Committee,	William S. Charlton
Committee Members,	David R. Boyle
	John R. Ford Jr.
	Charles M. Folden III
Head of Department,	Yassin A. Hassan

August 2013

Major Subject: Nuclear Engineering

ABSTRACT

A system for the analysis of urine bioassay samples for the purpose of inversely investigating an unknown exposure to uranium has been developed. This technique involves the use of a thin flow electrochemical cell in conjunction with an anodized glassy carbon electrode to selectively separate uranium atoms out of solution for later analysis on an inductively coupled plasma mass spectrometer. A series of uranium urinalysis bioassay sample results can be used to investigate the time frame and type of exposure. This analysis uses an exposure database and regression analysis to best fit urinalysis uranium excretion data to expected profiles using commercially available mathematics software. The least number of data points to determine an acceptable confidence interval is ten bioassay samples taken at least a week apart.

The system was benchmarked using a random sampling of urinary excretion samples from a known case at the Y-12 plant in the 1960's. The electrochemical system was characterized using U.S. Department of Energy synthetic urine quality assurance standards from an inter-laboratory exercise in 2012. The separation apparatus was able to consistently separate uranium from the synthetic urine solutions with a consistent recovery between ten and fifteen percent and up to fifty percent. The method is isotope independent and maintains the enrichment of any excreted material. This allows for the material to be compared to operational logbooks at facilities using multiple enrichments in the nuclear fuel cycle. This methodology is recommended for spot estimation in support of a traditional bioassay program.

DEDICATION

To my mother who has inspired me in more ways than I can count. I pray that one day I am half the person she is, and I will count myself lucky.

ACKNOWLEDGEMENTS

I would like to thank my committee chair and adviser, Dr. Charlton, and my committee members, Dr. Boyle, Dr. Ford, and Dr. Folden, for their guidance and support throughout the course of this research. I would also like to recognize the entire NSSPI research group for their support in so many endeavors over the past few years. It has been a blessing to watch NSSPI become the preeminent nonproliferation and safeguards academic program in the world.

I would like to acknowledge insight and guidance from the staff members in Chemistry- Nuclear and Radiochemistry group at Los Alamos National Laboratory specifically Dr. Robert Steiner, Dr. Michael Harris, Dr. Felicia Taw, Dr. Luiz Bertelli, Mr. Gerald Alfano, and Mr. Dale Melton. I am thankful to the entire C-NR group for welcoming me into their work family for three years while I completed my research experiments.

This research was performed under the Nuclear Forensics Graduate Fellowship Program, which is sponsored by the U.S. Department of Homeland Security, Domestic Nuclear Detection Office and the U.S. Department of Defense, Defense Threat Reduction Agency. I would like to thank the NFGF and its staff Samantha Kentis, Craig Williamson, and Nicole Huchet for their assistance throughout the fellowship.

NOMENCLATURE

AdSV	Adsorptive Stripping Voltammetry
Ag/AgCl	Silver/Silver Chloride (Reference Electrode Type)
AGC	Anodized Glassy Carbon
BASi	Bioanalytical Systems, Inc.
C-NR	Chemistry: Nuclear and Radiochemistry Group at LANL
CRM-145	Certified Reference Material 145 (Natural Uranium from NIST)
DCAL	Dose and Risk Calculation Software
DOE	Department of Energy
FT	Flow Through
FR	Flow Rate
HDCV	Hydrodynamic Cyclic Voltammetry
HNO_3	Nitric Acid
ICP-MS	Inductively Coupled Plasma Mass Spectrometry
ICRP	International Commission on Radiation Protection
i.d.	Internal Diameter
LANL	Los Alamos National Laboratory
M	Molar (as in chemical concentration)
NaCl	Sodium Chloride
NRC	Nuclear Regulatory Commission
ORNL	Oak Ridge National Laboratory

PEEK	Polyether Ether Ketone
PNNL	Pacific Northwest National Laboratory
SRS	Savannah River Site
TIMS	Thermal Ionization Mass Spectrometry
µL/min	Microliters per Minute
V	Volts

TABLE OF CONTENTS

Page

LIST OF FIGURES

Page

LIST OF TABLES

Page

CHAPTER I

INTRODUCTION AND LITERATURE REVIEW

One of the biggest challenges facing the world in the coming century is energy production. As the world's population increases so does demand on resources, specifically the demand on energy will continue to grow. Nuclear energy is poised to fill a large portion of that energy demand. Ensuring the safety of nuclear technology from cradle to grave is a vital component in meeting this energy need. The safe use of nuclear materials is not only limited to the safety of the facility, but even more important are the safety issues posed by the significant health risks involved in working with nuclear materials. One of the earliest nuclear scientists, Marie Curie, had significant health complications from nuclear material exposures that contributed to her death in 1934. [1]

The nuclear industry is predicted to expand at least a factor of five in the coming quarter century. [2] Thus all aspects of the nuclear fuel cycle (shown in Figure 1) from mining and milling to power generation and waste disposal will need to vastly increase both the number of facilities and the number of nuclear workers around the world. The United States alone already has over 400,000 nuclear workers.[3] This expansion will also spur innovation of new ideas and processes. These processes will need to be safe because the consequences of isolated accidents affect the entire nuclear industry. Therefore, every nuclear facility around the world has a vested interest in the safety of every other nuclear facility. This work will specifically focus on the monitoring of occupational exposures related to uranium processing.

Figure 1: The Nuclear Fuel Cycle[4]

Statement of the Problem

The US Nuclear Regulatory Commission (NRC) requires that facilities handling nuclear materials monitor workers for potential occupational exposures. This monitoring is often multi-faceted and typically involves an air sampling and biological sampling regime. The regime depends on the potential for exposures, the materials and chemical compounds being used, and the facility history. Specifically respiratory exposures are of

great concern. Not only are inhalation exposures most common, but they can occur without a worker's knowledge. Personal protective equipment, such as respirators and glove box enclosures, are often used to limit inhalations, but they are not used in all circumstances nor are they 100 percent effective. Typically, most nuclear processing facilities employ annual, biannual, and quarterly testing regimes. [5]

Motivations and Goals

Suppose that a new process has been developed for working with uranium materials which improves efficiency and costs by a large factor and is worthwhile to pursue. This hypothetical process has multiple steps and is still in the developmental phase or in pilot production testing, but during routine bioassay monitoring procedures, a worker surpasses the uranium bioassay threshold for an occupational exposure. The specific method and origin of exposure is unknown.

This work is interested in determining as much information about the occupational exposure that occurred during this new process at the pilot phase. Quantities of interest include but are not limited to approximating the time of exposure, determining the exposure pathway, and determining the material and chemical form of the exposure. Decreasing the analysis time and the minimum detection limits for analysis related to the uranium bioassay would improve the bioassay testing process. The largest emphasis of this work is increasing the accuracy of the time frame approximation and decreasing the complexity and analysis time for bioassay samples.

To accomplish these goals, the work has two major components. Considerable effort was expended to develop and characterize an electrochemical system used for

separating actinides from solutions for use in urinalysis. This effort involved a significant amount of work in apparatus design, fabrication, and testing as well as traditional separations and analytical chemistry utilizing state of the art inductively coupled plasma mass spectrometry (ICP-MS). The other goal is to examine the requirements to glean information related to determining the time frame of an exposure utilizing biokinetic modeling of uranium excretion profiles. This time frame estimation investigates the more complex issues related to understanding hidden facets of an exposure.

Previous Related Work

Each of these two fields has been studied previously. However, the two have not been studied together and applied to this type of problem. These previous efforts serve to guide initial research pathways to best launch into a new application of alternate methods. These previous works range in scope from analytical chemistry experiments to biological testing of uranium excretions in various animals.

Bioassay Programs

The starting point for addressing this problem involves examining the existing bioassay programs and procedures around the world. Since every country and nuclear facility has a vested interest in the health and safety of its highly skilled nuclear workforce, it comes as no surprise that a myriad of bioassay programs exist around the world. Some of the first bioassay programs were started at Y-12 in Oak Ridge, TN and the Savannah River Site (SRS) in Aiken, SC.[6, 7] Since Y-12 led the early US uranium enrichment programs, it also pioneered early uranium bioassay.[8] Likewise, the

Savannah River Site (SRS) pioneered plutonium bioassay techniques.[9] From these programs, techniques were developed to detect exposures via biological excretion pathways for several years following a major dosage.[10]

Bioassay methods and procedures can be both *in vitro* and *in vivo*. *In vitro* tests can include urinalysis, fecal analysis, blood analysis, or hair digestion. The most common *in vivo* test is radiation respiratory (lung) counting. Several types of tests may be utilized to fully characterize the exposure of an individual. Excretions can be analyzed using various techniques including alpha spectroscopy, thermal ionization mass spectrometry (TIMS), inductively coupled mass spectrometry (ICP-MS), neutron activation analysis (NAA), and phosphorometry. Each has advantages and disadvantages based on analysis time and cost. For example, alpha spectrometry is inexpensive, but has a large uncertainty in regard to concentration measurements. Additionally, peak resolution in alpha spectroscopy can be poor in complex samples with a large number of nuclides. TIMS is expensive, but precise when measuring trace material signatures. NAA is both expensive and labor intensive in addition to requiring a well characterized neutron source and other material handling facilities. The two most widely used are alpha spectroscopy and thermal ionization mass spectrometry.[8]

Uranium Bioassay

Uranium bioassay is a complex problem because of the large amount of background uranium in human excretions. This background is a much more difficult problem than plutonium bioassay. Since plutonium is manmade, plutonium is assumed to have a nominal or nonexistent background signature.[11, 12] This is a direct result of

uranium intake in food, air, and water. Water has the largest effect on an individual's uranium background level. Significant efforts have been made across the world to estimate uranium excretion background with varying degrees of success. Ultimately every individual has a different background signature based on their particular lifestyle habits.[13] Due to typical background concentrations between 5 and 15 µg/L, all of these bioassay programs rely on threshold measurements which means that the test solely determines if an individual is above or below a certain level of exposure. For example, the uranium threshold is 15 µg/L in a 24 hour urine sample (one day worth of urinary excretion) as per US NRC guidelines.[5]

Los Alamos National Laboratory (LANL) has a uranium bioassay program. The most recent literature and validation of their program reports the capability to detect and monitor uranium excretions greater than 54 pg/mL (equivalent of ppb).[14] The program at LANL also reports the ability to recover approximately 70 percent of uranium excreted using a calcium phosphate precipitation on samples when detailed isotopic analysis is desired, which has been more efficient than other reported methods.[15] The overall detection limits on this procedure are determined by the ICP-MS instrument being used to analyze the samples. Recently, new instruments have been added to the program at LANL and should result in much lower minimum detection limits. The flow sheet for the LANL process is shown in Figure 2.[14] The LANL bioassay program is predominately focused on plutonium bioassay as the overall mission directive of the laboratory involves significant plutonium handling.

The two assay programs are coupled, but have significant differences. Uranium bioassay procedures call for one standard measurement on an ICP-MS instrument, while the plutonium system utilizes both alpha spectroscopy and Thermal Ionization Mass Spectrometry (TIMS). The plutonium samples have a significant amount of chemical processing prior to any quantitative analysis, and an individual sample requires more than one week of processing time. Americium bioassay is similar to the plutonium procedure and is also very common at LANL. The uranium processing takes a similar amount of analysis time, but does not have a fully functional production line as the plutonium program does. These programs are threshold programs which determine if an exposure is above or below a specified limit.[16]

The uranium bioassay program at the Y-12 facility in Oak Ridge, TN has a large throughput and is consistent and ongoing. In contrast to the program at Los Alamos, the Y-12 program tests both urine and feces. From the biokinetic models of uranium in the human body, fecal samples have the largest initial excretion of uranium after an exposure. However, fecal excretion drops off much quicker than urinary excretion. Thus, the fecal signature of an exposure is significantly shorter lived. The two programs have similar performance and are appropriate for their institutions and missions.[17] Most uranium bioassay programs are similar, but vary accordingly to meet the specific goal of the work which they support.

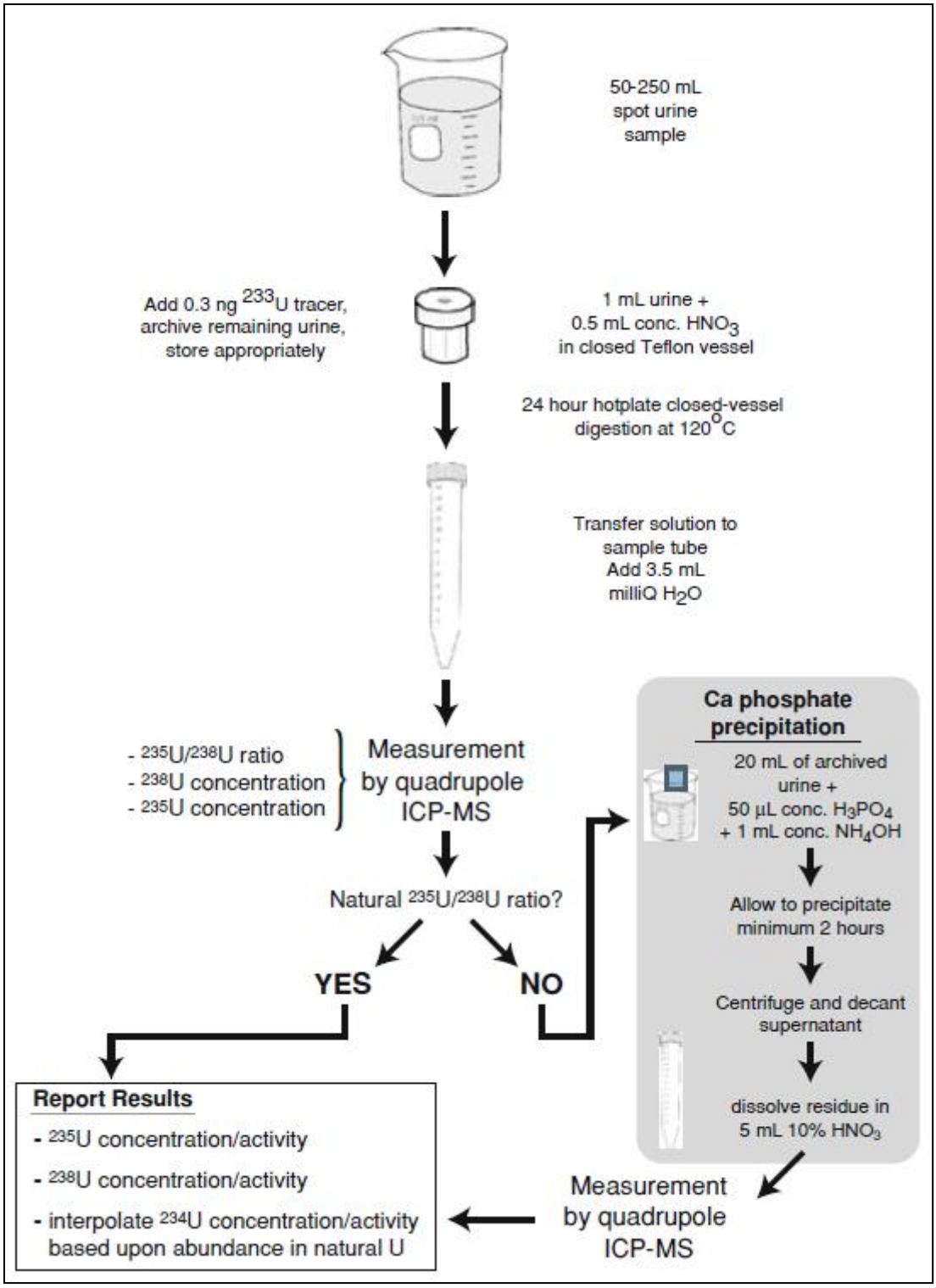

Figure 2: LANL Uranium Bioassay Flow Sheet[14]

Matrix Difficulties

Even though urinalysis is a common procedure in bioassay, it does not imply that urine is an easy medium to process. In fact, it is an extraordinarily complex matrix and this complexity is reflected in the required analysis time per sample. The matrix of a sample is defined as the materials contained in the surrounding medium. Human urine has no less than 168 constituents that could interfere with the test. A sampling of these constituents is listed in Table 1. Most of the constituents are organic and should disassociate from urine over time, specifically by off-gassing. This off-gassing is why urine samples are typically allowed to rest approximately a week or more before analysis. Rest periods can be shortened by the application of voltage to the sample, but this is only done under special circumstances.[18] The biggest issue with the direct measurement of urine by mass spectrometry is the build-up of salts and organics on the front end of the instrument where sample injection occurs. This build-up has been referred to as plasma loading and memory effects. These effects can significantly reduce the quality of analysis as well as increase the maintenance required on and instrument.[14]

Electrochemical Works

The extraneous constituents of urine create large measurement difficulties in both precision and accuracy of measurement. Currently, to combat these difficulties, bioassay processes require a great deal of work and staff hours to complete, and matrix elimination currently done for the urinalysis is by no means efficient or simple. As a result, this work investigates the suitability of an alternate matrix reduction technique for use in urinalysis.

Electrochemical separation has become popular to process uranium samples, but has not been applied directly to the urinalysis problem.[19] These works have shown that with use of chelating compounds, uranium can be separated from solution in an electrochemical flowcell. These cells contain a small volume between electrodes where voltage can be applied to a very small dynamic volume of fluid. Typical chelating agents used have been propyl gallate, cupferron, oxine, and N-benzoyl-N-phenylhydroxylamine. Cupferron and propyl gallate produced the best results and have been the most widely utilized.[20] In this adsorptive stripping method (AdSV), the chelating compound attaches to the uranium atom and is then selectively removed from solution using an appropriate electrochemical reaction. These chelation agents have drawbacks including a low saturation point on an appropriate working electrode.[21]

Anodized Glassy Carbon Electrochemical Separation

With the complexities already present in a urine sample, adding additional chemicals to be separated later is not an attractive option. More recent work has been focused on coupling these flowcells directly to a mass spectrometer in order to lower minimum detection limits as well as decrease total sample processing time. Studies at Oak Ridge National Laboratory (ORNL) and Pacific Northwest National Laboratory (PNNL) have shown that uranium and plutonium can be preferentially electroplated on an anodized glassy carbon (AGC) electrode for either online or offline processing of samples. These experiments have shown great promise in concentrating the actinide signatures of given samples.[22, 23] Formerly, this work has mostly been concerned with

proving the concept of preconcentration (selectively releasing various actinides using applied voltages) for online coupling with ICP-MS measurements.[24]

Table 1: Constituents of Human Urine[18]

Item	Formula	Formula Weight	Range mg/l	Range mg/l	Solubility Limit In A Binary Solution g/100g H_2O
Total Solutes			36,700	46,700	---
Urea	H_2NCONH_2	60.1	9,300	23,300	119
Chloride	Cl^-	35.5	1,870	8,400	---
Sodium	Na^+	23.0	1,170	4,390	---
Potassium	K^+	39.1	750	2,610	---
Creatinine	$C_4H_7N_3O$	113.1	670	2,150	8.7
Sulfur, Inorganic	S	32.1	163	1,800	---
Hippuric Acid	$C_6H_5CO{\cdot}NHCH_2{\cdot}CO_2H$	179.2	50	1,670	0.367
Phosphorus, Total	P	31.0	470	1,070	---
Citric Acid	$HOC(CH_2CO_2H)_2CO_2H$	192.1	90	930	208
Glucuronic Acid	$C_6H_{10}O_7$	194.1	70	880	S.
Ammonia	NH_3	17.0	200	730	---
Uric Acid	$C_5H_4O_3N_4$	168.1	40	670	0.00645
Uropepsin (as Tyrosine)	$HO{\cdot}C_6H_4{\cdot}C_2H_3(NH_2){\cdot}CO_2H$	181.2	70	560	0.04
Bicarbonate	HCO_3^-	61.0	20	560	---
Creatine	$HN{:}C(NH_2)N(CH_3){\cdot}CH_2{\cdot}CO_2H{\cdot}H_2O$	149.2	0	530	1.4
Sulfur, Organic	S	32.1	77	470	---
Glycine	$NH_2{\cdot}CH_2{\cdot}CO_2H$	75.1	90	450	23
Phenols	$C_6H_5{\cdot}OH$	94.1	130	420	8.2
Lactic Acid	$CH_3{\cdot}CHOH{\cdot}CO_2H$	90.1	30	400	∞
Calcium	Ca^{+2}	40.1	30	390	---
Histidine	$C_3H_3N_2{\cdot}CH_2{\cdot}CH{\cdot}(NH_2){\cdot}CO_2H$	155.2	40	330	S.
Glutamic Acid	$HO_2C{\cdot}CHNH_2{\cdot}(CH_2)_2{\cdot}CO_2H$	147.1	<7	320	1.5
Androsterone	$C_{19}H_{30}O_2$	290.5	2	280	i.;S.
1-Methylhistidine	$C_3H_3N_2CH_2CH(NH{\cdot}CH_3){\cdot}COOH$	169.2	30	260	
Magnesium	Mg	24.3	20	205	---
Imidazole Derivatives	$C_3H_4N_2$	68.1	90	200	S.
Glucose	$C_6H_7O_6(COCH_3)_5$	390.4	30	200	0.15
Taurine	$NH_2{\cdot}CH_2{\cdot}CH_2{\cdot}SO_3H$	125.2	5	200	6.4
Aspartic Acid	$C_4H_7O_4N$	133.1	<7	170	2.71
Carbonate	CO_3^{-2}	60.0	100	150	---
Cystine	$[HO_2C{\cdot}CH(NH_2){\cdot}CH_2S{\cdot}]_2$	240.3	7	130	0.01
Citrulline	$NH_2CONH(CH_2)_3{\cdot}CH{\cdot}(NH_2){\cdot}CO_2H$	175.2	0	130	S.
Threonine	$C_4H_9O_3N$	119.1	10	120	S.
Lysine	$(NH_2)_2C_5H_9{\cdot}CO_2H$	146.2	5	110	V.S.
Indoxylsulfuric Acid	$C_8H_7ON{\cdot}H_2SO_4$	231.2	3	110	
m-Hydroxyhippuric Acid	$C_6H_4COHC(CONH{\cdot}CH_2COOH)$	195.2	1	100	
p-Hydroxyphenyl-Hydrocrylic Acid			1	100	

The basis behind the preconcentration work at PNNL is the discovery that by pretreating carbon electrodes, the functional sites on the electrode can change properties.[25] In efforts to exploit these properties, it was discovered that by cycling voltage on a glassy carbon working electrode in the presence of 0.5M nitric acid as a pretreatment and cleaning procedure, an affinity for higher actinides can be obtained.[26] The current consensus behind the mechanism recreating this affinity is the creation of a "porous, nonconductive graphitic oxide surface to form a film [where] the film has increased oxygen functionalities compared to nonanodized glassy carbon, and cations are readily transported into the anodized matrix."[26, 27]

The anodized glassy carbon electrode system has been applied to a variety of problems and has performed well in most. Its unique ability to be used for the separation of selectable actinides including uranium, plutonium, americium, and neptunium make it an innovation ripe to be utilized across various aspects nuclear materials handling. One particular study tested the system on removing actinides from seawater.[22] Additional studies considered successive selective separations of various actinides.[28-30] Other efforts have been to computationally discover the exact mechanisms behind the uranium affinity of the AGC process.[24] However, much of the previous work focuses on the plutonium affinity over the uranium affinity. It has been touted as a robust procedure for eliminating difficult matrices (also known as harsh environment mass spectrometry), and therefore apt for the problem of urinalysis. One recent publication details the ability of similar systems to preconcentrate plutonium and uranium separately at opposing accumulation voltages. Essentially, plutonium is accumulated at +1.2 V and then

subsequently released at -0.2 V. Meanwhile, uranium is accumulated at -0.2 V and released at +1.2 V.[31] This system holds great promise for expansion into many other complex separations.

Expected Electrochemical Mechanisms

Building on the work at PNNL and ORNL, this work investigated a similar unique and uncommon experimental setup for minor actinide electrochemical separations. One departure from traditional electrochemistry is that the experimental apparatus consists of a thin layer flowcell. Thin layer flowcells have been utilized for electrochemical experiments since the early 1960's for a variety of applications including liquid chromatography and electrochemical detection. Yet the use of thin flowcells remains infrequent as compared to traditional bulk/bath electrochemical experiments. Three reasons for utilizing this technology are the selectivity, low detection limits, and modest cost.[32, 33]

Furthermore, this work utilized a three-electrode configuration as opposed to a two-electrode configuration. Traditional two-electrode configurations measure the current and voltage across an entire cell. These two- electrode cells use the counter electrode (also often referred to as an auxiliary electrode) as both the counter electrode and reference electrode. However, in three-electrode configurations, the reference electrode and counter electrode purposes are split. The reference electrode provides a constant, well-known, and unwavering standard potential for the flowcell. Meanwhile, the counter electrode completes the current connections within the cell. In this work, the working electrode was the site of the electrochemical activity. The working sense

electrode was connected at the same point as the working electrode. This setup was specifically designed to measure the potential on one-half of the electrochemical cell, and this potential was measured independent of any changes or reactions at the counter electrode. This isolation allows for a specific site or reaction to be studied with confidence and accuracy.[34] A traditional electrochemical diagram is shown in Figure 3. It is important to note that the voltage was measured relative to the reference electrode. The current was measured relative to the counter electrode.

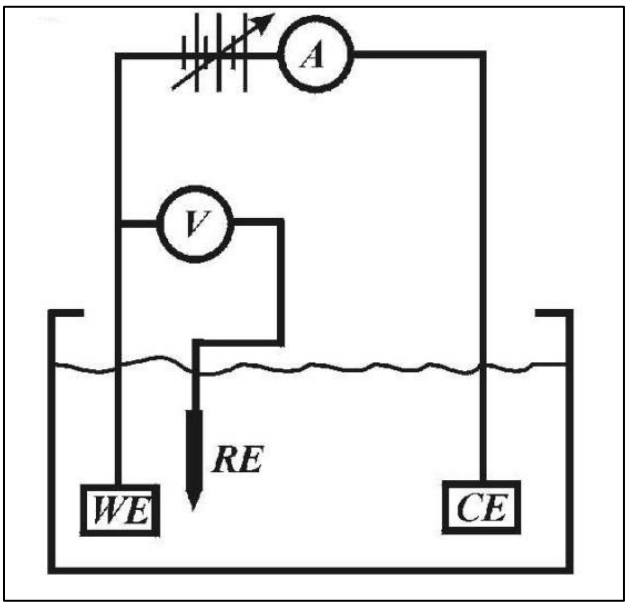

Figure 3: Traditional Electrochemical Diagram of the Flowcell[33]

The traditional diagram for a bath type electrochemical cell does not alone adequately describe this work. The traditional diagram above (Figure 3) was included to better elucidate the electrical connections between the flowcell and the potentiostat. Due to the thin flowcell configuration, the flowcell cross sectional diagram in Figure 4 is a

better representation of the geometry and configuration being studied. The left side of Figure 4 depicts the reduction during the Accumulation phase of this work. Correspondingly, the right side depicts oxidation during the Elution phase of this work. Additionally, much of traditional electrochemistry is performed under steady-state conditions. This work in contrast was hydrodynamic and the small sample volume (1-4 μL) was continually replaced under laminar flow conditions.

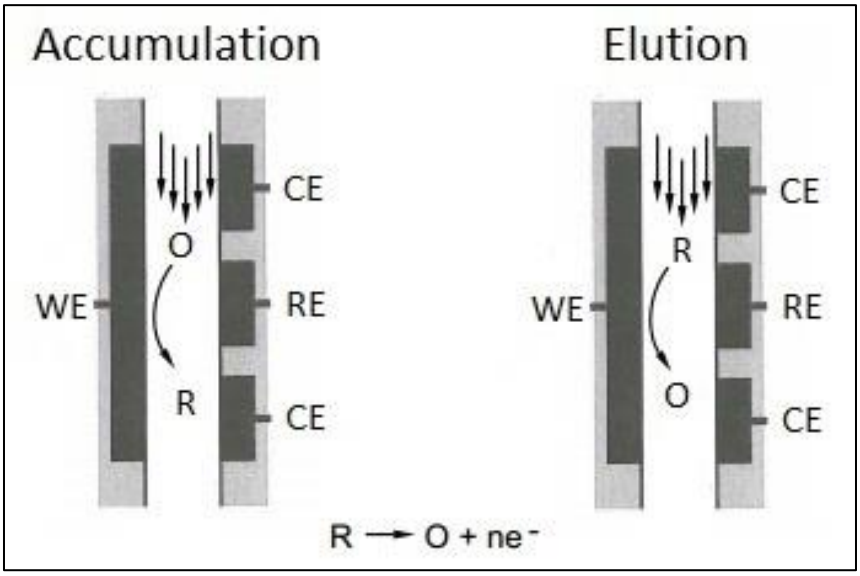

Figure 4: Thin Flowcell Diagram of Accumulation (Left) and Elution (Right) Phases

Additionally, this work was centered on an affinity for higher actinides using a modified glassy carbon electrode approach referred to as anodized glassy carbon (AGC). Unmodified glassy carbon electrodes showed no affinity to preferentially sequester higher actinide atoms by adsorption at Working Electrode – Fluid interface.[35] "With GC electrodes, cycling the potential to positive values in acidic media causes a porous,

nonconductive graphitic oxide surface film to form. The film has increased oxygen functionalities."[27] This oxidative reaction, which forms the surface groups, allows for covalent attachment of a higher actinide atom/molecule. Only limited studies on this adsorption functionality have been conducted. The leading study delves into a surface complexation model which "is likely dictated by electrostatic interactions between charged ions in solution and pH dependent, protonated, neutral, and deprotonated binding sites at the surface-water interface."[24] These reactions are described by

$$SOH + H^+ \Leftrightarrow SOH_2^+$$

$$SOH \Leftrightarrow SO^- + H^+$$

where *S* stands for the surface or substrate material. The formation of functional groups on a carbon substrate has been graphically represented in Figure 5.[33] This expected oxygen functional group on the glassy carbon working electrode is shown at the top of the figure. All of the oxygen functional groups are most likely formed during the anodization process; however, the functional group at the top of Figure 5 is the functional group related to the uranium affinity which forms the basis of this work.[24] One of the probable expected covalent chemical adsorption mechanisms is thought to be governing the adsorption of uranium is

$$SOH + UO_2^{2+} \underset{AGC}{\Longleftrightarrow} SOUO_2^+ + H^+$$

The full mechanism of this adsorption has not been fully elucidated and has sparked several ongoing research projects related to fully understanding this complex

mechanism.[24] Figure 6 shows a modified thin flowcell diagram with oxygen functional groups and an adsorption.

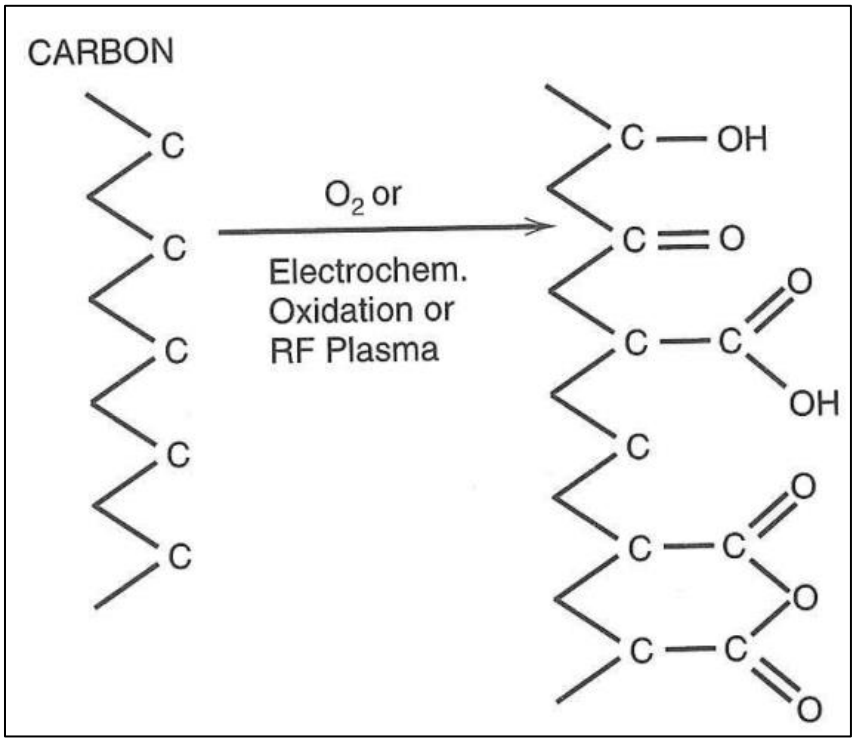

Figure 5: Oxygen Functional Groups Bonded to a Carbon Substrate[33]

The speciation of the uranium in solution can have an effect on the adsorption mechanism. In order to fully understand the speciation of the test samples, Figure 7 contains the Pourbaix diagram for uranium.[36] This work utilizes solutions with low pH (pH of 1-3) and an Ag/AgCl reference electrode with a constant potential of +0.209 V. As a result, the Pourbaix diagram predicts that aqueous solutions (between the two dashed lines) with the specified pH and reference electrode voltage (versus the Standard Hydrogen Reference Electrode) that UO_2^{2+} should be the dominant ion in the system.

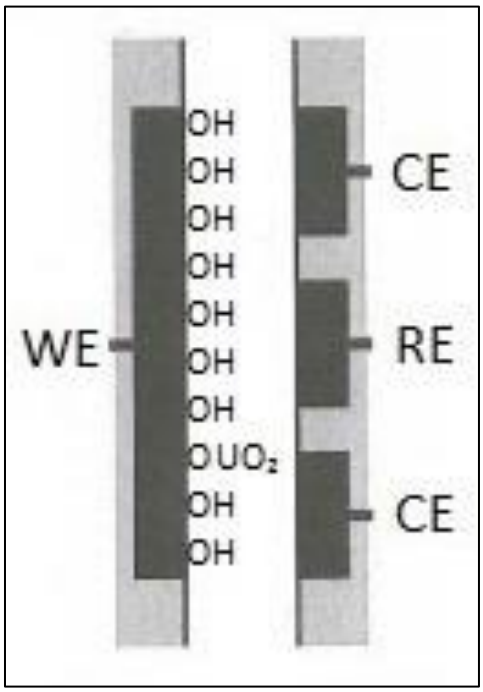

Figure 6: Thin Flowcell Diagram of Anodized Glassy Carbon Working Electrode with an Adsorption of a UO_2 Molecule

The active site density of the glassy carbon working electrode has been estimated as 2.3×10^{18} sites/m^2.[24] This work utilized a 6 mm diameter round glassy carbon working electrode. Thus the area of the working electrode was 2.8×10^{-5} m^2. As a result the total active sites of a glassy carbon working electrode used in this work was 6.5×10^{13} sites. Assuming that each site can bind no more than one molecule, then 100 percent saturation of the working electrode should occur with approximately 25.7 ng of uranium. Significantly lower quantities than the saturation amount were studied during the experimentation phase of this work.

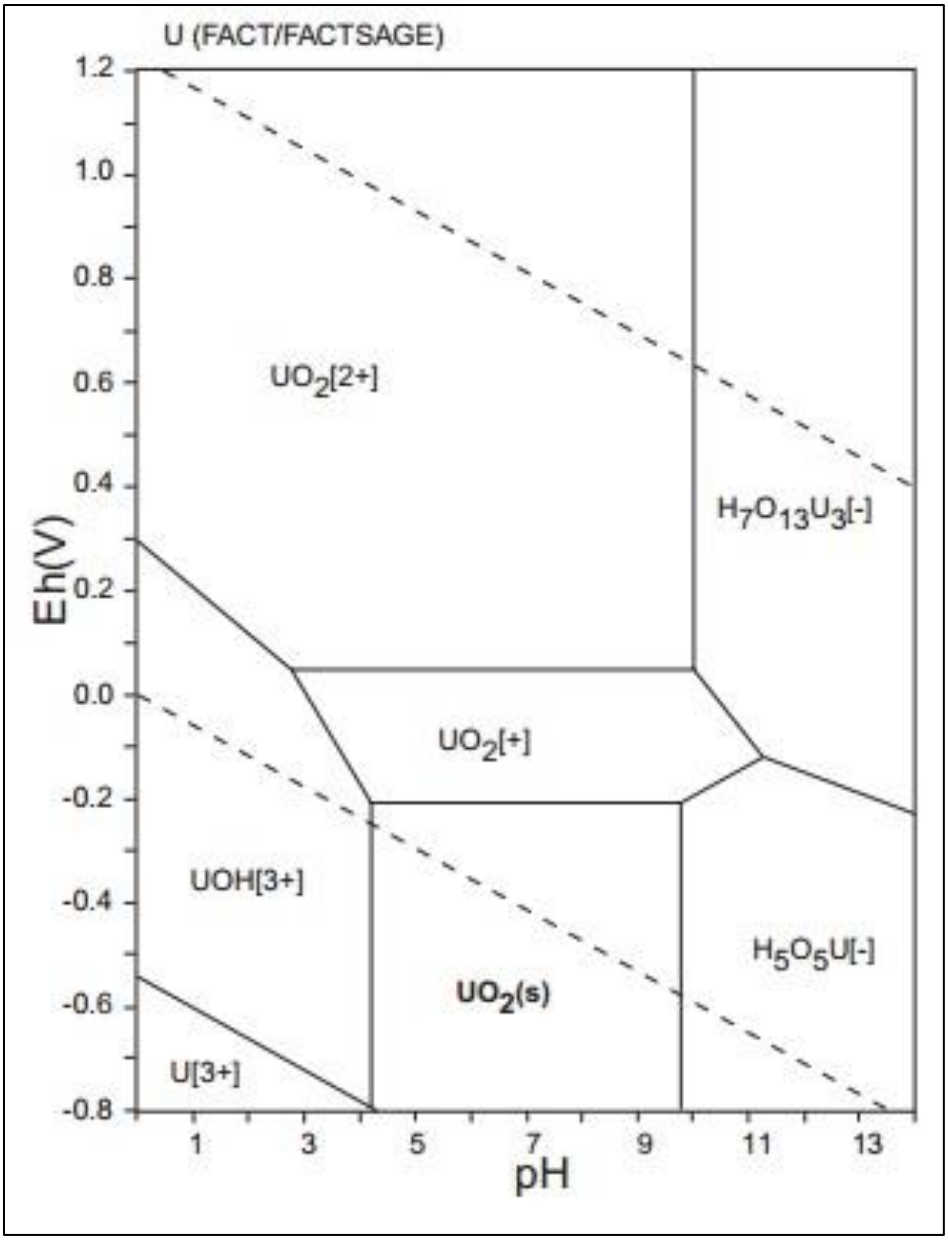

Figure 7: Pourbaix Diagram for Uranium (Standard Hydrogen Reference Electrode Potential in Volts vs. pH)[36]

Electrochemical Separations of Urine

Electrochemical procedures have seen limited application to urinalysis for the selective measurement of various elements. In one specific case, researchers

successfully separated manganese directly from a urine and electrolyte solution.[37] One of the most important factors in adapting this concept to analyze urine samples with higher atomic number elements is the interference of other materials and fouling of the electrode anodization from the organic components of urine during the separation process.[38] In order to overcome this fouling, appropriate levels of digestion must be accomplished before processing the sample. The most common method of digestion is by heating the sample in closed vessels; however, promising results are being produced by several researchers using microwave digestion to hasten the breakdown of miscellaneous organics contained within urine samples.[39] Anodized glassy carbon as a urine analysis tool remained unexplored until this work.

Biokinetic Modeling Works

If the problem solely consisted of detecting uranium through urinalysis, the issue would be purely chemistry related. However, there are additional complexities that arise when studying a biological system. Biological systems are influenced by a vast number of factors. Previously, the problem of a naturally occurring uranium background was briefly discussed. This background uranium content can be related to many factors from geographical location, diet, occupation, and personal biological make up, with the largest being background arising from drinking water as part a diet.[40] Something as simple as moving across a city to change water sources can significantly affect the expected background in an individual. Thus, it is important to understand the pathways and biological reactions for uranium when studying this problem.

A significant effort in the health physics community to understand the biokinetic pathways of a variety of nuclear materials has been underway for several decades. Widely accepted results for biokinetic models are contained in the International Commission on Radiological Protection (ICRP) Publications. These models are constantly evolving and being updated. Some recent work has focused on understanding the alternate excretion points such as fingernails and hair. However, most biokinetic models have remained the same for several decades. These standard models for uranium excretions are contained in ICRP 67 through ICRP 72. These models were developed from a compilation of data and experience from studies from the 1950's and include monitoring the excretion of both animals and humans. Most of the human data is due to accidental exposures in both the nuclear industry and the United States military-industrial complex. As a result, the data varies in its breadth and quality due to the variety of sources.[41-44] Additional studies have been undertaken to understand the effects of using depleted uranium munitions in war and the accompanying exposures.[45] This work only utilizes the highest quality accidental occupational exposure data. The ICRP sixteen compartment and pathways model is shown in the Figure 8.[46]

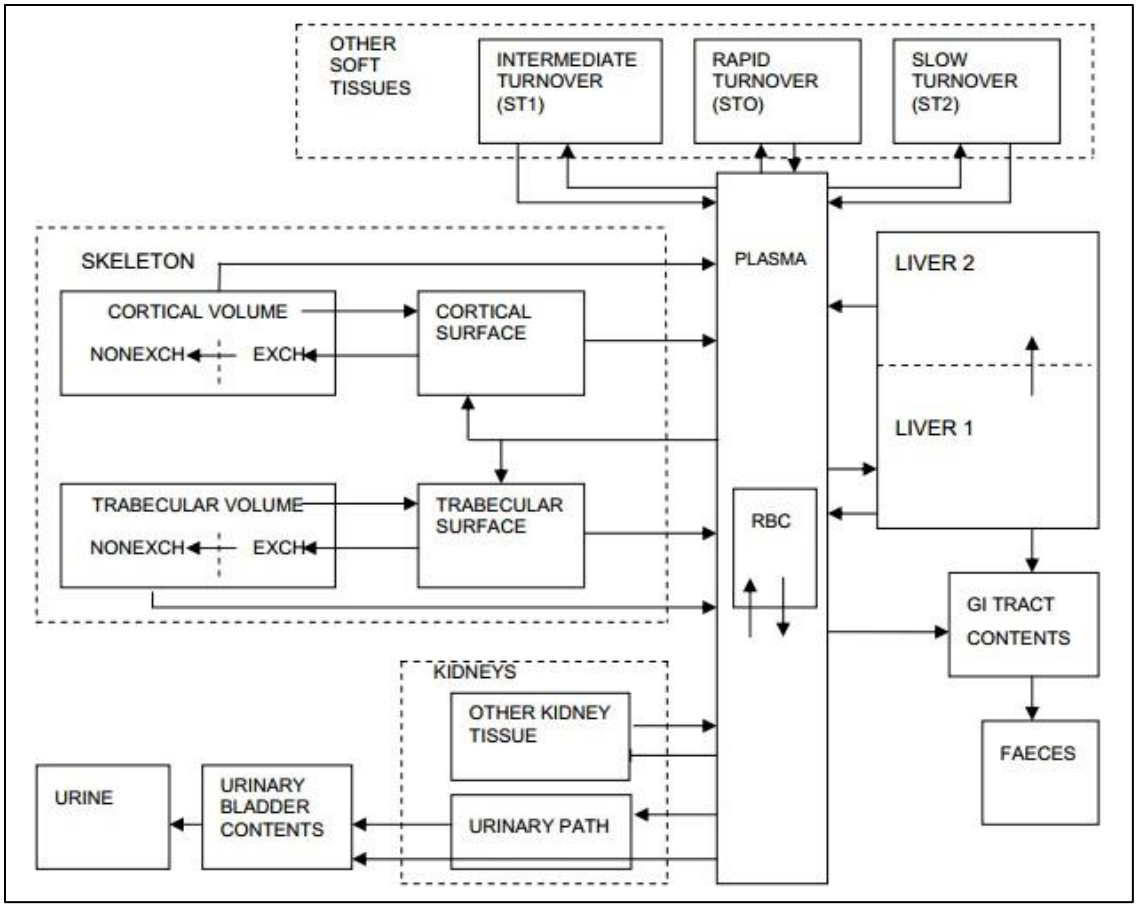

Figure 8: ICRP Compartments for Uranium Biokinetics[47]

One previous effort that is important to this work was from the 1960's where the significance of uranium urinalysis was examined. The first relevant conclusion was that limited numbers of samples could not be interpreted accurately to make proper conclusions from bioassay data. The second conclusion was that samples must have some time gap between one another as well as the exposure incident to be reliable.[48] Thus, understanding the number of samples needed to reliably determine the intake from an exposure is an important factor to investigate.

One of the most accepted models is the Dose and Risk Calculation software (DCAL) developed by the Biosystems Modeling team at Oak Ridge National Laboratory.[49] DCAL is an unclassified and freely available code distributed by Oak Ridge National Laboratory. It has become a widely accepted and used code through the health physics community in the United States. The models and software calculate the expected body burden and excretions based on the material, biological introduction pathway, and age of the subject.[50]

Some additional work undertaken to update the model has been to better understand the differences between various chemical forms of uranium in regard to pathways and excretion from the body. A big step forward was to understand the differences between the various excretion rates of different materials. This is related to the solubility of the particular chemical.[51] Typically, the models divide materials into fast, moderate, and slow. As more data becomes available and different chemicals are tested, it has become apparent, that no material fits exactly into the fast, moderate, or slow categories. Rather, each material tends to fall in between two classifications. By adjusting the absorption factors (differences in the classifications) in the code, different chemical absorption and excretions can be modeled.[52] This development is based on empirical observations and not well trusted yet. These standard models and data serve as the basis for expectations related to the excretion of uranium from urine. These multiple factors related to urinary excretion of uranium form a complex problem and must be carefully considered when determining the minimum requirements of an effective inverse modeling of urinary excretion data.

CHAPTER II

EXPERIMENTAL DESIGN AND DEVELOPMENT

The experimental design and development was a significant effort in the completion of this work. The experimental design went through several phases to continually refine the procedures and practices to best separate uranium from the complex solutions. Successive iterations saw improvements in both results and experimental methodologies. The initial stages of design were based on the literature found from the ORNL and PNNL efforts to pioneer similar systems for online preparation of samples.[21, 22, 26, 28, 35] Since this approach and samples are unique, the previous efforts were only used as a spring board into further more sensitive methods. Previous efforts were designed for online separation; however, this work is using a batch method due to sporadic ICP-MS availability. The experimental system underwent several design refinements in producing a functional uranium separation methodology. These refinements involved materials selection and replacement, optimization of experimental parameters, and appropriate sample selection to mimic real world scenarios. This chapter details each refinement and the impetus behind each change as the experimental process was improved.

Preliminary Geometry Experimental Setup

The basics of the experimental setup include a thin flow electrochemical cell with an adjustable volume determined by thin Teflon® gaskets. While in the active volume of the flowcell, the samples will be subject to a voltage such that uranium atoms

can be preferentially stripped from the solution and held on an electrode. Later, these uranium atoms will be eluted and collected in a clean nitric acid matrix while the contaminants in the sample pass through the cell without accumulating on the working electrode. The overall system utilizes a variable speed peristaltic pump, a sensitive voltage supply (potentiostat), a control computer, and appropriate Teflon® coated plastic tubing. The overall flow diagram of the experimental setup is shown in Figure 9.

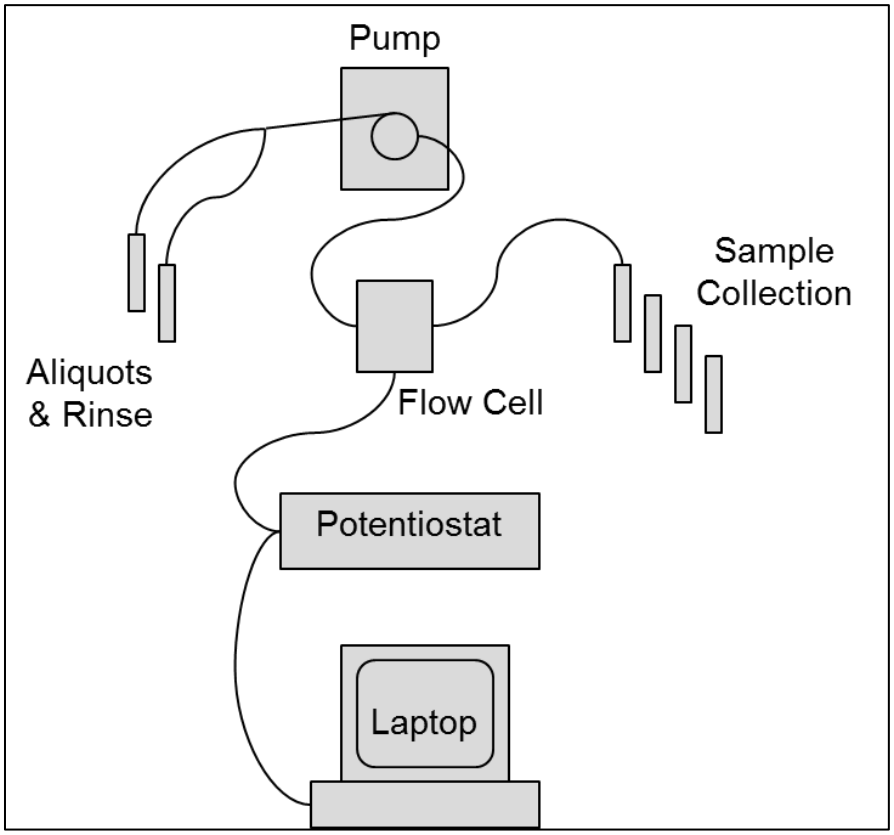

Figure 9: Experimental Flow Diagram

Due to the ubiquitous nature of uranium, these experimentations must be done in a clean room rather than a standard chemistry laboratory. This keeps the unwanted

uranium background to a minimal level. The available clean room space at LANL was a class 10,000 room which means there are less than 10,000 particles larger than 0.5 microns in one cubic foot of air. To further ensure the cleanliness of the experimental space, the apparatus and the peripherals used to prepare the experiment were housed in a class 100 hood. The hood has no more than 100 particles larger than 0.5 microns in one cubic foot of air. This is achieved by utilizing air handlers equipped with high-efficiency particulate air filters. These laboratory spaces are certified annually during the first week of November. Further, all of these spaces are maintained by periodic cleaning performed by each lab space user. This is done using clean room procedures as established at LANL. The clean room set up is shown in Figure 10.

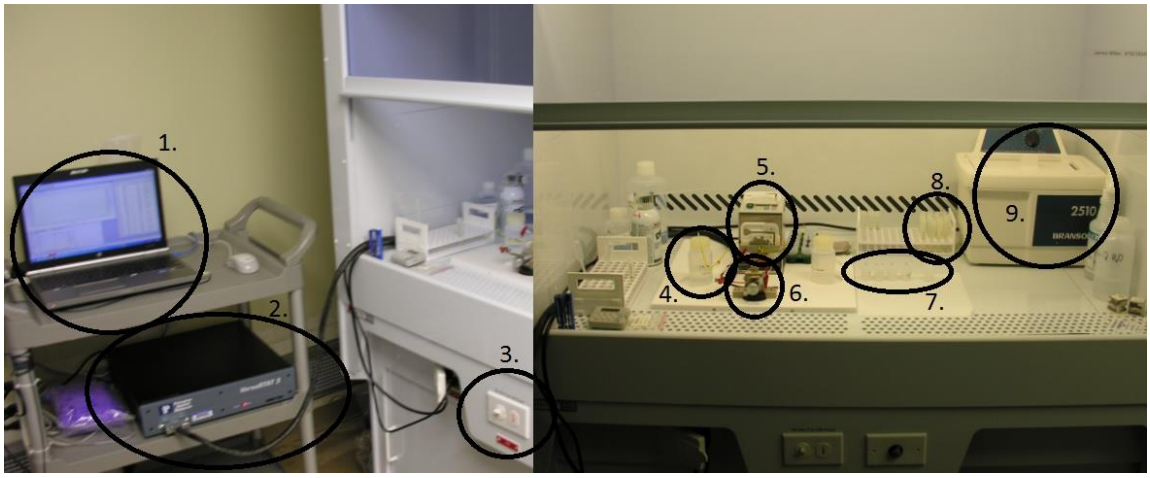

Figure 10: Clean Room Laboratory Space and Chemical Hood Setup (1. Control PC 2. Potentiostat on Cart 3. Fume Hood Controls 4. Nitric Acid Rinse Bottle 5. Peristaltic Pump 6. Flowcell 7. Teflon® Vials 8. Sample Storage 9. Sonication Bath)

A standard optical microscope was used for additional analysis and experimental checks, which has an optical range from 10x magnification to 40x magnification. This

microscope was located inside the clean room and within its own microscope hood to maintain the cleanliness of samples and is shown in Figure 11. The microscope was used to examine the functional sites and materials in higher resolution than the naked eye would allow. This microscope was used to take pictures of many portions of the experiment, including the working electrode, counter electrode, and dried samples for qualitative comparison.

The cleaning regime for equipment is very important when performing trace uranium analysis. To aid in this cleaning, an ultra-sonic bath (sonicator) was acquired and used to ensure no errant particles from the working electrode cleaning polishes or previous experiments were introduced into any samples. This sonicator is shown in the back right corner of the chemical hood in Figure 10 (on far right). The sonication bath was changed periodically and filled with 18 MΩ-cm filtered water.

Figure 11: Microscope Inside the Clean Room

Figure 12: Princeton Applied Research VersaSTAT 3

Based on the aforementioned literature, several items were acquired to proceed with experimentation.[22] The first and most important new acquisition was the potentiostat. This is by far the most expensive and essential piece of equipment needed for the experiment. The potentiostat provides the voltage to the electrochemical system. The applied voltage must be precise and unwavering. Furthermore, a quality potentiostat has a current feedback sensor to detect power overloads that will destroy experimental equipment. This experiment cannot be accomplished with a standard voltage supply. The potentiostat used was a Princeton Applied Research (Amtec) VersaSTAT-3 with accompanying VersaSTUDIO software, which is only compatible with a Windows PC. Further, the VersaSTUDIO software is available in both 32-bit and 64-bit packages and must be the appropriate version for control PC. The potentiostat is

shown in Figure 12. The computer and potentiostat were housed on a moveable cart next to the experimental hood (shown in Figure 10 on the left) in order to allow them to be easily moved when other scientists needed to use the shared laboratory space.

The fluid supply was controlled using a digital variable peristaltic pump from Reglo. The fluid handling system is not exceptionally unique, but it must be consistent, easily programmed, and most importantly, useable for a broad range of flow rates. The flow rates range from a few microliters per minute to hundreds of microliters per minute. This particular pump had a bias moving fluid slightly quicker than programmed when operating near the lower limit the flow rate window. This bias was observed using several nitric acid samples with a known volume and a digital timer. The time needed to transport all the fluid was compared to the expected flow rate. The overall bias was approximately one microliter per minute. The window of flow ranges is set by the inner diameter (i.d.) of the peristaltic pump tubing. Smaller diameter Teflon® tubing allowed for a lower flow rate which was proportional to the inner diameter. The smaller tubing is available with flared ends which aids in connecting the inlet and outlet port tubing with the flowcell. These connections can be made by forcibly placing the smaller tubing into the flexible peristaltic pump tubing. Often, the harder, smaller tubing needs to be trimmed to a point at the end to facilitate placement within the peristaltic pump tubing.

The apparatus (potentiostat, sonicator, peristaltic pump, control PC, and chemical hood) remained in place throughout all phases of the experimental process. However, several of these pieces needed refurbishment throughout the process. That refurbishment is discussed later.

Commercially Available Flowcell

A thin flowcell kit is commercially available from Bioanalytical Systems Incorporated (BASi). Ideally, a commercially available flowcell would make this experimental process very simple and straight forward. Reasons why the commercially available package was not appropriate for trace uranium analysis are discussed in this section. The BASi kit contained polishing supplies (polishes, bases, and pads), an auxiliary electrode, reference electrodes, tubing, inlet and outlet flanges, and Teflon® gaskets. Ultimately, the auxiliary electrode base was not used, but the accompanying components were utilized. Further, this stainless steel flowcell served as a reference to craft a custom flowcell from clean room compatible materials. The thin flowcell from BASi is diagramed in Figure 13. Additionally, the flowcell comes with several working and silver/silver chloride (Ag/AgCl) reference electrodes. The standard working electrode in the kit contains dual 3 mm diameter glassy carbon working electrodes; however, this work requires a larger surface area and thus several 6 mm diameter single glassy carbon working electrodes were acquired from BASi.

With all of the components in hand, a test of the apparatus was performed. The first step in preparing the apparatus for use is a thorough cleaning of all components using the sonication bath as well as polishing kits. When the flowcell was assembled as shown in Figure 13, the electrical leads for the potentiotstat were connected to the counter electrode (black), working electrode (green and grey), and reference electrodes (white) accordingly.[34] Immediately it was clear that the electrical attachments placed significant strain on the placement of the flowcell causing it to topple. The flowcell

needed to be anchored in place to prevent slippage, leakage, and poor performance. A backer plate was created with assistance from the Chemistry: Nuclear and Radiochemistry (C-NR) machine shop to anchor the flowcell in place and hold the experimental pieces in place. The anchor system consisted of a base plate and two blocks to hold the flowcell base in place via two hexagonal head stainless steel screws and corresponding nuts sunken in the base plate.

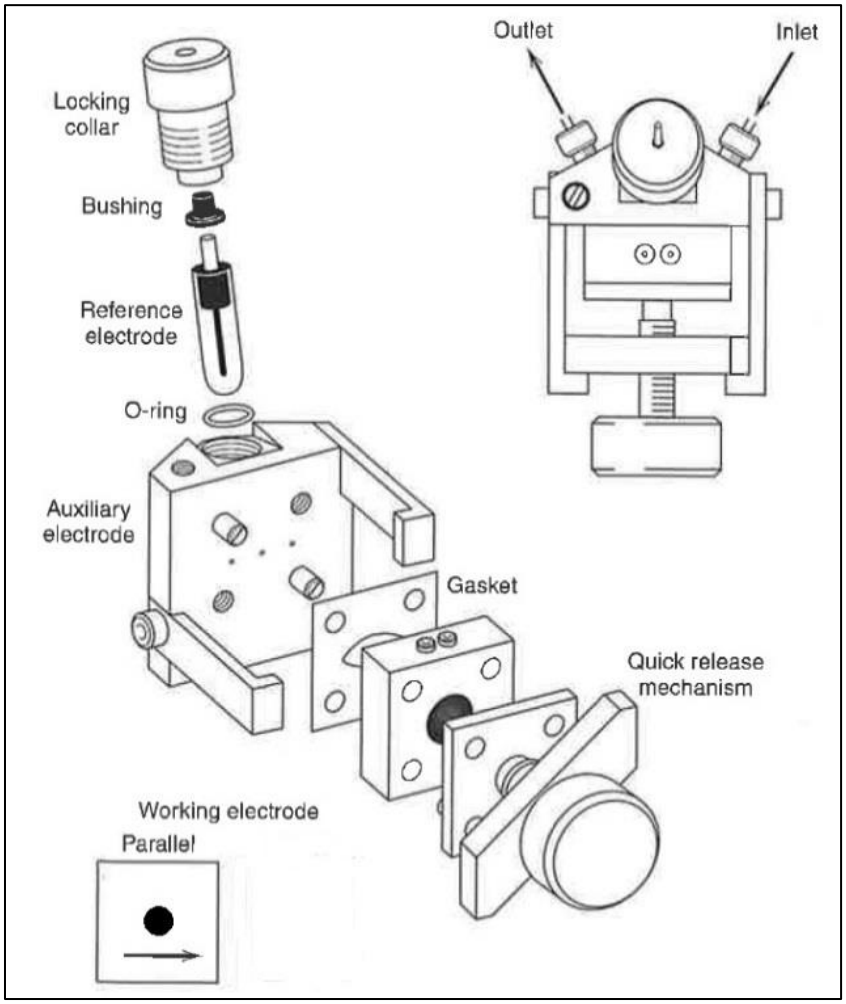

Figure 13: BASi Thin Flow Electrochemical Cell[33]

The next step in preparing the apparatus for uranium separations was to polish the working electrode and to anodize it to accept uranium on a homogeneous layer of oxygen across the surface of the working electrode. This anodization is the crux of the entire experiment. Should anodization not be accomplished, then no separation should be expected. As previously mentioned, the anodization creates a thin layer of oxygen on the surface of the electrode which has an affinity for uranium. This thin oxygen deposition alters the functional sites on the surface of the electrode.[26, 27, 32] From the literature, the anodization is complete when "following pretreatment, the glossy finish of polished GC [glassy carbon] was replaced by a flat matte surface; iridescence was apparent, along with an underlying metallic blue or green tint."[22] From the ORNL and PNNL work, the expected uranium(VI) reduction reactions in this low pH system are[32]

$$UO_2{}^{2+} + e^- = UO_2{}^{+} \ (E^0_{redox} = -0.15V)$$

$$UO_2^{2+} + 4H^+ + e^- = U^{4+} + 2H_2O \ (E^0_{redox} = +0.13\text{V})$$

The voltages for the preceding redox reactions are for the given system with respect to the reference electrode setup. The Ag/AgCl reference electrodes used in this work have a standard reduction potential of +0.209 V when saturated with 3 M sodium chloride. A different saturation during storage or wear on the electrode can have a small effect (less than -0.05 V) on the reference electrode voltage.

The first anodization experiments were based on the experiments in literature performed at ORNL.[22] The anodization cycles were set for a 60 second voltage application at +1.85 V followed by a 30 second rest period at +1.00 V. These voltages are relative to the reference electrode voltage. At least five anodization cycles were

performed to ensure anodization. While anodizing, 0.5 M HNO_3 Optima® acid was used at a flow rate of 1 mL per minute.

This particular setup had some electrical loading issues. Specifically, the flowcell would overload and cause the voltage supply to turn off. This usually was a failure of adequate flow from the flowcell volume to the reference electrode reservoir and back. If any air bubble was present within the reference electrode reservoir, the air bubble would insulate the reference electrode from the rest of the cell causing the overload. The commercially available stainless steel flowcell had a consistent issue with overloads caused by air bubbles. When overloads occurred during the anodization cycles of the experiment, the reference electrode was simply manually re-wet with some of the nitric acid being used during anodization by disposable transfer pipet and restarted.

Assessing the anodization state of a working electrode is a difficult task. The literature merely describes an anodized glassy carbon electrode as having a blue luminescence.[22, 53] Eventually a low quality image was found to demonstrate the blue luminescence; however, this image was not available for the first iterations of the experiment.[29, 53] There is a very distinct possibility that one of the overriding factors contributing to failure to separate uranium using the stainless steel commercially available flowcell was inadequate anodization. When a glassy carbon electrode is fully anodized, it should have a very distinct blue color that in unmistakable (and is shown in a more in depth discussion of anodization in Chapter III). Ultimately if there is any

doubt, then the working electrode is not anodized. This was a lesson learned through extensive trial and error.

After cycling through several anodization steps and visually checking the working electrode for acceptable anodization, the separations step were conducted. The early tests consisted of between 1 and 5 ng known sample loads in 5 mL of solution. These samples were standard matrix (no interferences) solutions. They were clean 0.5 M HNO_3 acid solutions and contained up to one part per billion (ppb) natural uranium. Following what would become the best practices, all of the fluids from the experiments were collected including the rinses between phases of the separation. Separations were conducted in accordance with the literature.[35] The uranium was separated with the application of -0.15 V for five minutes (time necessary for the entire sample to be pumped through the flowcell). The uranium was eluted at +1.15 V for an equal time to the separation. The samples were then dried on a hot plate overnight to then be volumetric normalized for mass spectrometry analysis. The samples were digested using clean 0.5 M nitric acid and transferred to test tubes for ICP-MS analysis. The samples were analyzed using a low resolution fifteen pass scan on a Thermo Element XR single collector ICP-MS. The minimum detection limit for this ICP-MS instrument is approximately 0.001 ng uranium.

Intermediate Geometry Experimental Setup

After several trials with the stainless steel electrode and with no significant separation of uranium from the samples, several changes were made to the methodology. These changes were made after a thorough fresh analysis of the literature.[26] Two

discrepancies were found between the literature and the previous experimental process. The first discrepancy found was that one percent nitric acid was used for the separation, while two percent nitric acid was used in the initial experimentations. This was not likely the cause of such poor performance. The second discrepancy, which is fairly significant, was that newer literature papers described a custom flowcell that was only modeled on the commercially available stainless steel version.[30] Additionally, the nitric acid seemed to be stripping several portions of the stainless steel counter electrode when using the commercially available setup. This was seen visually and in the mass spectrometry data. This normally should not be a problem for stainless steel equipment, but the unique environment of acid combined with significantly variable applied currents creates a situation in which the stainless steel is not durable enough for this experiment. As a result, it was decided to build a custom flowcell using acid resistant plastics in conjunction with the machine shop in the Chemistry – Nuclear and Radiochemistry group at Los Alamos National Laboratory.

Additionally a series of personal communications between one of the authors (Dr. D. Duckworth of PNNL) from the literature revealed that newer publications were in preparation which indicated the need for much smaller uranium loads (an order of magnitude) due to electrode saturation of the working sites.[53] In the same communication, it was conveyed that the flow rates used for such trace analyses were almost an order of magnitude lower than was originally reported in the literature and used in the initial tests.[35] As a result, a custom flowcell using acid resistant plastic

(PEEK) was fabricated in conjunction with the machine shop in the C-NR group at LANL to replace the existing stainless steel setup.

Flowcell Replacement

Several pieces from the original flowcell were recycled into this custom device. Specifically the base, arms, and working electrode quick release mechanisms were used in conjunction with the new plastic flowcell. The full CAD diagrams are attached in Appendix B and the front face of the custom flowcell is shown in Figure 14. Mr. Dale Melton, a skilled machinist, oversaw the fabrication as per laboratory regulations.

The new flowcell is made from polyether ether ketone (PEEK). PEEK was chosen because of its high resistance to degradation when in the presence of acids. Also, it is commonly machined in engineering applications and a sizeable scrap was available for this fabrication. The fabrication took almost a month to complete.

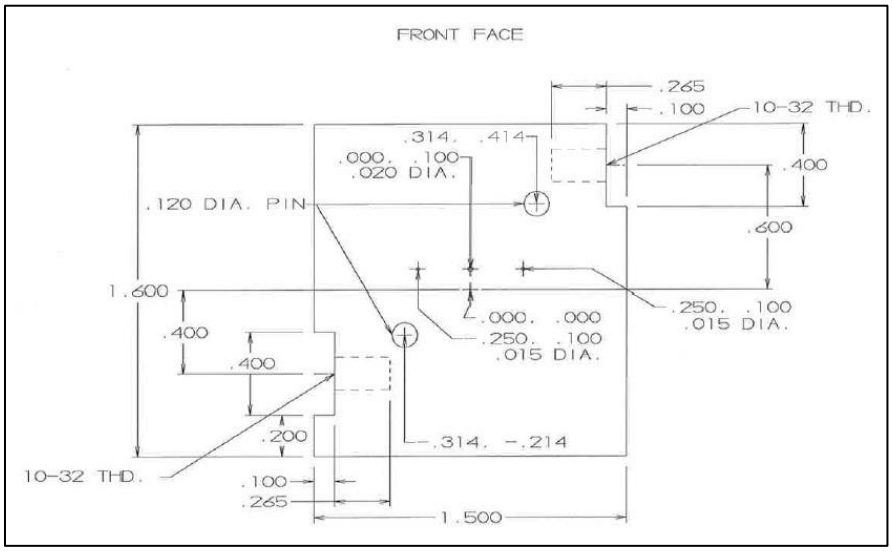

Figure 14: CAD Diagram of the Custom Flowcell Front Face

Counter Electrode Replacement

Since the previous flowcell was a combination counter electrode and flowcell, an additional piece needed to be fabricated to replace the counter electrode. As seen in the initial testing of the flowcell, this counter electrode is subject to a unique environment.

Material Selection and Acquisition

The material chosen for the new counter electrode must be more resistant to both electrical and acidic environments. Stainless steel is not an option for the same issues that were observed in the previous flowcell. Also, copper, which is widely used in electrical systems, is very acid adverse and is a poor choice. Platinum was chosen for the counter electrode since it is exceptionally chemically resistive and widely used in electrochemical experimentation.[33]

Platinum is a very costly, precious metal, which could impede the acquisition process. To get an appropriately sized (2 cm by 2 cm by 0.1 cm) thin foil of platinum from the Department of Energy precious metals supplies would have cost about 4,000 dollars and would have required at least eight weeks. Private suppliers were able to provide an appropriate piece in a more reasonable timeframe, but at much greater expense. The laboratory had several platinum pieces available including strips and wire, but neither had the surface area needed to adequately replace the counter electrode. And creating a foil from pieces of wires and strips would not provide a smooth face inside the flowcell, which makes non-turbulent flow inside the cell impossible. After some inquiry with various teams within the Chemistry division, a one inch diameter platinum disk was acquired from the alpha spectrometry lab, which often used the disks as planchets for

electrodepostion of active samples.[16] From this one inch disk, a circular counter electrode was fabricated. Thus some design parameters had to be modified in order to use this platinum since it was thicker than originally desired. This disk had three holes: an inlet port, a reference electrode port, and an outlet port. The disk was fabricated such that the pegs to hold the working electrode in place could be used to keep the counter electrode in position. The fabricated counter electrode is shown in Figure 15. It is also of note that the counter electrode must have a larger surface area than the working electrode. This particular setup is significantly larger (1000 times more surface area) than the 6 mm diameter glassy carbon working electrode.

Figure 15: Original Custom Counter Electrode

Counter Electrode Electrical Connection

With a platinum counter electrode available for contact within the flowcell, an electrical connection between the counter electrode and the potentiostat must be made. When the flowcell is assembled, the counter electrode is completely covered by the one inch by one inch working electrode block. As a result, attaching the counter electrode with a standard clip was not possible. Furthermore, attaching wire poses additional

complications. The first modification to attach the counter electrode was to remove a portion of the working electrode block to create clearance for the electrical lead. Sections of the corners at opposite ends of the diagonal were removed on the milling machine in the workshop.

Standard copper wire cannot be used due to its sensitivity to acidic environments and potential copper contamination within the samples. Thus a platinum wire would be needed for the same reasons outlined for the need for a platinum counter electrode. But traditional soldering methods are not effective with precious metals due to a need for consistent electrical transmission through the attachment.

Tack welding was the first method of attachment tried. In tack welding, the two pieces are clamped together and a large current is applied to the point of contact. This is designed to cause minor melting and solidifying to join the two metals together. It is routinely done as part of thermal ionization mass spectrometry to create rhenium filaments to contain samples to be analyzed. This method produced a very solid and consistent electrical connection; however, the connection was not able to withstand the successive cleaning and handling between experiments. After several uses, the tack weld would fail and the wire would need to be reattached. This flaw was discovered during the testing phase of this new flowcell geometry.

In order to create a more robust attachment to the counter electrode, both the counter electrode and flowcell base were modified. Two modifications were made to the flowcell base. The first included two screw receptacles added on the diagonal opposite the working electrode pegs. The second was to mill a less than one millimeter deep and

wide channel on the bottom right hand section to provide a recessed channel for the wire connection. Matching holes were drilled into the counter electrode to allow plastic screws to attach the working electrode to the flowcell base. The platinum lead wire had a loop added to the end and was attached by contact and held on with one of the plastic screws in the recessed channel behind the counter electrode. This approach could potentially generate an issue with embrittlement of the plastic screws should they be exposed to acid. Originally, stainless steel screws were used, but these screws had an oxidation issue related to acid exposure. Significant oxidation was seen on the counter electrode disk, Teflon® gasket, and machine screws. Plastic was deemed to be the appropriate replacement, but with the tradeoff that plastic screws would be susceptible to the aforementioned acid embrittlement. Occasionally the heads of the screws sheared off and the neck of the screw would need to be removed using a tap set. This issue can be mitigated for the most part by avoiding over tightening the screws when attaching the counter electrode. These modifications are shown in Figure 16.

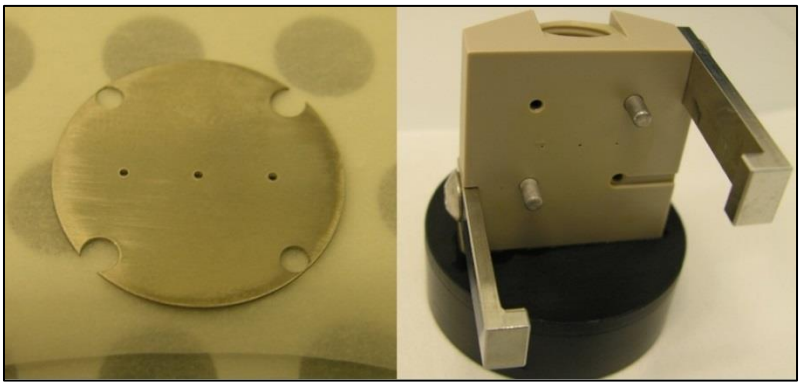

Figure 16: Modified Counter Electrode and Flowcell

Custom Flowcell Testing

In the same literature review that spurred the change to custom flowcell, updated parameters for anodization and separation were discovered. The parameters being used previously were updated significantly in a publication and were then confirmed via private communication.[29, 53] Thus a new set of experiments were conducted in order to determine any flaws or failures within the experiment.

Hydrodynamic Integrity Testing

With a new custom apparatus, the fluid retention capabilities of the flowcell were tested. The new geometry was much more complicated than the previous geometry of the stainless steel flowcell. This is a result of the counter electrode design. Previously, the fluid being analyzed would enter the cell directly into the void space created by the thin Teflon® gasket, cross the face of the working electrode, transition into the reference electrode reservoir, re-enter the flowcell void space while crossing the face of the working electrode, and exit the other port. The introduction of the new counter electrode added four more material interface crossings and seals to the flow path.

Initial tests of the new apparatus found a satisfactorily sealed flowcell. A variety of flow rates were tested and visually inspected. These tests were done with "clean" 0.5 M Optima® nitric acid (less than 10 pg/g natural U) to avoid any uranium contamination in either the flowcell or the chemical hood. One minor leak was noticeable. The leak appeared to be from the corner where the counter electrode was attached to the platinum wire. In order to mitigate this issue, the corner of the Teflon® gasket corresponding to the leak was trimmed. This allowed for a better seal between the working electrode and

the flowcell volume. After no noticeable leaks were seen at the edges of the component interfaces, the fluid that went into the flowcell was being conserved and removed from the flowcell with minimal loss of the desired sample. Next the system was tested while biased.

These tests failed. An unknown effect was causing the flowcell to overload consistently without any obvious cause. Constant and consistent overloads resulted in the explosive failure of several Ag/AgCl reference electrodes during anodization tests. The remaining reference electrodes were tested according to the supplier's instructions with a voltammeter and a 3 M NaCl bath. All remaining electrodes were found to be within factory specifications, thus another component must be at fault. Upon inspection under the microscope, it was found that the reference electrode inlet/outlet port was becoming partially obstructed. This blockage was causing the reference electrode to be insulated from the working electrode's active sites. This blockage would manifest itself in several ways including the explosion of the reference electrode, elution of platinum atoms from the counter electrode, and oxidation of the components of the flowcell. After another thorough cleaning with isopropyl alcohol and sonication, it was determined to use compressed air to actively clear the port before use. This effectively minimized the overloads and testing was able to resume. Due to the continual overloading issues, permanent fouling of the first glassy carbon electrode occurred. In doing so there was a residue akin to charring. This is shown in Figure 17. No amount of polishing seemed to return the working electrode to its original state. This residue was sampled by a Secondary Electron Microscope (SEM) equipped with a backscatter

detector and determined to be liberated stainless steel from the first set of screws fastening the counter electrode to the flowcell face.

Anodiziation and Separation Protocol Refinement

During initial tests of the new cell, overloads and null separations occurred frequently. After some refinements to the anodization protocols, the frequency of these overloads and null separations was drastically reduced. From the same newly acquired reference, the anodization input deck was modified from 60/30 second cycles to 20/20 second cycles.[29] Furthermore, the anodization time was increased from 5 minutes to 20 minutes.[29] This change corresponded to a slight change in voltage as well. The anodization voltage remained at +1.85 V, but the relaxation voltage was lowered from +1.0 V to +0.85 V. Further, from a graph of a real-time ICP-MS measurement of on-line preconcentration utilizing a similar flowcell, the accumulation voltage used by the group at PNNL was changed to -0.2 V as opposed to previous work using -0.15 V.[29]

Figure 17: Microscope Image of Permanently Fouled 6mm Diameter Glassy Carbon Working Electrode

Unfortunately, a few other minor differences in the experimental setup were discovered. Upon thorough review with the technical staff at Los Alamos National Laboratory, those minor differences were accepted as intrinsic biases of this particular system. The first difference is that the working electrode is offset to the back end of the flow stream such that the sample comes into contact with the reference electrode prior to crossing the working electrode. Meanwhile, this work has a different geometry where the sample will cross the working electrode both before and after contacting the reference electrode. The two systems differed in the make and model of both pumping systems and potentiostats. The concentration of acid was slightly different between the two systems. The other was using 0.46 M HNO_3 while this work used 0.5 M HNO_3. The largest difference was the working electrode's position in relation to the reference electrode.

One additional valuable report had pictures of both the flowcell used and an anodized glassy carbon electrode as opposed to written descriptions and computer generated diagrams.[28] The anodization is very difficult to represent in a photograph, however, this was the first visual of anodization past the written descriptors in previous work. From this image it was clear that the anodization was the defective portion of the methodology. Thus with a new set of parameters and knowledge of anodization, another round of experimentation was prepared.

Experimental Samples

Two sets of fluids were prepared for this experimental phase. One is a neat solution for overall performance testing. The other was an imitation urine sample. These both would be needed in characterizing the performance of the flowcell.

The former sample was made using Certified Reference Material 145 (CRM-145). This is a natural uranium sample which was certified by the New Brunswick Laboratory of the U.S. Department of Energy. It was combined with clean Optima® nitric acid (less than 10 pg/g natural U) for a 1.17 (±0.01) ng/g solution. Preparation of this sample was straightforward and merely required the CRM-145 and acid solutions to be homogenized by shaking and combined gravimetrically. The latter is a set of quality assurance standards acquired from the U.S. Department of Energy as part of the quality assurance program for bioassays across the various laboratories. The specifications for these samples are shown in Table 2. This set of samples contained both uranium loaded solutions and background blank solutions. They were designed to best mimic actual urine samples in elemental and isotopic composition.[12] The synthetic urine sample set consisted of eleven jars with approximately 17 grams of urine salts. These were then dissolved to a volume of 500 mL using 2% nitric acid. The sample set contained five background and six uranium spiked samples. The spiked samples had known levels of NIST traceable radionuclides. The known levels of radionuclides contained in Table 3 were experimentally verified by inductively coupled plasma mass spectrometry at Los Alamos National Laboratory in April of 2012. The synthetic urine specifications are included in Appendix C.

Table 2: Grams of Each Salt in Each 500 mL Synthetic Urine Sample

COMPONENT	g/sample
Urea (CH_4N_2O)	16.00
Sodium chloride (NaCl)	2.32
Potassium chloride (KCL)	3.43
Creatinine ($C_4H_7N_3O$)	1.10
Sodium sulfate ($Na_2SO_4 \cdot H_2O$)	4.31
Hippuric acid ($C_9H_9NO_3$)	0.63
Ammonium chloride (NH_4Cl)	1.06
Citric acid ($C_6H_8O_7$)	0.54
Magnesium sulfate ($MgSO_4$)	0.46
Sodium phosphate, monobasic ($NaH_2PO_4 \cdot H_2O$)	2.73
Calcium chloride ($CaCl_2 \cdot 2H_2O$)	0.63
Oxalic acid ($C_2H_2O_4$)	0.02
Lactic acid ($C_3H_6O_3$)	0.09
Glucose ($C_6H_{12}O_6$)	0.48
Sodium silicate ($Na_2SiO_3 \cdot 9H_2O$)	0.07
Pepsin	0.03

Due to extensive paperwork complications in obtaining approval to use donor blank urine as part of the plutonium bioassay program at Los Alamos National Laboratory as originally planned, the synthetic urine was deemed to be an appropriate substitute. These quality assurance synthetic urine samples were originally sent to Los Alamos National Laboratory to be analyzed for the certification of the bioassay program. Thus if they are adequate for an actual bioassay program, then they would be sufficient for the characterization of a novel bioassay approach.

Furthermore, if this work were to be certified as a process for actual bioassay samples, the procedure would need to be tested against a very similar set of samples. These samples had been stagnant for several months before being prepared for electrochemical analysis. The samples were homogenized using a magnetic stir plate

and corresponding magnetic bars. The stirring was done several times for at least one hour prior to gravimetrically measuring individual 0.l mL aliquot samples contained in 3 mL plastic test tubes.

Table 3: Synthetic Urine Uranium Concentrations

Sample	U Concentration (ng/g)	Uncertainty (ng/g)
DL51	1.24E+00	1.82E-02
DL52	1.24E+00	2.04E-02
DL53	1.23E+00	1.81E-02
DL54	1.23E+00	1.81E-02
DL55	1.24E+00	3.31E-05
DL56	1.23E+00	2.04E-02
BL1	1.32E-01	2.70E-03
BL2	1.38E-01	2.24E-03
BL3	1.41E-01	1.96E-03
BL4	1.40E-01	2.36E-03
BL5	1.45E-01	2.03E-03

Separations Testing

In addition to changing the protocols for the voltage for both anodization and separations, the size of the loaded samples would change as well. The overriding theory behind this was that the active sites of the anodized glassy carbon working electrode were being saturated. This could be doubly effective because anodization was not as thorough as desired with the previous procedure. But in order to move on, some characterization of the performance of the flowcell would be needed.

The initial tests of the new protocols and systems were promising. In contrast to the previous tests where almost no separation of the uranium was seen, vast improvements were seen in percent recovery. The first noticeable improvement was the

minimization of electrical overloads. With the apparent cause of the reference electrode becoming insulated from the system fixed, experiments were proceeding more reliably. The occasional overload occurred, but for the most part the experiments no longer were being interrupted.

The first variable optimized was flow rate. Several samples were run at various flow rates to observe the initial response of the system. The flow rate is a very important parameter as this determines residence time within the active volume of the electrochemical flowcell. Figure 18 shows five consecutive trials of 0.250 ng U CRM-145 samples at various flow rates. The accumulation voltage used was -0.20 V. The data contained in Figure 18 was from experiments on three consecutive days on one ICP-MS analysis. From these data points and other trials, fewer null separations occurred at lower flow rates. As a result, it was determined to focus on the lower flow rates and acquire tubing for the peristaltic pump capable of providing flow rates as low as 4 μL/min. But the elution phase of the experiment was left at a much higher flow rate. This was to ensure enough acid to completely wash out the flowcell as well as increase the shear force across the face of the working electrode aiding in removal of the separated uranium. Several samples were lost due to some issues of contamination as well. One sample registered 25 times the amount of expected uranium. As a result, everything involved in this process and the mass spectrometry instrument were cleaned to bring the uranium background levels back to nominal. It was not clear if the contamination was as a result of the electrochemical process or some cross contamination in the mass spectrometry laboratory.

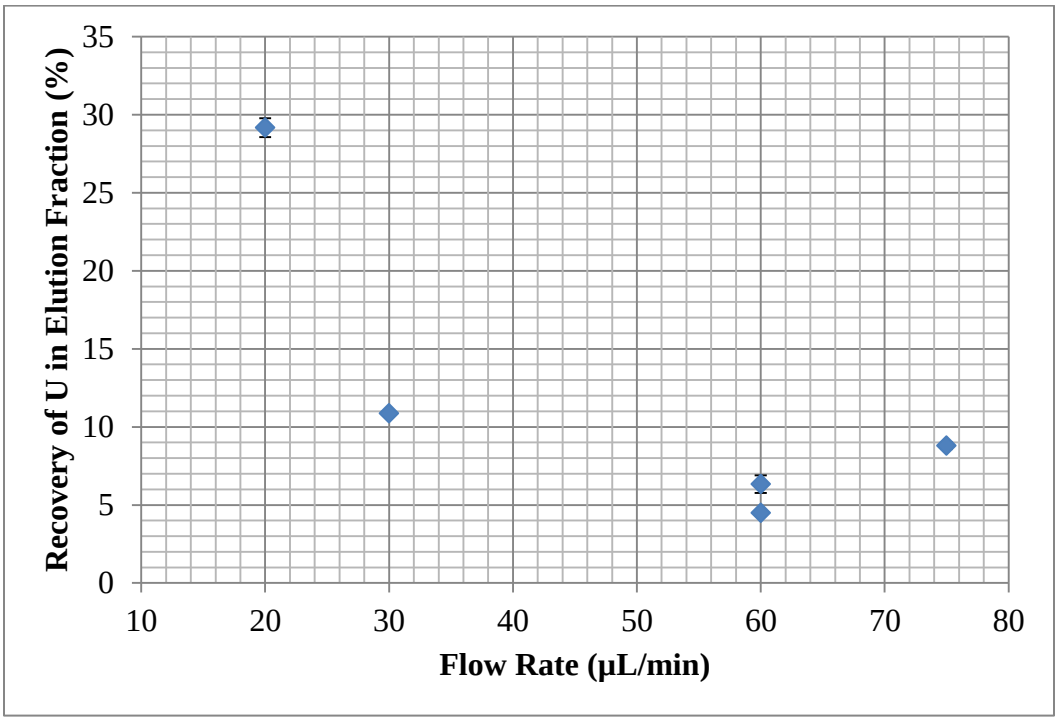

Figure 18: Initial Optimization Data of Percent Recovery vs. Flow Rate

During these optimization tests it was noticed that after dry down, the size of the residue has a correlation to the amount of uranium in each sample. Thus, pictures were taken of all the dried sample residues for a qualitative comparison which will be discussed in the results chapter of this work. Not only did the samples differ in size and color, but also in grain structure of the residue. These improved results were likely a result of the new anodization procedure as well as the new flowcell.

Lower flow rates were then used to test the apparatus. These on the whole were much more consistent than the higher flow rates. The lower flow rates did not have as many higher separation outliers, but the lower flow rate had many less non-effective

separations. The data from the lower flow rate separations using this geometry is shown in Figure 19.

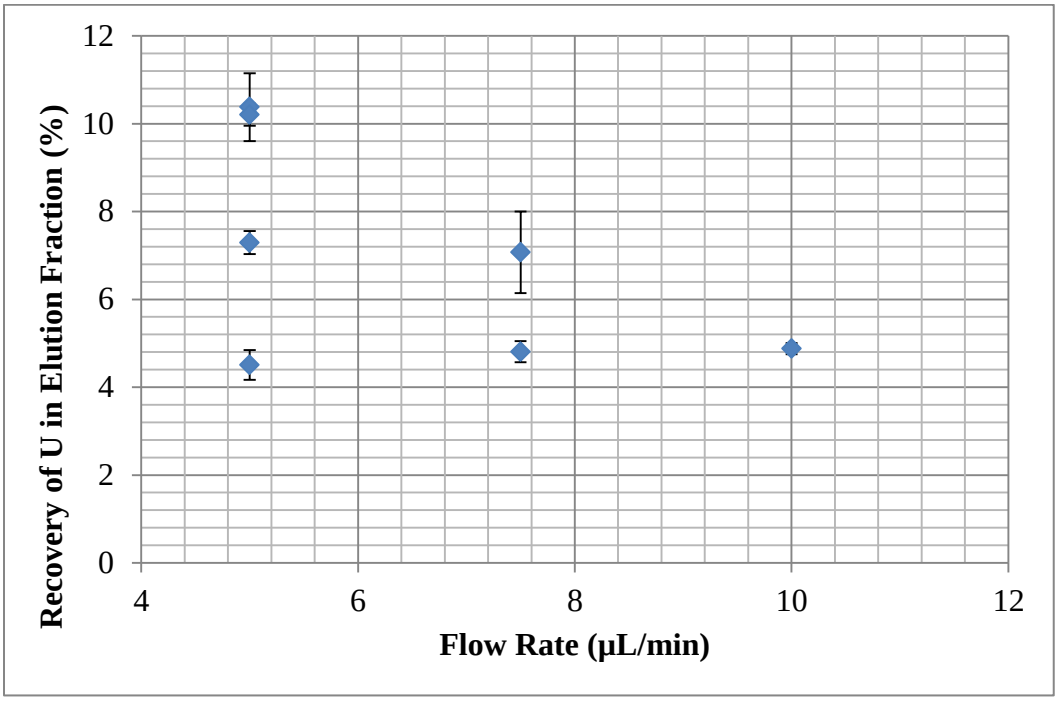

Figure 19: Low Flow Rate Separation Tests

Laboratory Flooding and Refurbishment

Following the initial successes of the new flowcell and geometry, an unforeseen flooding of the laboratory space occurred. This damaged the electronic components of the electrochemical apparatus as well as contaminated all of the equipment in the chemistry hood. Further, the water damage broke the clean room atmosphere inside the overall laboratory space which needed to be replaced. The ceiling providing the seal to keep unwanted contaminants from the laboratory environment needed the most extensive repairs. The potentiostat needed to be tested in order to determine its integrity

for further use. Fortunately, the potentiostat was not under electrical load during the flooding. After a series of diagnostics including dummy cells (known resistors of 1 Ω, 1.5 kΩ, 10 kΩ, 11 kΩ, and 30 kΩ) and internal component testing, the potentiostat was recalibrated and satisfactory for use. The rest of the laboratory restoration took ample time and several new components needed to be replaced including reference electrodes, Teflon® gaskets, and electrical connections. The computer controlling the potentiostat output was destroyed and unsalvageable. It was completely replaced. After a thorough cleaning and the replacement of the air filters, experimentation could resume. It is of significant note, that the flood water likely contained more uranium than was being analyzed in the samples so a less than adequate cleaning of the chemical hood would yield poor results.

Hydrodynamic Cyclic Voltammetry Scans (HDCV)

With the laboratory space ready to be used again, the optimization parameter testing could resume. The next parameter tested was the accumulation voltage. Since the various previous reports had some minor disagreement in the appropriate accumulation and elution voltages, finding the most appropriate voltage for this system would need to be a priority. In traditional electrochemistry cyclic voltammetry scans are done to find the appropriate voltages. In cyclic voltammetry, the working electrode's potential is cycled from one value to a higher value and back using a discrete voltage interval while the corresponding current is measured and recorded. The initial voltage in the scan is negative. For these scans, the top curve is measured first and then followed

by the bottom. The various scan rates were done in succession without polishing from the fastest scan rate to the slowest scan rate.

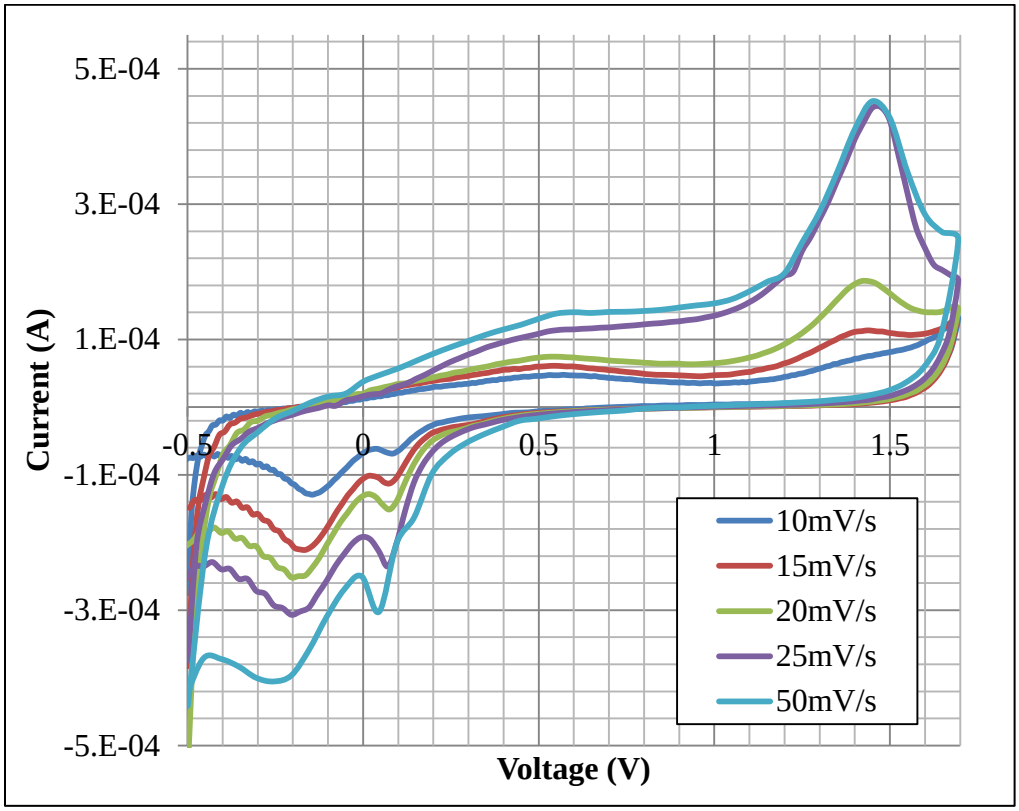

Figure 20: CRM-145 Solution Hydrodynamic Cyclic Voltammetry Scans at 5 µL/min

The optimal accumulation and elution voltages will be the local minima and maxima. However, this work is not a steady state problem. This work is done with a flowing volume. Thus a series of hydrodynamic cyclic voltammetry scans were taken using different voltage steps as well as flow rates (5, 7.5, and 10 µL/min) to investigate the electrical potentials needed to complete separation and elution. These were first done with the standard "clean" solution. The results of the 5 µL/min scan are seen in

Figure 20. The three flow rates provided very similar results. The voltammetry scans showed that optimal voltages for the clean solution should be set to +1.45 V for elution and -0.17 V for accumulation.

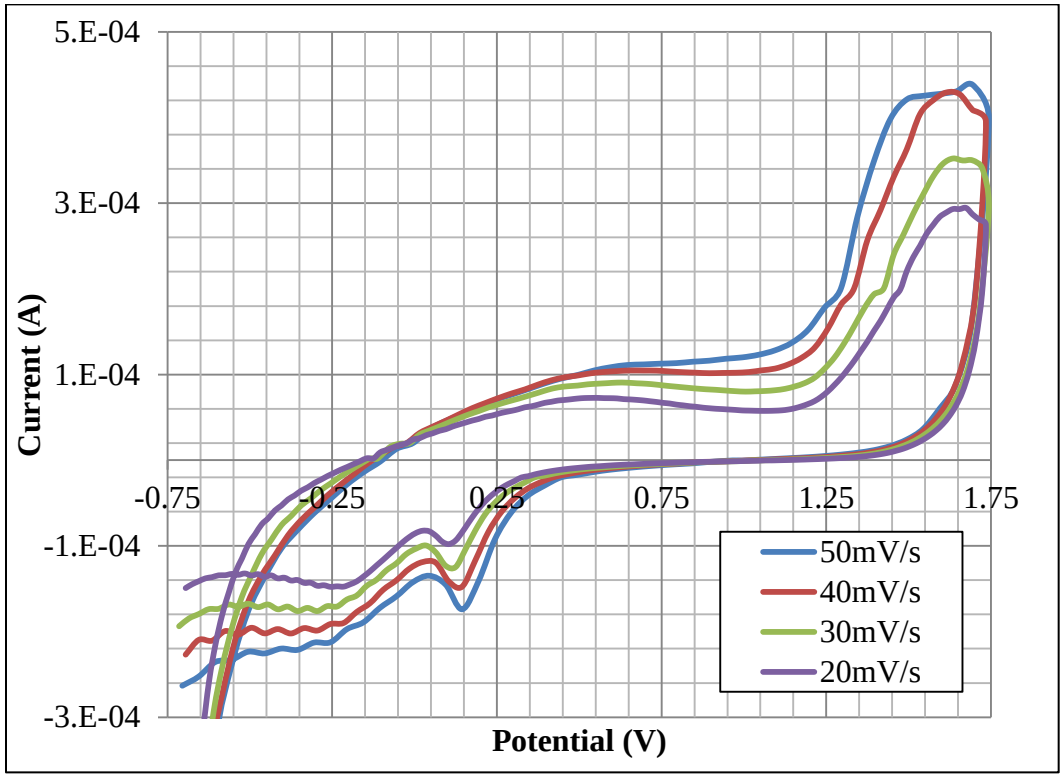

Figure 21: Synthetic Urine Hydrodynamic Cyclic Voltammetry Scan at 5 uL/min

In order to confirm the voltages for the synthetic urine separations, a similar set of hydrodynamic cyclic voltammetry scans were performed with a uranium-loaded synthetic urine quality assurance standard (DL51). The results from the synthetic urine hydrodynamic cyclic voltammetry scans are shown in Figure 21. These scans were similar to the "neat" solution, but these results had a few minor differences. Most likely these differences were a result of the potential matrix interferences within the solution.

Since the overarching motivation of this work is to investigate this electrochemical method with respect to the major urine interferences, these two graphs demonstrate the complexity added by the urine matrix. The synthetic urine scan showed that optimal voltages for the synthetic urine samples are an elution voltage of +1.64 V and an accumulation voltage of -0.22 V. These voltages are slightly different and would be tested with the synthetic urine separations experiments for confirmation.

The two scan setups yielded several similarities as well. There are two local minima in the accumulation ranges. This suggests that two separate accumulation actions could occur. Both minima could be results from uranium electrodeposition; however, one could be related to phenomena in the matrix solution. It is most likely a second uranium action related to another oxidation state of the uranium. Regardless, the voltages being applied during this work not electrodeposit uranium using that second mechanism at +0.13 V. But should this second action be a predominant separation due to the contents of the sample, it could negatively affect the separation fractions. The elution peaks are similar but not as defined in the synthetic urine sample in contrast to the very clean elution peaks in the neat solution. This is definitely due to the additional ions in the solution in the more complex synthetic urine solution. Both show a similar plateau near +0.5 V followed by a steep increase starting at +1.2 V. This is likely why the literature uses an elution step at +1.2 V. In order to cover the range of maximum elution, this work used a step increase beginning at +1.2 V and ending at 1.65 V. These scans were done to ensure that every possible uranium atom is detached or adsorbed at the working electrode during the collection and accumulation phases of the experiment.

Another significant characteristic of the system was discovered during these scans. The scans were done successively, and the working electrode was not polished and anodized between the steps. The successive scans started with the largest voltage step and proceeded to the smallest. It is expected that the larger steps would lead to larger amplitudes in the current. However, the degradation of the anodization (the fouling of the electrode surface) exacerbated this difference over the course of the scans and the clarity of the local minima and maxima reflect this process. The two elution peaks at the highest two scan rates for the clean test solution are likely a result of restarting the highest scan rate several times due to overload issues. This was noted during the scan but does not affect the information gleaned from the process.

The reason for performing so many different scan rates is to test the physical process for its reproducibility. In standard cyclic voltammetry, the reproducibility of an electrochemical reaction is good when the voltages of the minima and maxima at different scan rates are the same.[32] Ideally all of the scans should have matching voltage values when varying only one parameter (flow rate or scan step). The series of scans taken matched on local maxima and minima location. Even though these voltages are not exactly the same, the voltages are very similar number and support this accumulation and elution as being a reproducible process.

With the scans complete and a picture forming for testing various voltages for accumulation, an experimental test plan became clear. The rest of the samples to be run would consist of the synthetic urine samples to best understand the specifics of the performance in regard to complex matrices. Many additional synthetic urine

experiments were run in the following experiments. During this time, the ICP-MS instrument being used to analyze the separated samples needed significant maintenance. The ultimate issue was resolved with the replacement of the nebulizing equipment. A pool of fluid had collected in the nebulizer and several analyses across several projects were affected. During this maintenance period, another flaw in the flowcell design and apparatus was discovered and corrected.

Final Geometry Experimental Setup

While disassembling the flowcell and its various components for a thorough cleaning during the ICP-MS outage, a small amount of fluid appeared to be leaking from the bottom of the flowcell volume. Specifically, this fluid was leaking between the counter electrode and the flowcell base block. This was most likely due to an imperfection in the counter electrode disk. The disk had a minor bend in it most likely due to machining and thus was not completely flush against the flowcell face. This flaw had been previously noted. It was thought that the pressure from the quick release mechanism holding the working electrode to the face of the flowcell would compensate for this issue. Due to the amount of corrosion and oxidation on the back side of the counter electrode disk, this was a much bigger issue than originally thought. The corrosion was evidence that at least a portion of the sample was flowing behind the counter electrode and possibly not contacting the working electrode. This would significantly vary the performance of the system since the working electrode is removed, polished, and replaced between every successive experiment. There was no way to ensure the exact same pressure on the counter electrode disk between trials. Thus the

geometry would need to be altered once again. Further, two samples were passed through the system with no attempted accumulation and elution. Those two samples only recovered 75 percent of the expected uranium when analyzed on the ICP-MS further supporting an unaccounted mechanism removing uranium from the system.

Counter Electrode Geometry Refinement

After some lengthy discussions with several Los Alamos National Laboratory personnel from scientists to technicians, several alterations were designed for the flowcell to correct the geometry issue. The main issue relates to the counter electrode geometry. The easiest and most effective method of correcting this geometry issue would be to simplify the flow path of the sample through the apparatus.

Previously, the sample would have several materials interfaces to transit. By removing these transitions, the flow path behind the counter electrode would be removed. This was accomplished by creating a 0.047 cm deep channel in the face of the flowcell. This would extend from below the flowcell void volume created by the Teflon® gasket to above the top of the flowcell for electrical lead attachment which is a distance of 2.54 cm. The width of the channel was 1 cm and the platinum disk would be trimmed to fit exactly in the channel. This would create a minor gap in the corners of the channel – counter electrode. This gap would be filled using a silica two-part epoxy. Several different acid resistant epoxy resins are available commercially, and after an extensive conversation with a technical representative from Masterbond®, a suitable two-part epoxy was chosen to bond the counter electrode to the flowcell as well as fill any minor gaps on the face of the flowcell block.

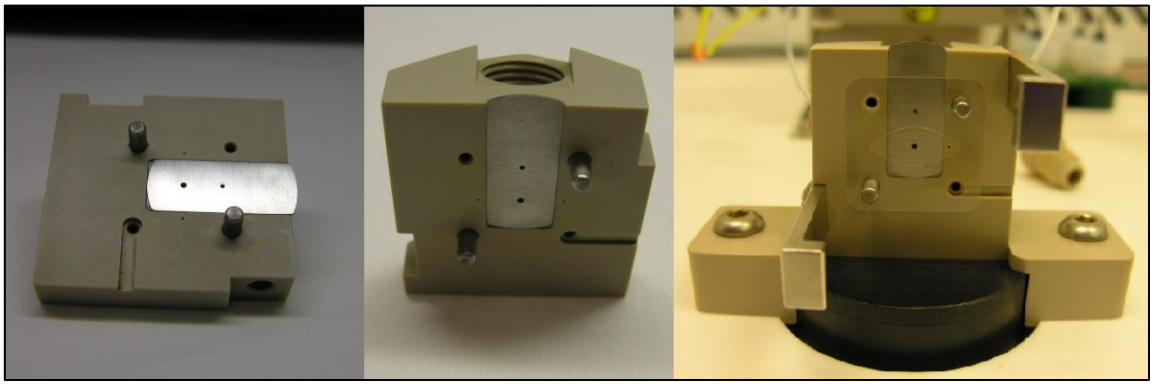

Figure 22: New Flowcell Geometry

The counter electrode disk would also need to be altered to fit the channel. The counter electrode also had some small holes remaining from the previous geometry. Those would not be near the active volume of the electrochemical cell and would also be filled with the same two part epoxy. While creating a new reference electrode port in the counter electrode strip, the port in the plastic flowcell block would also be enlarged two thousands of an inch. While attaching the platinum to the flowcell, a pin of the exact reference electrode port diameter was used to ensure the port remained clear. Since the interface between the various components of the flowcell face must be flush to avoid further leakages, the face of the flowcell was lightly sanded with 600 grit paper (after the counter electrode was attached). The resulting flowcell is shown in Figure 22. The ports were all checked visually and under the microscope. The resulting fit was impeccable.

Since the new counter electrode extended above the top of the plastic flowcell assembly, the complications of attaching an electrical lead to the counter electrode were put to rest. This small extension was less than two millimeters, but this was ample space

for an electrical clip to be attached to the disk. Several clips were tested, and a stainless steel with the most robust connection was selected.

Final Performance Testing

With the flowcell rebuilt, the testing and characterization of the system resumed. A large set of synthetic urine samples were prepared in the method discussed previously. These tests were completed over the various voltages determined in the cyclic voltammetry scans. A very small amount of fluid transited along the counter electrode – flowcell interface to the top of the working electrode assembly. As a result, some acid made contact with the counter electrode lead. This was easily fixed by wrapping the counter electrode lead with laboratory grade Parafilm®.

After these samples were tested according to the procedures in Chapter III, several trends were noted. The first of which was that the trials had a more consistent recovery. This recovery was better than the previous geometry, but it was improved as much as was expected. Additionally, the overall percentage of uranium detected in each set of samples increased. Previously, many of the samples were not yielding the total expected amount of uranium across the samples. But with the new geometry, the total uranium detected was much closer to the amount loaded in each sample. Further, the samples which contained the lowest levels of uranium had the best performance. This suggests that the electrode might be saturating with trace levels of uranium. A more in depth discussion of the experimental performance of the final system is found in Chapter IV.

CHAPTER III

PROCEDURE AND BEST PRACTICES

The experimental procedure for handling a single sample is quite involved and complicated. This procedure is a culmination of many trials and experiments which were discussed in Chapter II. Each experimental procedure helped build a final methodology and best practices which are outlined here. As a result, there are seven processes which all require significant attention and care to complete. The overall process takes about one day to complete per set of samples. This experimental procedure was done in batch mode instead of using an on-line instant analysis approach as was used in many of the works referenced in the literature chapter. This was due to available resources and limited availability of the ICP-MS for analysis. This batch mode does not reduce the overall analysis time as would be ultimately possible with an online immediate feedback setup. This is particularly noted due to increased wet chemistry preparation steps needed to prepare the samples prior to mass spectrometry analysis.

Experimental Preparation

As with any delicate experimental process, each step builds on the previous work. The preparation is of the utmost importance as improper preparation will spoil the results. This particular procedure is complicated and has many intricacies, any one of which could affect the overall performance of the system. The preparation of the glassy carbon working electrode is the crux of the entire experiment and its conditioning creates the uranium affinity this work exploits.

Electrode Preparation

The first step in performing one of these experimental procedures is to prepare the electrodes. This experimental setup uses three separate electrodes (reference, working, and counter/auxiliary) which have different preparation requirements. The reference and counter electrodes are fairly easily maintained and prepared; however, the glassy carbon working electrode is the most sensitive piece requiring preparation. Since the active sites and actual electrodeposition occurs on the face of the glassy carbon electrode, the working electrode was re-prepped between each set of samples. This preparation is designed to return the working electrode to a baseline clean state. Further, with prolonged use after preparation, it is common to see electrode fouling which can consist of deposited particles as well as reduced electrical response. This polishing is of extra importance due to the extraordinarily complex matrix of contaminants being reduced using the flowcell as well as to prevent any cross contamination between successive samples.[54]

Mechanical Polishing

The type of working electrode used will determine the proper polishing methodology. Since this experiment utilized glassy carbon electrodes embedded in plastic (acid resistant PEEK), that choice dictated mechanical polishing utilizing an alumina slurry. Diamond slurry polishing would destroy the surface of the working electrode by creating non-uniform gouges in the active surface area of the glass carbon.[54]

Bioanalytical Systems Incorporated (BASi) supplies polishing supplies with its glassy carbon electrodes. These polishing kits contain supplies for various types of electrodes, but the glassy carbon electrode polishing procedure requires only a portion of these. First, the electrode is rinsed with isopropyl alcohol (70%) and clean distilled water (18.2 MΩ-cm). A methanol or acetone rinse is not required after this polishing process because the alumina polishing slurry used is not oil based. However, rinsing with either methanol or acetone could be done to further ensure the removal of any polishing materials. These materials are shown in Figure 23.

Figure 23: Rinse Fluids for Before and After Mechanical Polishing

Then using a heavy glass plate with an adhesively attached microcloth polishing pad, alumina slurry and clean water is added to the pad. It is important to ensure that the polishing pad is attached without bumps or bubbles to create a uniform polishing surface. The polishing pad and slurry bottle are shown in Figure 24. It is important to

vigorously shake the alumina polish as it will separate after sitting for several minutes. If the slurry sits much longer than a few minutes, the suspended solids will become hardened and attached to the bottle. This can require up to five minutes of vigorous shaking. Ideally the consistency should and color should resemble that shown in Figure 24. The polishing pad can be used several times, but these pads accumulate dried polish which will need to be rewetted for each use. Similarly, rinsing the polishing pad can reduce the encrusted material and prolong polishing pad life. Ideally, the polishing pad will remain soft and velvety to the touch.

Figure 24: Polishing Stages (L to R): Polishing Pad, Slurry and Electrode; Applied Alumina Slurry; Polishing Face Down

The glassy carbon working electrode was then polished face down on the pad with smooth even motions. Polishing was done minimally for two minutes. The electrode was rotated 90° frequently (approximately every thirty seconds) to ensure uniform wear on the electrode. The mechanical polishing process is shown in Figure 25 as taken from a BASi polishing instructions guide.[54]

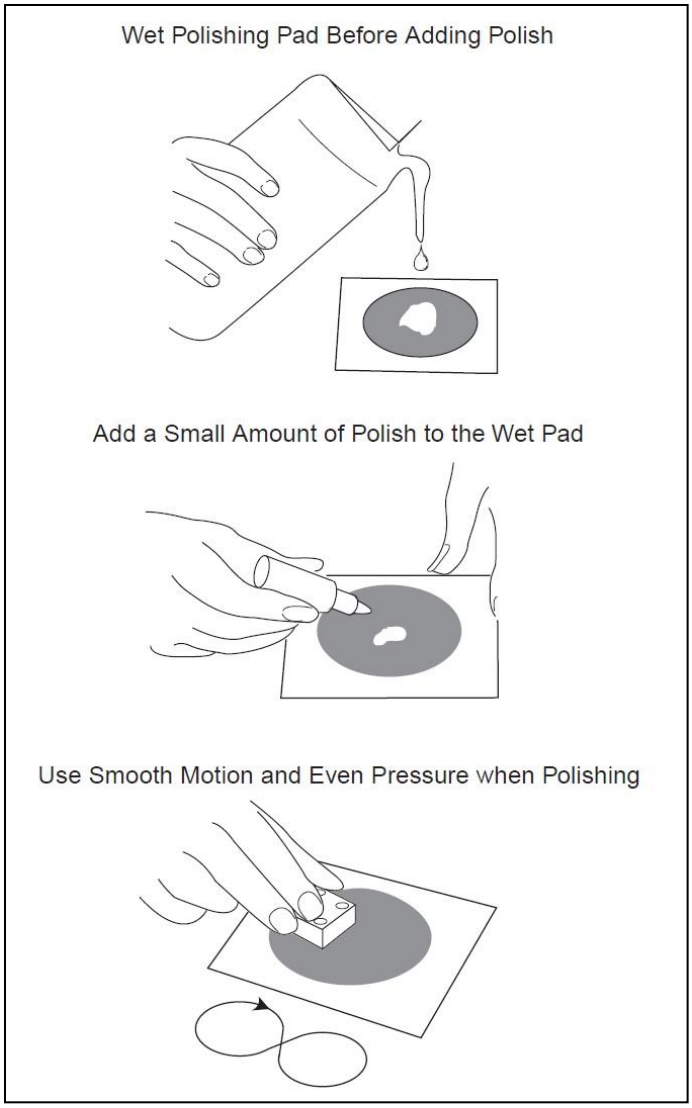

Figure 25: Mechanical Polishing Instructions from BASi[54]

Sonication

Following the mechanical polish, the electrode was rinsed again with isopropyl alcohol and clean water. The rinsing continued until all visual traces of white residue polish were removed. Following the rinse, the electrode was sonicated for up to five minutes in a low power ultrasonic cleaning bath. Sonication for longer than five minutes

could damage the electrode due to overheating. After sonicating, the electrode was rinsed again. The electrode will quickly air dry or can be dried using a clean room tissue. The face of the electrode was not dried manually, but fluid was occasionally wicked away with a tissue. To reiterate, the electrode surface was kept away from all objects including fingers to avoid any extraneous damage. Using a secondary container to hold the electrode during sonication ensured that the surface of the glassy carbon working electrode does not contact any other objects in the sonicator. Further, the secondary container kept any legacy contamination from the sonicator or other processes by creating a sterile environment within the sonciation bath.[54] This procedure is shown in Figure 26.

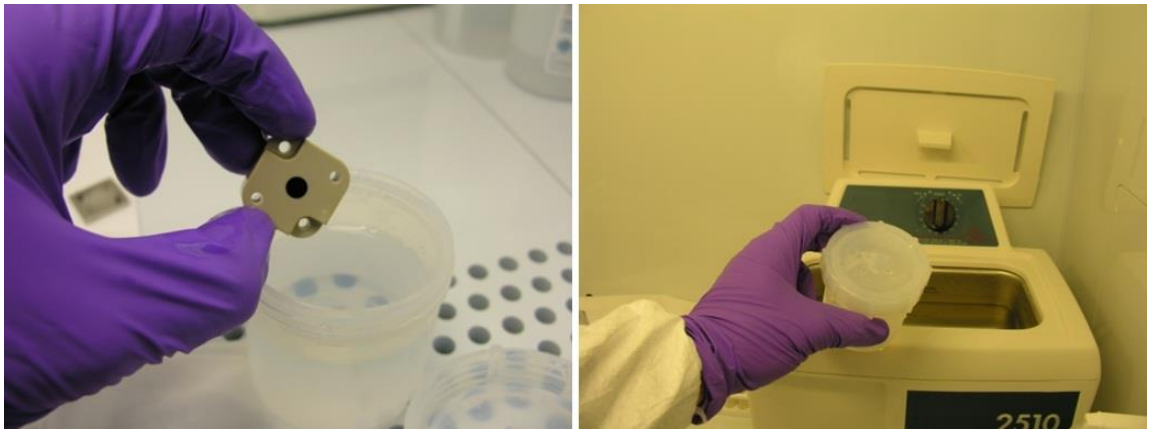

Figure 26: Sonication Capsule and Sonication Bath

The flowcell base tended to have residual sample contamination after several uses. In order to keep cross contamination between samples to a minimum, periodic cleaning of the flowcell was performed. The flowcell was rinsed and sonicated daily

when under heavy use. Also, rinsing and wiping the flowcell dry between samples was used to prevent cross contamination. Typically the flowcell was sonicated for at least 20 minutes, but sonication was extended up to one hour if there was any visual indication of contamination or residue. Similar cleaning procedures were followed after any machining of the base or components of the flowcell.

Collection Vial Preparation

In order to best ascertain the uranium composition of the sample fluids at all points of the experimental trial, various fractions were taken. Ideally, all fluid introduced into the system was collected. Some minor losses of sample were expected, but great care was taken to ensure these remained as small as possible. The different fractions were taken by collecting different vials of fluid on the outlet tubing. Each vial was manually switched during the appropriate experimental step.

The collection vials were 7 mm Teflon® vials with screw top enclosures. In order to prevent any leakage or accidental loss of sample, the vials were covered with Parafilm®. The outlet tubing was then placed through the covering. Four samples vials were prepared for every experimental trial. The vials were labeled using special makers designed for writing on Teflon®. The vials were labeled with the date, sample id, and the fraction designation.

Flowcell Assembly

After the flowcell and components were cleaned and ready for use in experiments, the entire flowcell was assembled. The flowcell base attached to a large plastic plate. This was attached with two plastic blocks and hexagonal head machine

screws to prevent the flowcell from tipping over while in use. In order to maintain consistency between experiments, the order and method of assembly was specifically followed.

Flow Tube Placement

Even though the tube placement seems fairly elementary, improper installation of the flow tubes can cause complete failure of the experiment. The best tubes for this specific setup were determined to be 0.13 mm i.d. three stop Tygon peristaltic pump tubing with flared ends (acquired from Thermo Fisher). The flared ends were incredibly important as the peristaltic pump tubing was attached to small lengths (approximately 4 inches) of hard Teflon® 0.20 mm i.d. tubing. These hard tubes were connected to the inlet and outlet ports of the flowcell using flangeless thumb screws. One millimeter of tubing extended past the thumbscrew in order properly seat the exit point of the tube as close to the face of the flowcell as possible. Improper connection to the inlet and outlet ports resulted in the loss of a sample. If the tubing extended too far past the end of the thumbscrew, then the end of the Teflon® tubing became pinched and impeded sample delivery or recovery.

Typically the peristaltic pump was attached to the stoppers closest to the flowcell on the inlet and outlet tubes. This allowed for the most flexibility in placement for samples and collecting vials. Further, the tubing between the pump and flowcell was not moved during the experimentation to prevent unquantifiable stresses on the apparatus.

The end of the tubing led to a small one inch Teflon® vial. These were used to collect the samples for analysis later. Keeping the tubing in the Teflon® vial was much

easier if the vial was covered with Parafilm® and the tubing was put through the Parafilm® to anchor it in place. This ensured no fluid was lost. Due to the trace amounts of uranium and small fluid volumes, even one lost drop could have had a significant impact on the experimental trial.

Teflon® Gasket

Several Teflon® gaskets were available from BASi for this type of electrochemical flowcell. These vary significantly in both geometry and thickness. The cross flow geometry was the most appropriate for the desired flow pattern based on this experiment. Two Teflon® gaskets were acquired for experimentation. The difference between these gaskets was in the thickness of the Teflon®. One had a thickness of 0.02 inches and the other had a thickness of 0.005 inches. The thicker of the two was most appropriate for this setup as minor surface roughness created minor cell leakage when the thinner gasket was installed. The thicker gasket had enough volume and compressibility to allow for water tight operation. The gasket was held in place by two metal pins which were on the diagonal of the flowcell. The Teflon® gasket can be seen in Figure 22 on the right side image.

Most experiments left a minor amount of liquid on both surfaces of the Teflon® gasket which was seen when disassembling the apparatus. This pathway could have potentially led to a loss of sample if not mitigated through proper assembly of the flowcell. In order to prevent this liquid from causing cross contamination between samples, the gasket was wiped with a clean room tissue between experimental trials.

Working Electrode

A polished and sonicated working electrode must be installed flush against the Teflon® gasket. The active side of the working electrode was 6 mm in diameter and glossy. The electrodes used in these experiments were acquired through BASi. They were modified by milling out the corners to accommodate the previous geometry. The electrode was installed such that a non-milled corner was on the upper corner of the inflow side. This helps reduce the amount of upper electrode leakage. An example of typical leakage during an experiment can be seen in Figure 27. This fluid will eventually be pulled back into the electrode flowcell at the completion of an experimental trial. Since this liquid droplet is present from the priming of the assembly with 0.5 M HNO_3 and does not change throughout the trial, it is reasonable to assume that this is a clean nitric drop and does not contain any sample.

After installing the working electrode, the backer plate was placed behind the working electrode. The two pegs on the backer plate were installed such that they are opposite the two metal pegs extruding from the flowcell face. In this particular flowcell, contact between the two sets of pegs probably does not have an effect on the performance of the system. However, in alternative setups where the flowcell and counter electrode are both machined from metal, an electrical short between the working electrode and counter electrode can be caused through the backer plate and flowcell through the pegs. This short would circumvent any electrical field being applied across samples introduced to the flowcell.

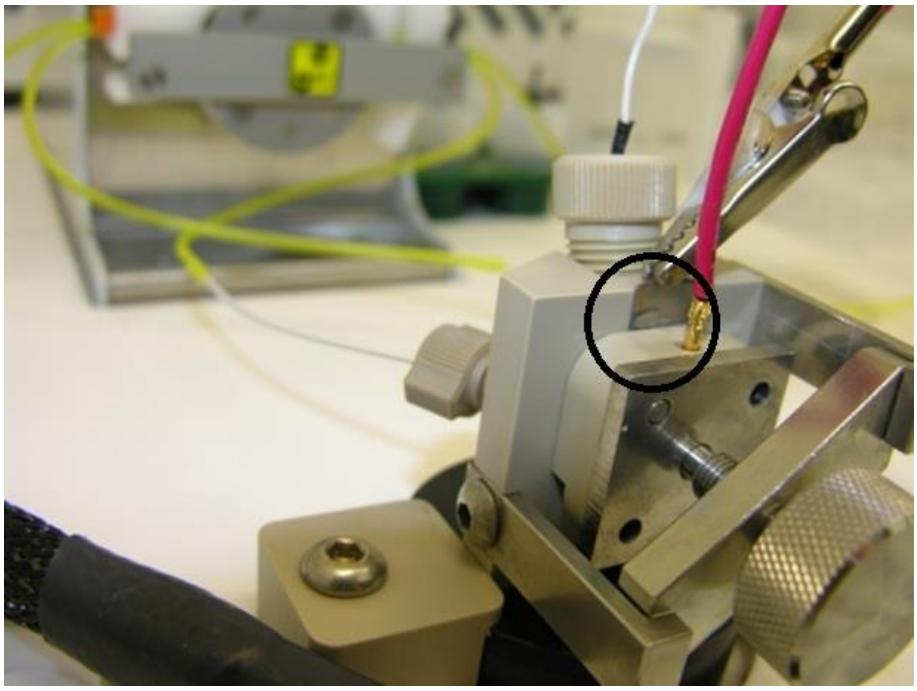

Figure 27: Typical Leakage at the Top of the Flowcell (Circled)

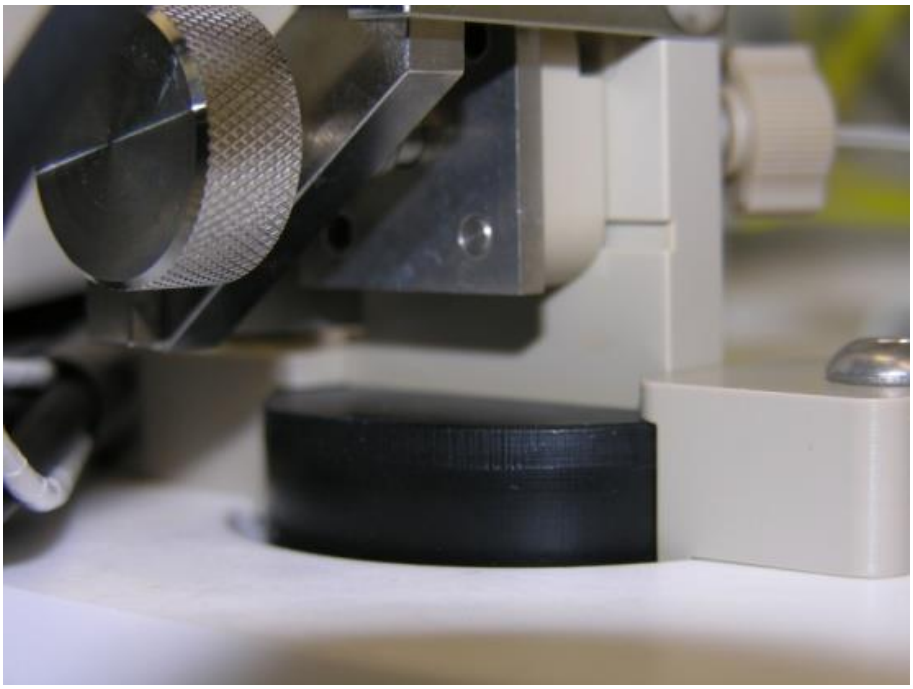

Figure 28: Area to Check for Improper Flowcell Assembly

Holding all of these pieces in place was a thumb screw and torque bar assembly. The thumbscrew was set in a divot on the back plate, and the torque bar contacts two arms attached the flowcell base. In order to ensure consistent pressure and sealing across the working electrode, it is advisable to tighten the thumbscrew as much as possible. This is typically not advisable in most instances, but if the assembly is not tightened properly, the flowcell will leak underneath the working electrode in the area show in Figure 28.

Reference Electrode

After the flowcell was been assembled, the tubes were primed with clean nitric acid. When priming the tubes and flowcell, it is important to only have the inlet portion of the pump/tubing assembly functioning. This can be seen in Figure 29. With the peristaltic pump, one section of the pump can be disabled by unhooking the plastic guide.

The priming of the tubing can be accelerated using the "max" setting on the peristaltic pump. The pump will fill the tube, flowcell cavity, and reference electrode port. The reference electrode port needs to fill with at least two millimeters of fluid in order to complete an electric circuit. The Ag/AgCl reference electrode was then inserted into the port. The black rubber O-ring was pushed into place by the screw-on collar. The progression of installing the reference electrode is shown in Figure 30. The O-ring and collar provide a fluid tight seal to the reference electrode. Failing to tighten this collar will cause air to surround the reference electrode during experimentation and thus an overload. The tightening of the reference electrode collar and the sealing of the

rubber O-ring will cause a small amount of the HNO_3 in the cell to force out of the small gaps between the Teflon® gasket and flowcell block. This was expected and can either be removed with a clean room tissue or allowed to remain throughout the experimental trial. It will be similar to the droplet seen in Figure 27.

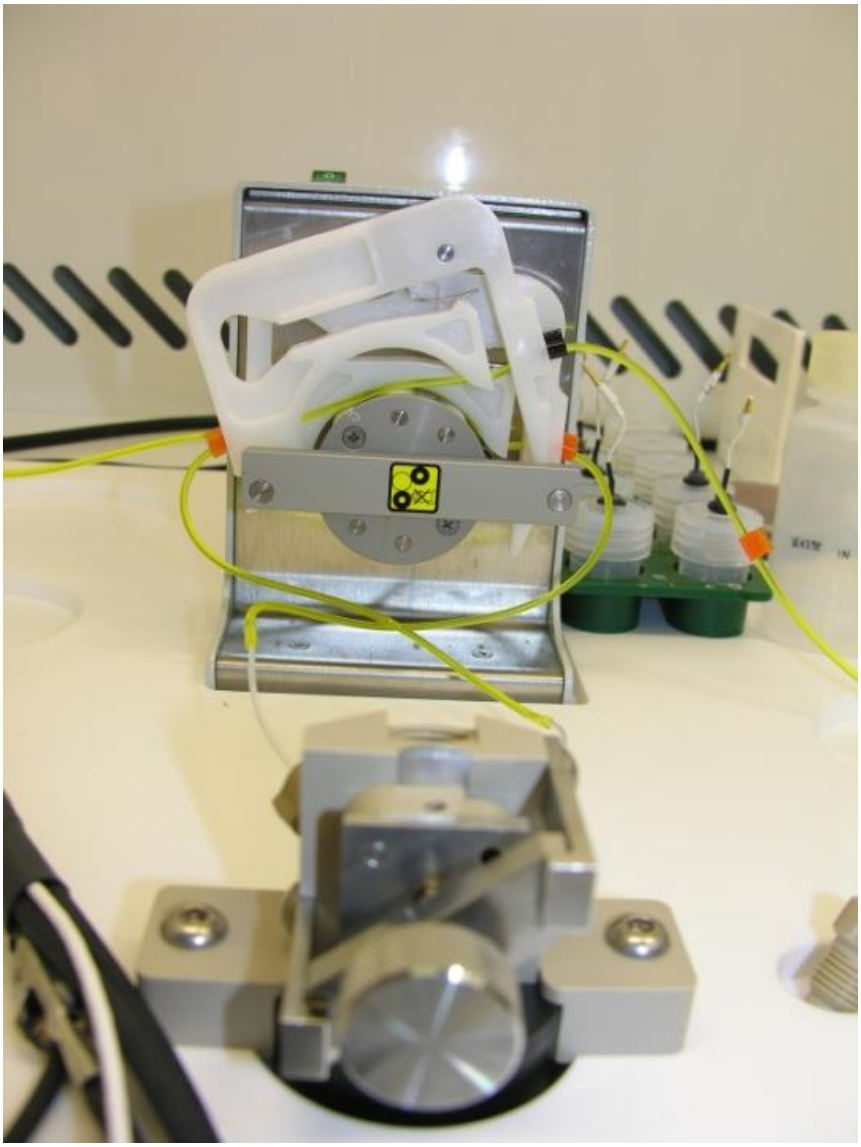

Figure 29: Peristaltic Pump with the Front Gate Open

The flowcell will not maintain the correct flow pattern without installing the second pass through the peristaltic pump. The second pass is on the outlet tubing side of the flowcell. This created a push/pull method to ensure uniform flow through the cell volume between the platinum counter electrode and glassy carbon working electrode. The installation of the second pump pass is shown in Figure 31.

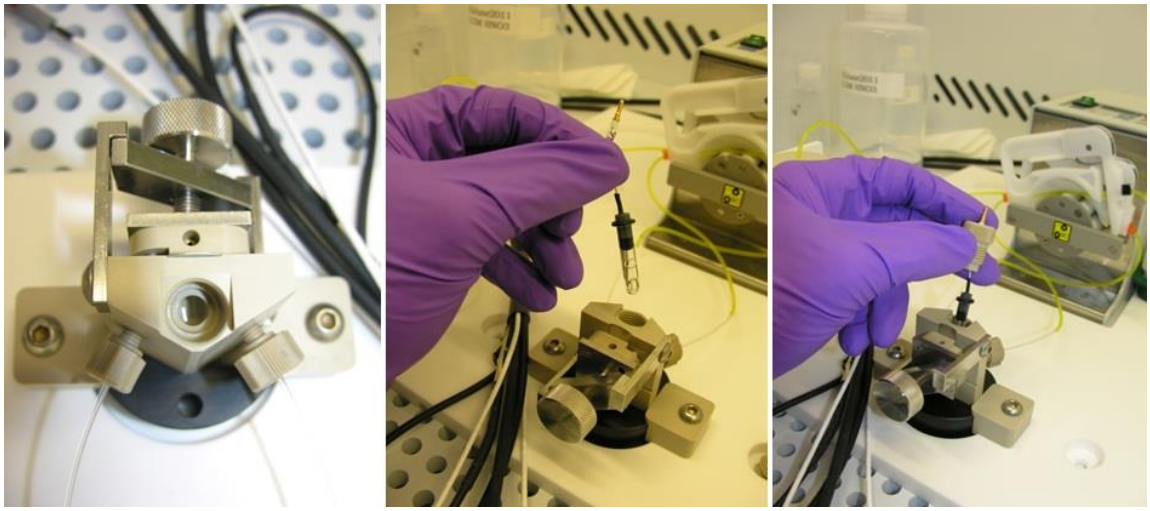

Figure 30: Placement of the Reference Electrode (L to R): Filled Reservior; Reference Electrode with O-ring; Retaining Collar Placement

The reference electrodes must be stored properly in order to maintain their electrical properites. The Ag/AgCl gel contained within the electrode can become stripped of chloride ions. In order to prevent loss of chloride ions, the reference electrodes were stored in 3 M NaCl solution. Additionally, the reference electrodes need to be suspended within that fluid. This was accomplished by utlizing 7mm Savillex Teflon® vials with ¼ inch holes in the lids. This allowed each reference electrode to

have its own 3 M NaCl bath to maintain its chloride saturation. The storage configuration is shown in Figure 32.

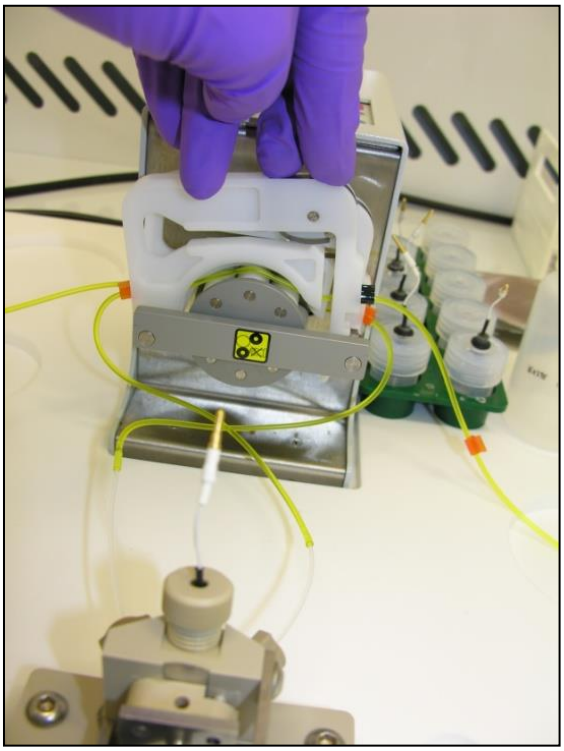

Figure 31: Attaching the Peristaltic Pump Front Gate to Complete Fluid Flow

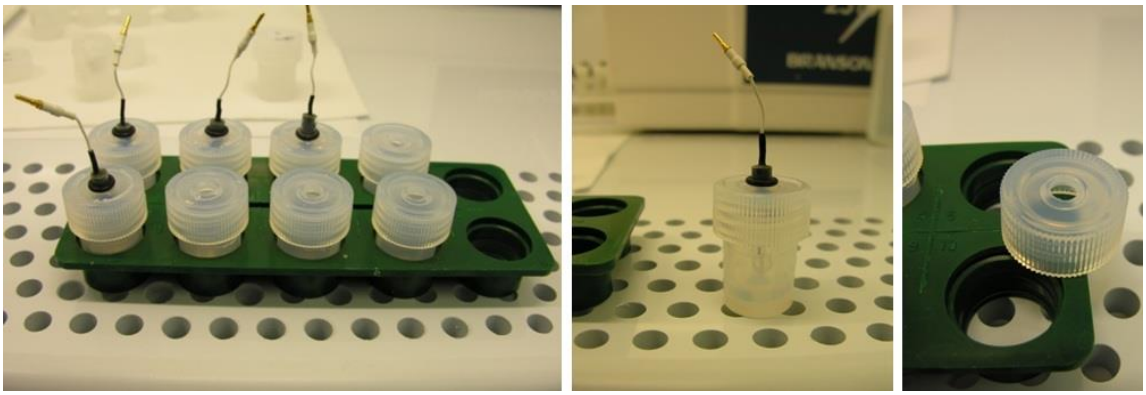

Figure 32: Proper Reference Electrode Storage in 3 M NaCl

Potentiostat and Electrical Attachments

After the previous steps have been followed, the flowcell was ready for attachment to the potentiostat. Since this experiment was a three electrode setup, multiple connections were made in succession. Prior to any connections being made, the lead for the glassy carbon working electrode was installed. The port and installation is shown in Figure 33. The lead was modified by extension with standard 12 gauge copper wiring to increase the available surface area to connect to the potentiostat as the standard lead is not long enough for two connections.

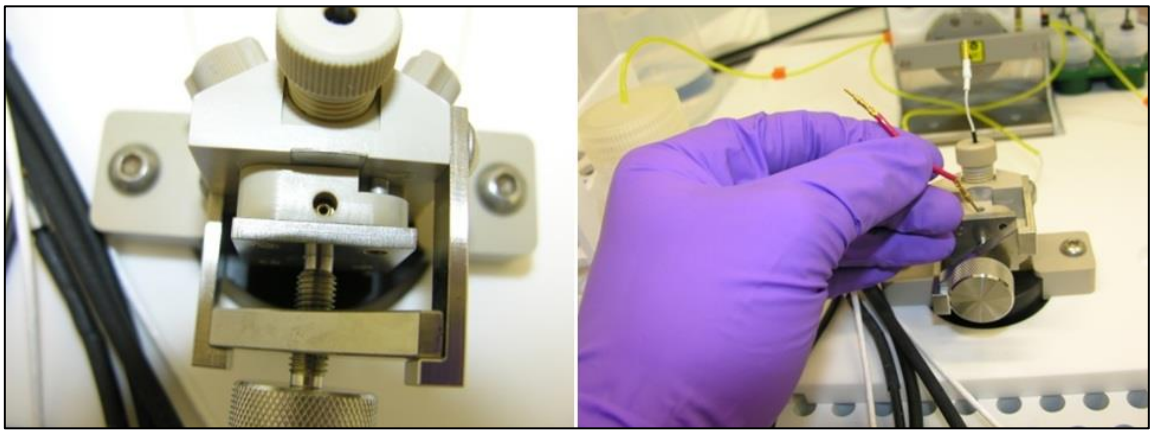

Figure 33: Working Electrode Lead Attachment

Before attaching any electrode leads to the flowcell, the potentiostat was powered on. With no attachments to the flowcell, the virtual voltammeter shown on the computer will have wild fluctuations in voltage between +10/-10 V. As soon as the electrodes were attached to the flowcell, the fluctuations stopped with the voltage slightly above zero. Attaching the electrical leads prior to powering the potentiostat can

lead to damage of the reference and working electrodes. The electrodes were attached in the following order and to the corresponding electrodes:

- Counter Electrode (RED)
- Working Electrode (GREEN)
- Sensing Feedback Electrode (GREY)
- Reference Electrode (WHITE)

The counter electrode clip was the most delicate. The surface area available for it to connect with the platinum strip is slightly smaller than 1 mm by 8 mm. This electrode lead can be wrapped in Parafilm® to ensure no contact with any acid droplets which have escaped from the flowcell volume. If some acid comes into contact with the counter electrode lead, some metal contaminates could be introduced to the samples including but not limited to iron, copper, silver, or nickel. In particular, contamination from leads comprised of copper led to dried down samples with a neon green hue. This Parafilm® wrapped connection is shown in Figure 34.

Next, the green lead was attached to the brass lead of the working electrode. Additionally, further up the brass lead, the grey sense lead was attached. Attaching these leads in an awkward configuration can cause the counter electrode to lose its connection. Altering the positions of the wires in respect to the red counter electrode lead alleviated this issue. The final attachment was of the white lead to the reference electrode. This set the baseline of currents from which all other applied voltages were measured. Typically, if an overload or issue arose during an electrochemical process, the reference electrode was at fault. If in doubt, the reference electrode was re-wetted. This was the

most common cause for failures and overloads throughout the experimental processes. Figure 35 shows the flowcell before and after attaching the electrical leads.

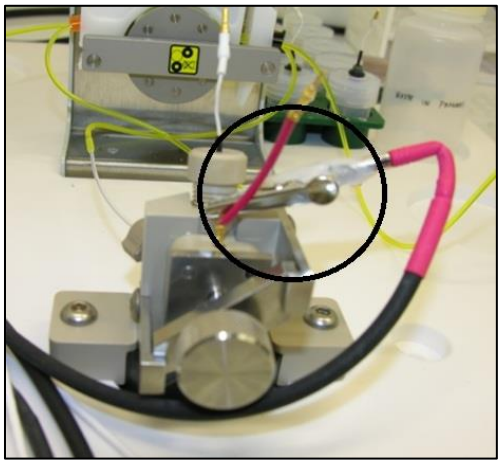

Figure 34: Counter Electrode Clip Covered with Parafilm®

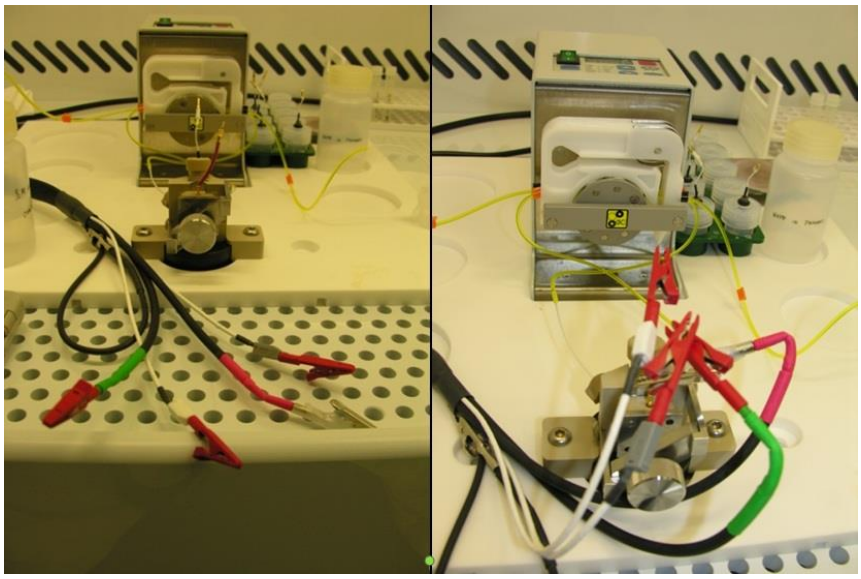

Figure 35: Flowcell Before Electrical Without Electrical Connections (L) and With Electrical Connections (R)

Anodization

At this point, the flowcell was ready for electrochemical experimentation. However, it was not ready for the separation of uranium from complex matrices. The working electrode must be properly conditioned to accept uranium. This process is anodization. The goal for anodization is to deposit a fairly uniform deposition of oxygen on the active sites of the glassy carbon working electrode. This deposition is believed to be fairly thin and no more than a few atoms in depth with the deeper depths seen at the rough blemishes on the face of the electrode. This oxygen layer creates the heavy metal affinity which allows the separations process to occur. Without proper anodization, all other steps are moot.

In order to create this thin layer of deposited oxygen on the face of the glassy carbon electrode, a square wave function was applied to the working electrode with the flowcell containing 0.5 M nitric acid. Throughout this process, the nitric acid was flowing at 30 µL per minute. The square wave was periodically applied to the working electrode in 40 second cycles. A voltage of +1.85 V was applied for 20 seconds followed by a rest period of +0.85 V applied for 20 seconds. The voltage and currents from a typical anodization are shown in Figure 36. Typically at least thirty cycles were applied to the working electrode to ensure uniform preparation of the working electrode. The minimum number of cycles to have fairly complete anodization was fifteen based on visual inspection of a series of anodized glassy carbon working electrodes.

The anodization current profile was very unique and consistent across anodization. The previous anodization step wave graph was modified to show the

specific anodization plateau in Figure 37. The rest portion of the cycles were removed, and a trend line showing the plateau of the final current measured on +1.85 voltage application was added. If the current was not moving toward a plateau as shown, then anodization was not complete and sufficient to provide the affinity for uranium separation as desired

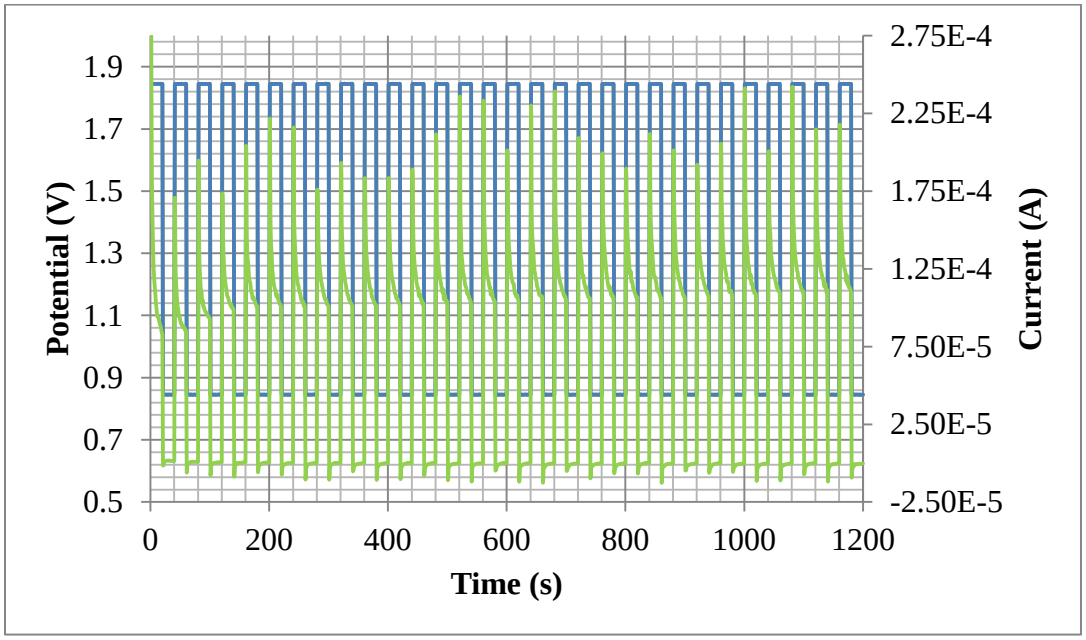

Figure 36: Anodization Stepwise Graph for 30 cycles (Voltage - Blue, Current - Green)

The quickest and most reliable indicator of complete and adequate anodization was visual. The anodized glassy carbon electrode would have a blue-green iridescence that was unmistakable. This was a difficult condition to document; however, Figure 38 shows the best available illustration of an anodized working electrode (left) next to a non-anodized working electrode (right).

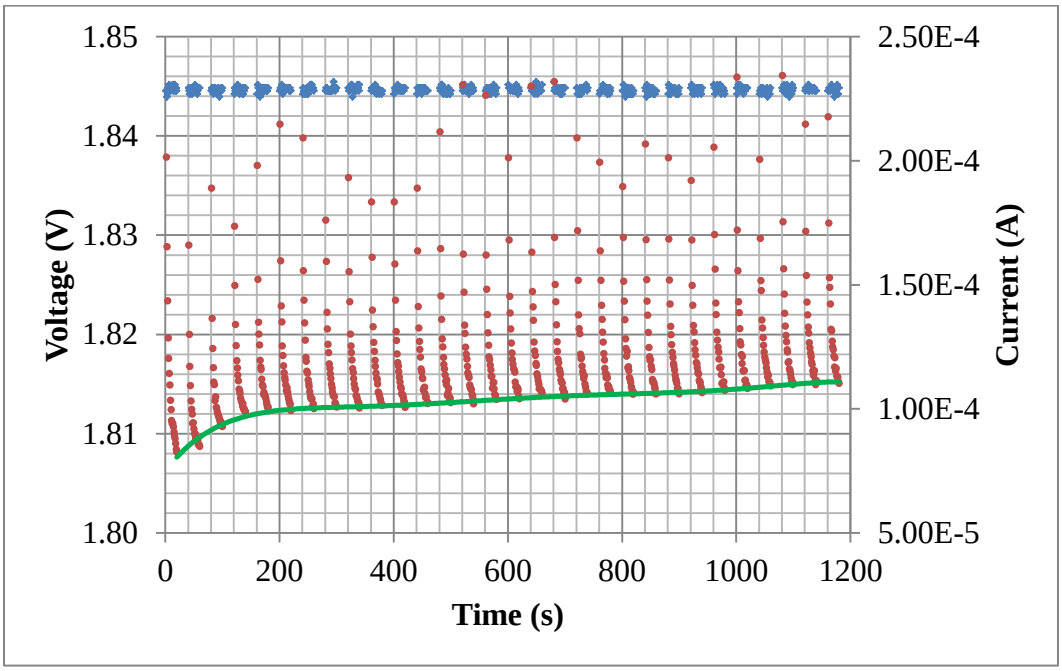

Figure 37: Anodization Stepwise Graph(Voltage - Blue, Current - Red) with Anodization Plateau (Green)

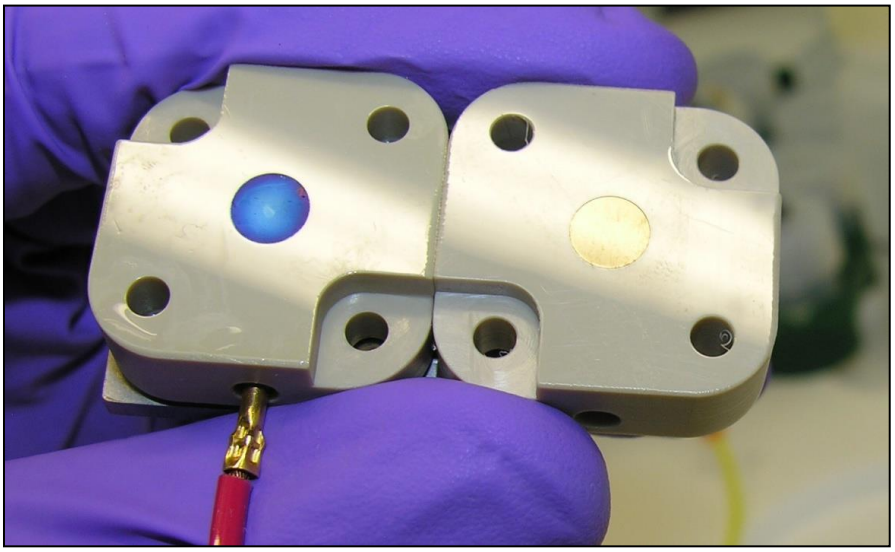

Figure 38: Anodized Glassy Carbon Working Electrode (Left) and Polished Glassy Carbon Working Electrode (Right)

In order to better understand the differences between an anodized and non-anodized electrode, an anodized (left) and non-anodized (right) electrode are shown together in Figure 39. These images were taken under an optical microscope. The images are approximately a 30 times magnification. The left image is a freshly polished and cleaned working electrode. The center image is an anodized electrode. The right image is an anodized electrode with deposited uranium from a synthetic urine experiment. The oxygen deposition appears as a cloudy film under the microscope. The right image is interesting because it shows that some of the anodization is lost when processing a sample. Thus when working on several samples consecutively, the working electrode was polished and anodized between experiments.

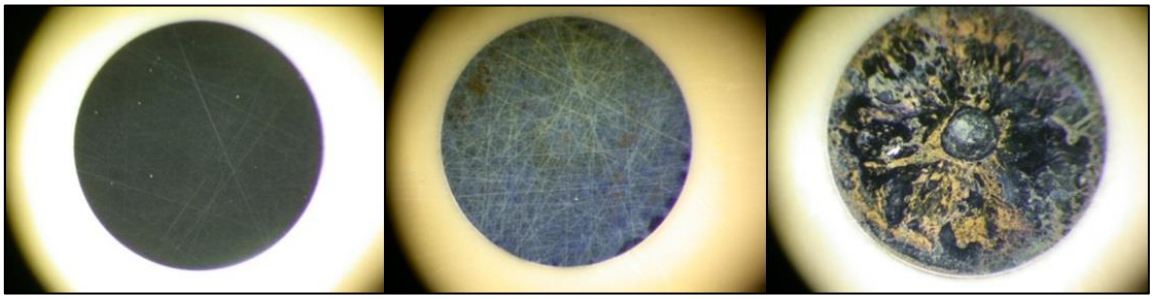

Figure 39: Microscope Pictures of the 6 mm Glassy Carbon Working Electrode (Left: Polished, Center: Anodized, Right: Uranium Accumulation)

Electrochemical Separations

Now with proper preparation of the glassy carbon working electrode surface, separations were done using the apparatus. Since the working electrode was checked visually, the flowcell was reassembled and all tubes primed. All fluids were collected to ensure continuity of knowledge for all uranium and effluent in the system. This

separations process would take some time and had several steps. Thus a digital timer was useful in tracking the various steps.

The selective separation of the uranium from the urine matrix happens when the appropriate voltage was applied to the anodized glassy carbon working electrode in the presence of the desired sample. From the literature, this voltage was between -0.15 V and –0.20 V.[30] Also, the elution of uranium from the electrode was above +1.20 V. Having several steps to higher voltages ensured complete elution from the electrode. All voltages are listed in respect to the reference electrode. Different reference electrodes had intrinsic voltages. It is important to note that the potentiostat used had a slight negative bias of 0.05 V. Thus this bias was accounted for when programming the experimental procedure on the computer.

Electrodeposition

If the working electrode was removed to visually check the anodization of the working electrode, it should be reassembled with the aforementioned procedure with nitric acid as the priming fluid. This was done at an accelerated flow rate of 60 µL per min to expedite the experimental procedure. After the flowcell was reassembled, the sample was primed into the flowcell assembly. The typical time to prime the front end of the apparatus was 5-6 minutes. This priming was done at the desired experimental flow rate (typically 5 µL/min). Thus, priming the sample for approximately three minutes before applying the accumulation voltage to the sample ensured that the first part of the sample reaches the flowcell right after the voltage stabilized. A digital timer, similar to the one in Figure 40, aided the tracking of changes to be made quite well.

Before priming the sample, the timer was set to count down for 13 minutes. Figure 40 also shows the input tubing placed in the test tube. The placement of the test tube was such that the tubing reaches the bottom of the test tube to adequately provide fluid for the entire sample. Some sample would remain in the bottom of the test tube, but this was addressed later.

Figure 40: 3 mL Test Tube for Sample Introduction and Digital Timer

After the tubing has been properly primed with sample, the potentiostat was activated to apply the desired accumulation voltage (typically -0.20V). The current took about a minute to stabilize after the voltage was applied. Typically the output was similar to that shown in Figure 41. At the same time as the voltage is applied, the collection vial was changed from Anodization/Before Blank (A/BB) to Flow Through (FT). This vial change buffer rinse time caused some blank to be contained in the FT sample, but since the chemicals are very clean; this additional blank in the sample fraction should have had very little impact on the uranium content of the FT sample.

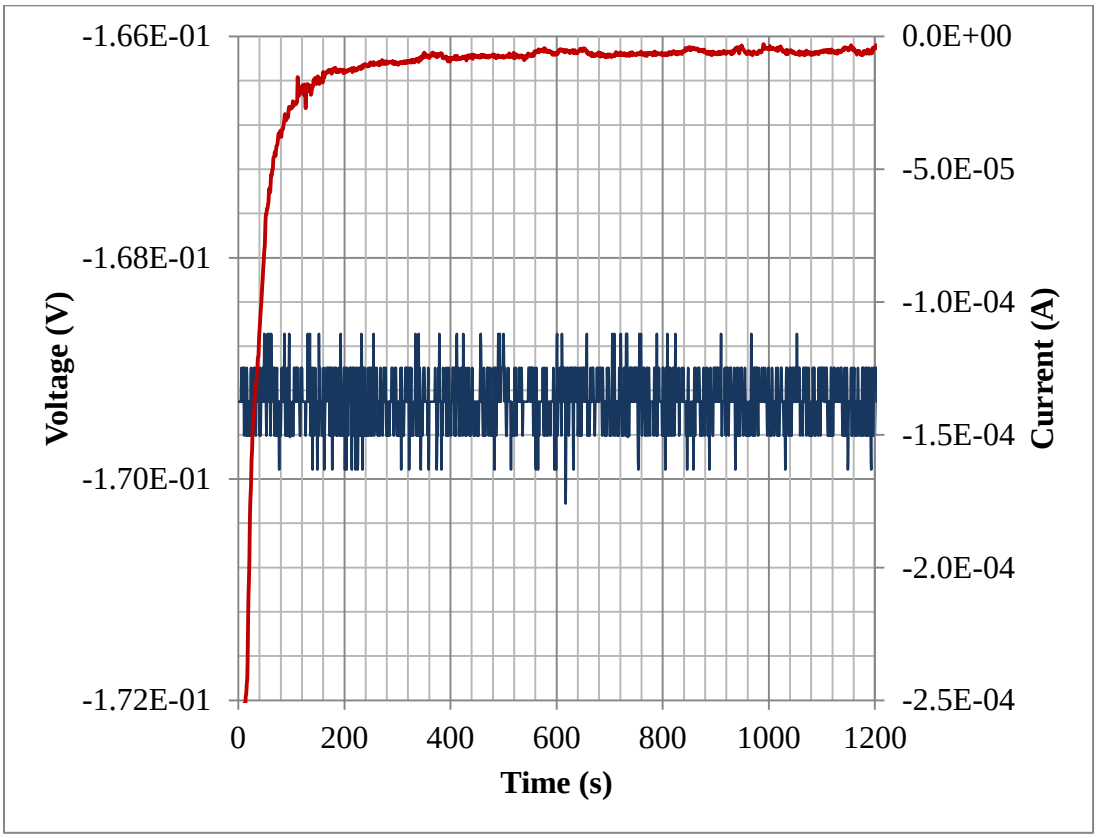

Figure 41: Uranium Accumulation Protocols (Voltage - Blue, Current - Red)

After the timer reached its 13 minute countdown, the sample input was switched to a clean rinse of nitric acid. The pump was briefly stopped in order to switch the tube. If the pump was not stopped, then an air bubble was introduced into the line. This would cause the flowcell to overload if the air bubble insulated the reference electrode from the electrical connection with the working electrode. Such an occurrence shut off the voltage and voided the experimental trial. Due to the programming used by the potentiostat, terminating the bias on the flowcell was the intrinsic safeguard to prevent destroying the electrochemical cell.

After the rinse had been introduced, a six minute rinse at the experimental flow rate provided ample time to purge the flowcell of sample. Then another three minutes of rinse at double the experimental flow rate emptied the back end of the apparatus. Next the flow rate was advanced to 60 µL/min. Each change of flow rate or sample took approximately 15-20 seconds to smoothly change the speed to avoid air bubbles. This change in pump speed gave added rinse time to ensure no contamination of the elution sample.

Elution

Now that the sample had been separated and the uranium sequestered onto the anodized glassy carbon working electrode, the voltage to elute the uranium was applied. This voltage was at least +1.2 V and was performed as a series of voltage steps. After the voltage had been advanced, the vial to collect the elution was changed. The elution vial contained some of the blank rinse acid. This blank rinse should also have been very clean and not affected the total uranium content in the elution sample. The cleanliness

of the rinse acid (in regard to natural U content) was confirmed by several unsuccessful separations where no detectable uranium was measured in the elution fraction. A typical elution voltammogram is shown in Figure 42. Each elution voltage step would last 120 seconds. The bulk of the elution was complete after the first 60 seconds, but some minor amounts could be eluted later. Additionally, the rinse which caught the uranium elution was ultra clean Optima® nitric acid and did not have any uranium contribution to the overall sample. After the voltage finished and the potentiostat cycled off, the input tube was removed from the rinse and air purged the flowcell and collected the final fluid contained in the apparatus. After the tubing was dry from pulling air through the apparatus (all of this fluid was collected in the elution vial), the electrodes were disconnected and either stored or cleaned. The final parameters for the experimental procedures are contained in Table 4.

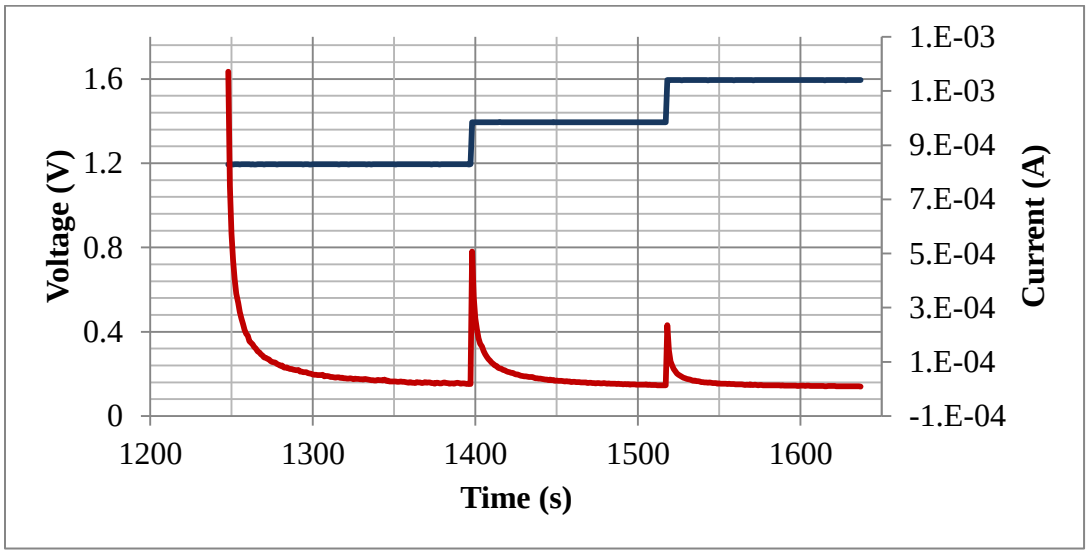

Figure 42: Elution Protocols (Voltage - Blue, Current - Red)

Table 4: Final Parameters for Electrochemical Procedures

Step	FR(µL/min)	Voltage	Time
Anodization	30	+1.85/+0.85 V	20 mins
Accumulation	5	-0.175 V	15 mins
Rinse	5	-0.175 V	6 mins
Rinse	10	-0.175 V	3 mins
Rinse	60	-0.175 V	1 min
Elution	60	+1.25/+1.45/+1.65V	6 mins
Rinse	60	0.0 V	5 mins
Remainder	n/a	n/a	1 min

The last step needed to finish sample collection was to collect the remainder. The amount of volume in the sample remainder was quite low, therefore, adding a small amount of nitric acid with a transfer pipet aided in the collection. This was placed in its own Teflon® vial for analysis on the ICP-MS. Additional blanks were occasionally collected between the aforementioned steps to confirm the cleanliness of the process; however, based on numerous methodology development trials, these four collection steps were sufficient for understanding the uranium distribution and separations of this apparatus.

Sample Analysis

In order to understand the effectiveness of the experimental conditions, the sample was analyzed on the mass spectrometer. However, due to various sample volumes and effluents, a series of wet chemistry processes were used to first normalize the samples. The idea in the analysis was to determine the total number of picograms of the uranium phase of the experiment.

Dry Down

The major overall difference between the samples was related to total volume. The Before Blank/Anodization samples were approximately 750 µL. The Flow Through samples were approximately 175 µL. The Elution samples were 500 µL. The Remainder samples were approximately 100 µL. Thus, normalizing these samples to the same volume was important to understanding the effectiveness of selectively separating uranium from the urine samples. In order to best accomplish this, the samples were heated to 100 ºC. The vials were placed in PEEK vial racks to transport them and ensure uniform heating on a standard laboratory hot plate in a fume hood. The dry downs took approximately 8 hours. This process was best run over night in order to ensure completeness. The dry down temperature was chosen to be 100 ºC in order to be on the threshold of the nitric acid's boiling point. Thus, no splattering and cross contamination of the samples should have occurred. Also, dry down for periods much longer than 8 hours did not affect the samples. For example, they did not burn if the dry down was much longer than 8 hours. While the samples were being heated, the caps were stored in corresponding order face down on a fresh piece of clean room lint free paper. This was to eliminate the potential for contamination to be introduced via recapping from any particulates in the air. This was important due to the minute quantities of uranium being analyzed, and the multi-user nature of the facility. This setup is depicted in Figure 43. A set of samples in a heating block is shown in Figure 44.

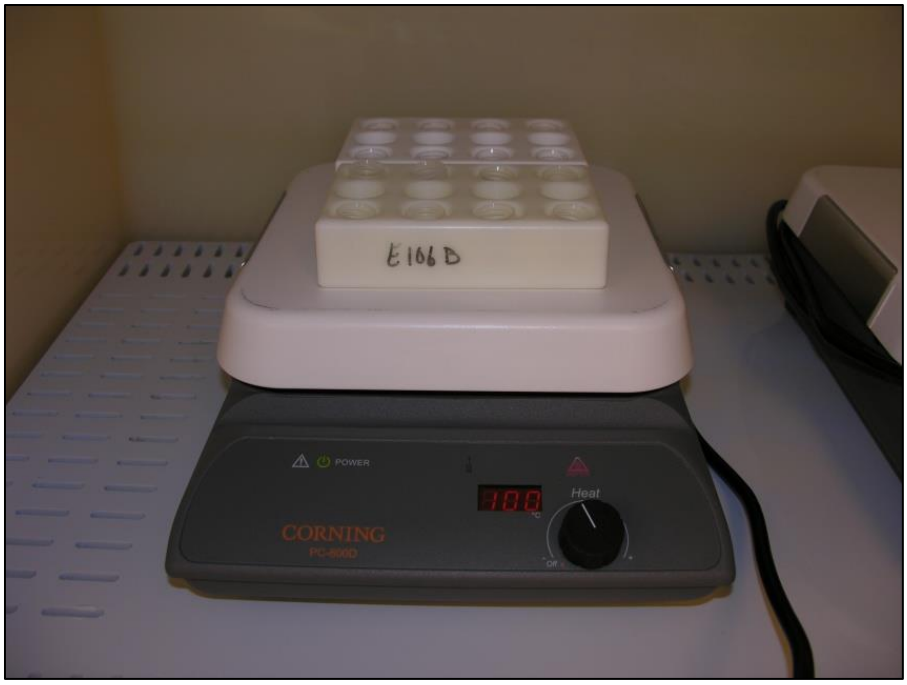

Figure 43: Samples Drying Down on a Hot Plate in a Vented Fume Hood

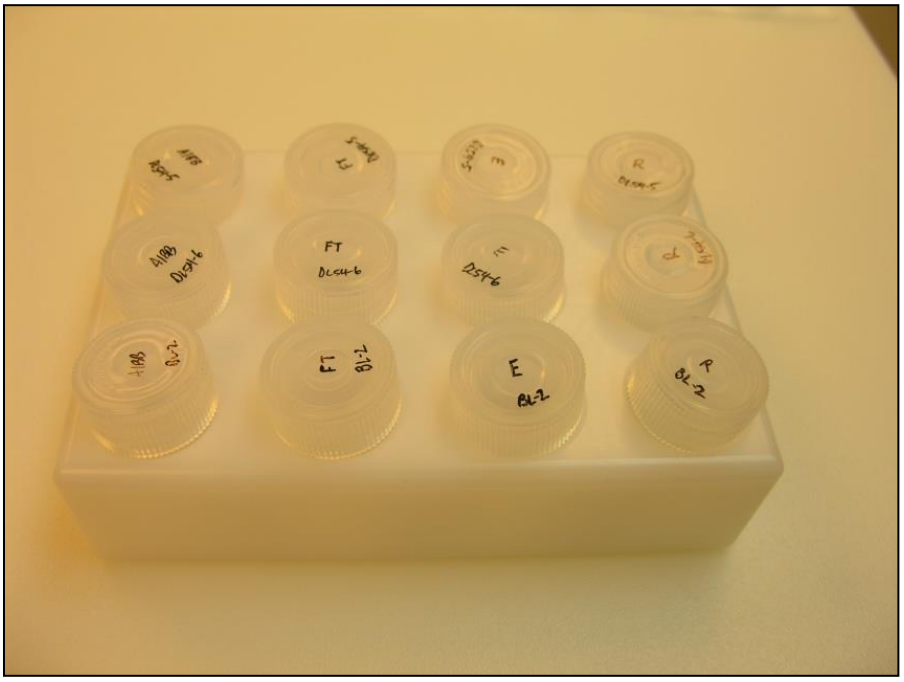

Figure 44: Samples (with Caps) Waiting to Undergo Dry Down

After the samples had dried down, the residue was crystalline in structure and had a visual indication of how much uranium was in each sample. Figure 45 shows the visual indicators of the samples after dry down. The rough amount of sample was seen in each vial. These particular images come from sample DL56-6 which had a 17.9 percent recovery based on ICP-MS analysis.

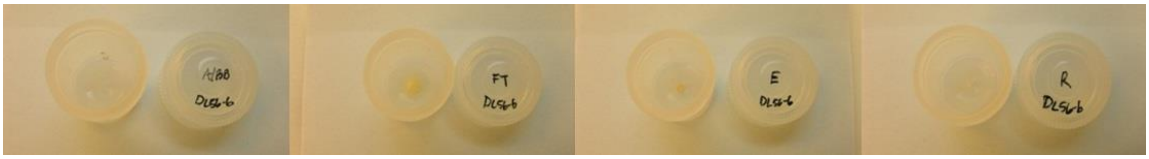

Figure 45: Dried Synthetic Urine Samples (L to R: Anodization/Before Blank, Flow Through, Elution, and Remainder)

Figure 46 contains microscope images of the same DL56-6 samples. These microscope images show the differences in structure of the residues. Qualitatively, a significant amount of the matrix was reduced from the Flow Through sample to the Elution sample. All of the samples were still largely crystalline in nature, but the amount of salt clearly was significantly larger in the Flow Through sample as compared to the others, which was a desired effect of the experiment and was visualized prior to analysis using the ICP-MS.

Re-digestions

The dried down samples cannot be analyzed on the ICP-MS. First these were re-digested or re-suspended. In order to ensure normalization of the samples, each was re-constituted to a volume of 2 mL using 2% Optima® nitric acid and recorded gravimetrically. This served in the analysis phase to calculate the total amount of

uranium present in the sample from concentrations determined on the ICP-MS instrument. The setup used to re-suspend the samples is shown in Figure 47.

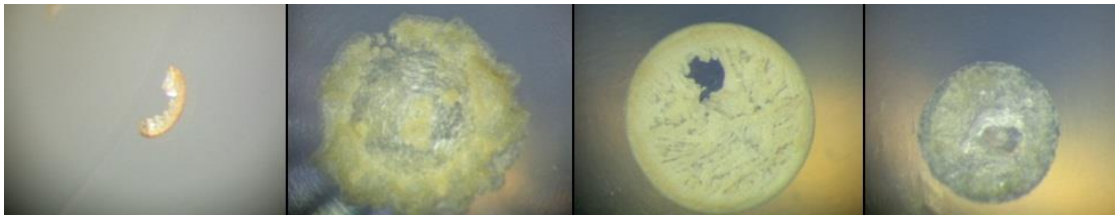

Figure 46: Microscope Images of Dried Synthetic Urine Samples (L to R: Anodization/Before Blank, Flow Through, Elution, and Remainder)

Figure 47: Calibrated Scale and Pipet in the Wet Chemistry Laboratory

After replacing the cap, re-digestion was accelerated by vigorously shaking the vial. The re-digestions were visual to the naked eye. At least one hour was allotted for the re-digestion to be complete. Several vigorous shakes of the vials during that time period helped the process but were not necessary. After the re-digestions were completed, the samples were transferred from the Teflon® vials to test tubes for analysis

on ICP-MS. The samples were either pipetted into the tubes or they were poured. As long as the sample was transferred in its entirety, the transfer mechanism did not matter. It was customary to also label the sample test tubes to keep them organized as they were transferred several times between sample racks before final analysis by mass spectrometry.

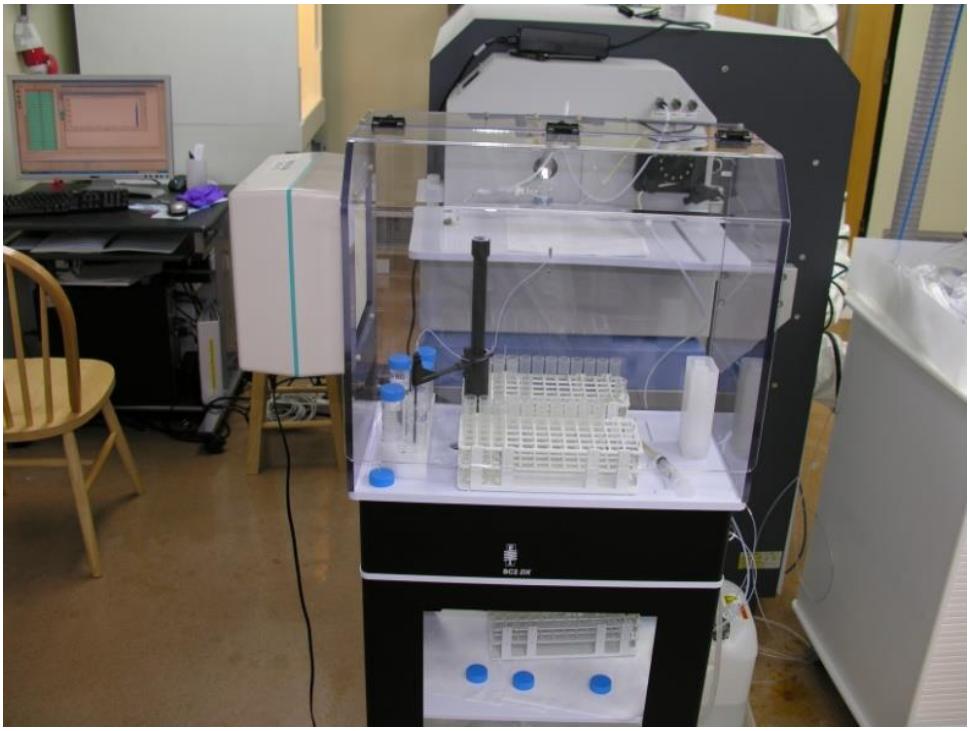

Figure 48: ESI Auto Sampler Connected to Thermo Element XR ICP-MS at Los Alamos National Laboratory

Mass Spectrometry Analysis

The samples were analyzed on a Thermo Element XR single collector ICP-MS. This particular ICP-MS was equipped with an auto-sampler to aid in the analysis of large sample batches. The detection limit of this instrument and the particular setup being

maintained at Los Alamos National Laboratory was approximately 1 pg. The instrumentation and auto sampler can be seen in Figure 48.

The testing methodology for these particular samples, due to their expected composition, was a low resolution scan of five different isotopes including U-238, U-236, U-235, U-234, and U-233. Each sample was scanned 15 times which took approximately 17 s in total. Since all samples analyzed were specifically natural uranium, U-238 dominated the measured spectra. Due to the high salt matrices of the samples, drift was expected throughout the analysis runs. This was quantified and corrected using a three standard method comprised of natural uranium standards on par with the expected sample uranium concentrations every ten samples. To further reduce the drift of the instrument, long rinse times were used to help keep the buildup of salt residues to a minimum. Traditionally on this instrument, rinse times were 200 percent of the sample take up time; however, 300-400 percent rinse times improved the precision of the instrument. The rinses were two staged and consisted of a 10 percent nitric acid and 0.1 percent hydrofluoric acid rinse followed by a 2 percent nitric acid rinse at equal intervals. In addition, acid blanks were run between every sample of the 2 percent nitric solution used during re-digestion. The nebulizer and front end of the instrument is shown in Figure 49. The glass nebulizer was routinely switched out to reduce sample build up and fluid sequestration. This particular instrument had issues with fluid buildup in the nebulizer. This complication resulted in several batches being destroyed.

After the analysis was complete, the data was downloaded and analyzed using a standard isotope dilution spreadsheet. The method used three known uranium standards

run in succession between every ten samples to create a concentration regression. Then after subtracting the average of blanks before and after each run, the concentrations of each uranium isotope were calculated using the regression. The last step was to volume correct each of the samples to find total uranium content in each portion of the fluids. This was an adaptation of a standard analysis done at Los Alamos National Laboratory.

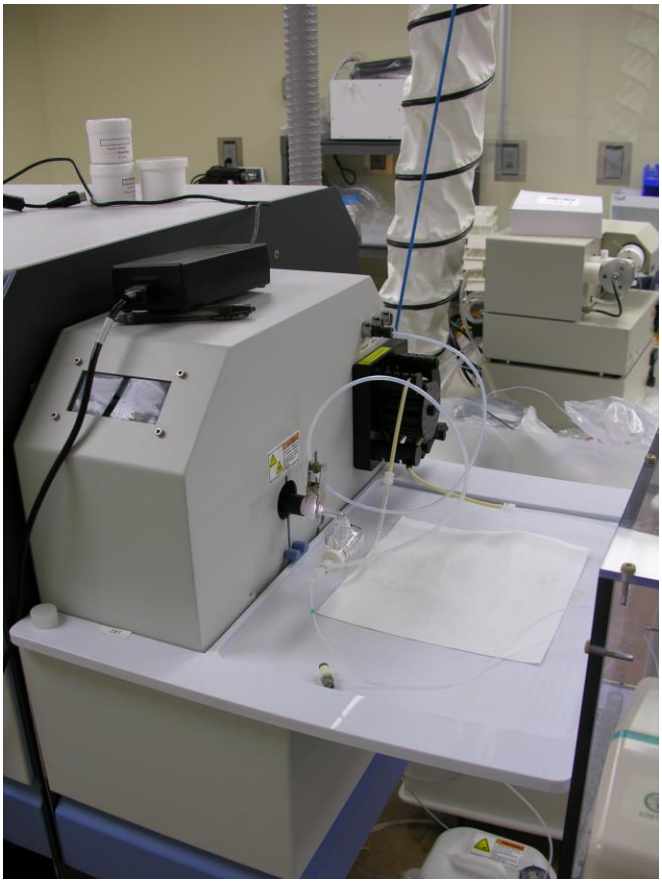

Figure 49: Nebulizer and Input for a Thermo Element XR ICP-MS at Los Alamos National Laboratory

CHAPTER IV

EXPERIMENTAL PERFORMANCE AND RESULTS

Over the course of several months, numerous samples were prepared and analyzed using the previously discussed procedures. The results of these experiments varied. As was discussed in Chapter II, several modifications were made to the procedure as well as the geometry over the course of experiments. The data has been grouped and ordered into sections according to the development of the experimental procedure and apparatus. Both quantitative and qualitative analysis was performed on these samples.

The samples being separated and tested were in line with the standard natural uranium solution and synthetic urine solutions discussed previously. They were made using ultra clean laboratory acid. The samples were tested on a Thermo Element XR single collector Inductively Coupled Plasma Mass Spectrometer. The mass spectrometer is maintained by the Chemistry – Nuclear and Radiochemistry group at Los Alamos National Laboratory. It is housed in the clean room facility at Technical Area – 48. The ICP-MS lab is a class 10,000 clean room facility. A standard ESI glass nebulizer was used on the front end of the machine. Sample introduction was through an ESI auto sampler. All of this equipment is maintained by a certified technician on staff at Los Alamos National Laboratory. Initial sample analyses were done under supervision by the technician, but later analyses were done independently when the instrument was available.

Separation Results

There are no appreciable results to share from the initial commercially available geometry since all five trials resulted in less than one percent separation. The total mass of uranium recovered during these trials was less than later experiments despite the initial sample loadings containing more than forty times the amount of later trace analyses. The results of separations experiments are presented using a simple percent recovery equation. The percent recovery was calculated using

$$Recovery = \frac{m_{Elution}}{m_{Elution} + m_{FlowThrough} + m_{Blanks}} * 100$$

where m is the mass of the appropriate sample fraction. The ICP-MS instrument blanks were taken into consideration when reducing the data from the instrument. The data reported in the following figures is the recovery of Elution sample fraction. This is the desired fraction in which recovery should be seen. Typically the background was near the minimum detectable limit. The acid blank used on the instrument was the same batch of acid used throughout the entire experiment for both digestions and rinses. As a result, the mass in each sample was not corrected for an additional uranium background. However, a blank was included in each trial to ensure that no extraneous uranium contaminated a set of samples. For typical blank acid results, a 750 µL blank sample (processed in the same manner as the other samples) was measured to have 0.001 ± 0.000 ng uranium which is the equivalent concentration of 1.3 pg per gram which is much less than one percent of the samples being examined. The amount detected in that sample is the minimum detectable limit (mdl) of the ICP-MS instrument used for these analyses. A typical uncertainty in each sample measurement was less than one percent

and is indicated by the error bars in the figures. Each measurement uncertainty is available in the data charts contained in Appendices D and E.

Custom Geometry

Some of the data points were shown in Chapter II for reference in justifying methodology and geometry refinements. That was only a portion of the available data. The initial custom geometry was used to test 21 clean solutions spiked with natural uranium. Another 20 synthetic urine standards were tested using this geometry. Several other samples were disregarded due to a contamination issue in the ICP-MS instrument. Eight sample sets in all were selectively excluded from this data due to those issues.

CRM-145 Standard

The two main variables being tested using the custom flowcell were flow rate and accumulation voltage. The flow rates were varied from 100 microliters per minute to 5 microliters using the two different accumulation voltages taken from the literature. The recovery increased as the flow rate was decreased. This increase is likely due to increased residence time in the active volume of the electrochemical flowcell. This prolonged exposure to the active functional sites of the working electrode allow for better system performance. Based on this data, the later trials would consist solely of flow rates less than or equal to 10 microliters per minute. The data comparing uranium recoveries to flow rates is shown in Figure 50.

Additionally, the standard natural uranium standards were tested against the voltage. Even though some of these were at different flow rates, the data shows a clear trend toward a more negative voltage (-0.20 V) performing better than a less negative

voltage (-0.15 V). Thus the voltage in future tests was changed to reflect this trend. The data from these tests are shown in Figure 51.

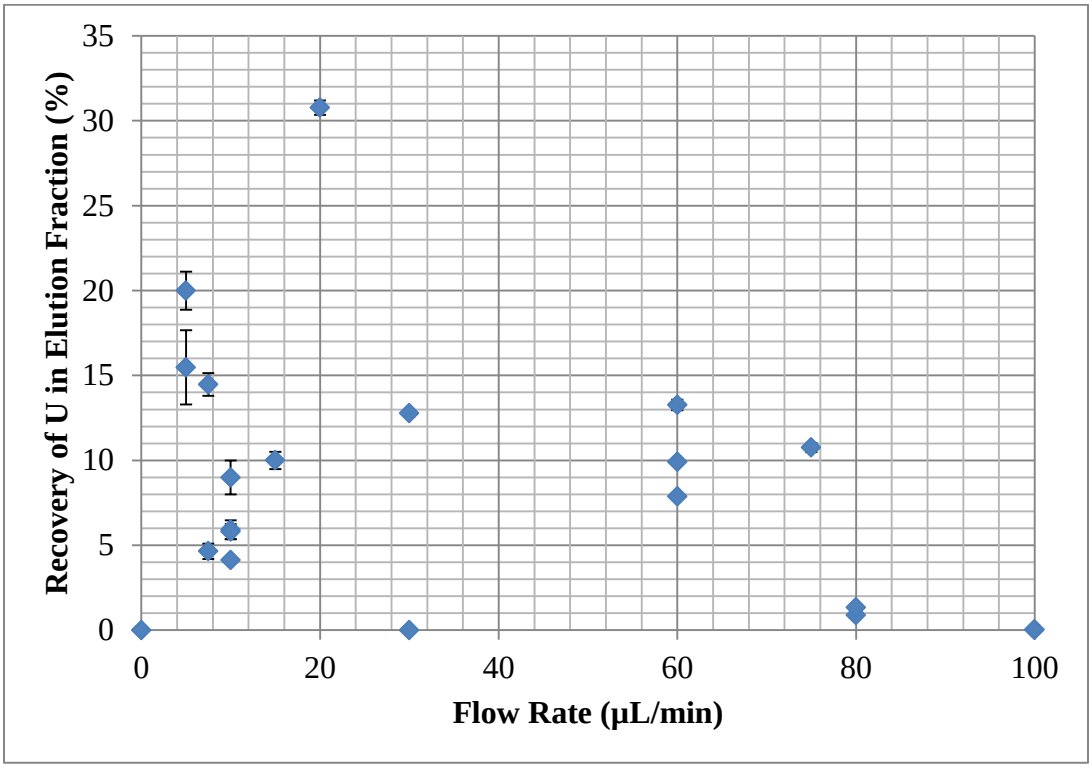

Figure 50: Initial Custom Flowcell Results for Standard Solution (Percent Recovery vs. Flow Rate)

Since a significant number of trials used -0.20 V for the accumulation phase, a subset of the data can be examined. The dataset shows more consistent performance at lower flow rates. This supports the decision to concentrate any subsequent data on lower flow rates for ascertaining the performance of the system against synthetic urine solutions. This data subset is shown in Figure 52.

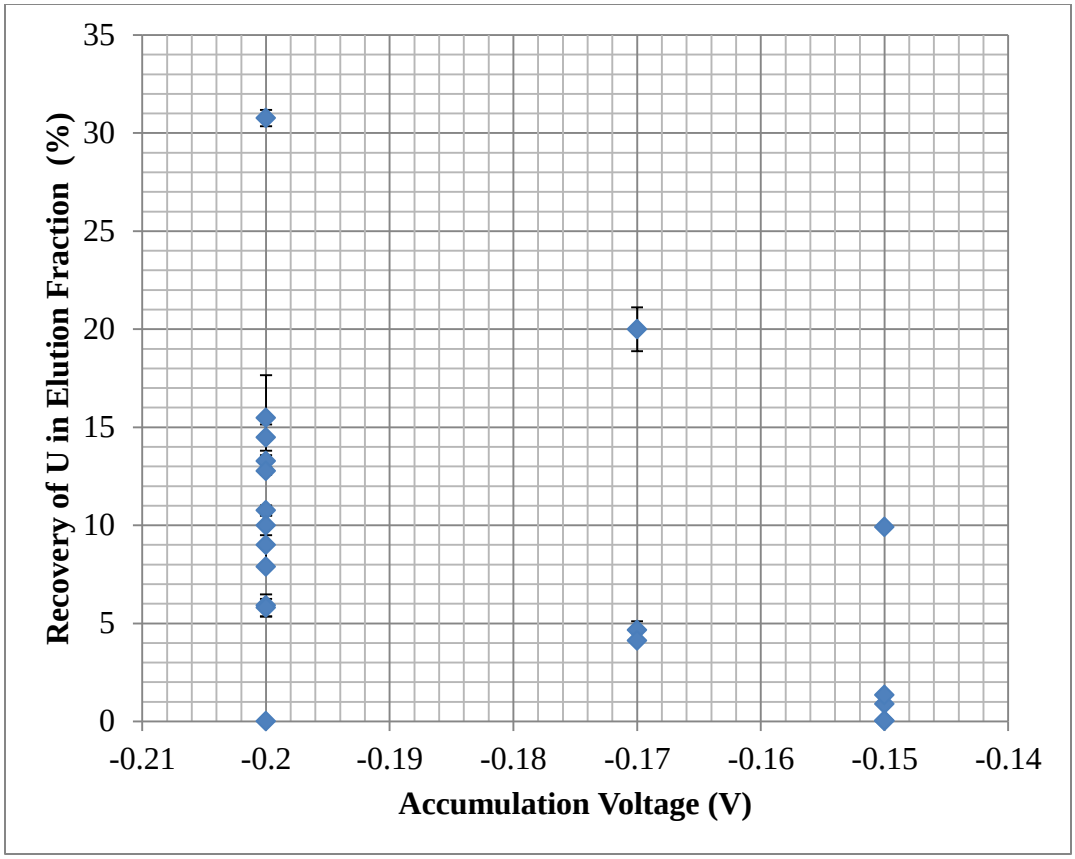

Figure 51: Initial Custom Flowcell Results for Standard Soultion (Percent Recovery vs. Accumulation Voltage)

The custom flowcell tests of clean matrix solutions proved that selective separation of uranium using this flowcell setup is possible. The custom system did not perform to the same efficiency as a similar system in previous works; however, the system did function and show observable trends related to both flow rate and accumulation voltages.

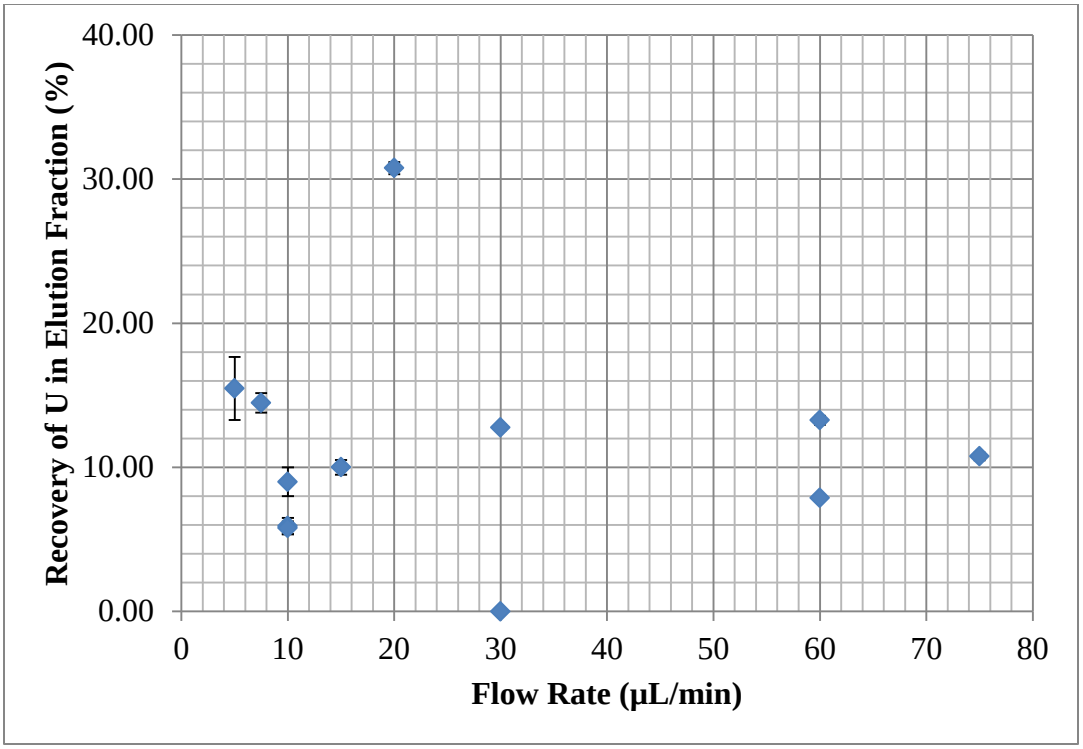

Figure 52: Initial Custom Flowcell Results (Percent Recovery vs. Flow Rate when V_{acc} = -0.20V)

Synthetic Urine

After significant testing of the clean uranium spiked solution, the switch was made to test synthetic urine samples using the custom flowcell geometry. These samples were run at a variety of flow rates and voltages. The predominate flow rate was 5 microliters per minute. The accumulation voltages were chosen due to previous results using the spiked uranium solution and the hydrodynamic cyclic voltammetry scans which indicated that a slightly more negative voltage would be most appropriate for this system.

The synthetic urine separations had lower recovery percentages than the standard solutions, but were more consistent than before. This is likely due to process refinement

and increased operator aptitude after many trials. The dataset for these synthetic urine samples are shown in Figure 53.

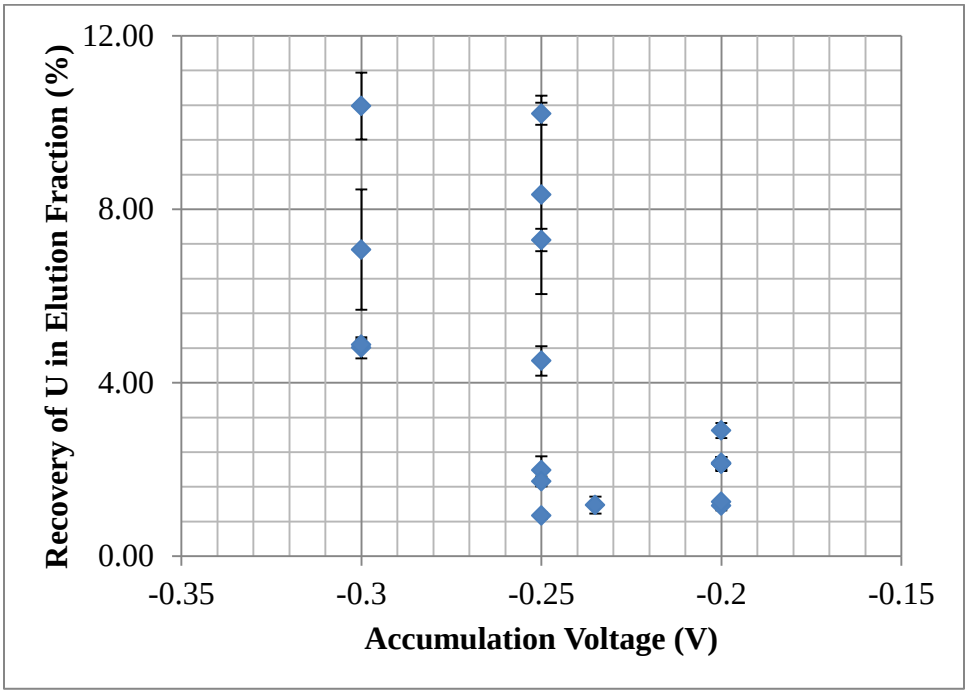

Figure 53: Initial Custom Flowcell Synthetic Urine Results (Percent Recovery vs Accumulation Voltage)

Final Geometry Results

All of the samples tested on the final geometry system were synthetic urine. Additionally all of these samples were run using a 5 microliter per minute flow rate. Sixteen synthetic urine samples were tested in total. An additional four were accidently disposed of and were unable to be analyzed on the ICP-MS instrument after separation, dry down, and digestion. The results of these samples are shown in Figure 54. The standard deviations of this data set are contained in Table 5.

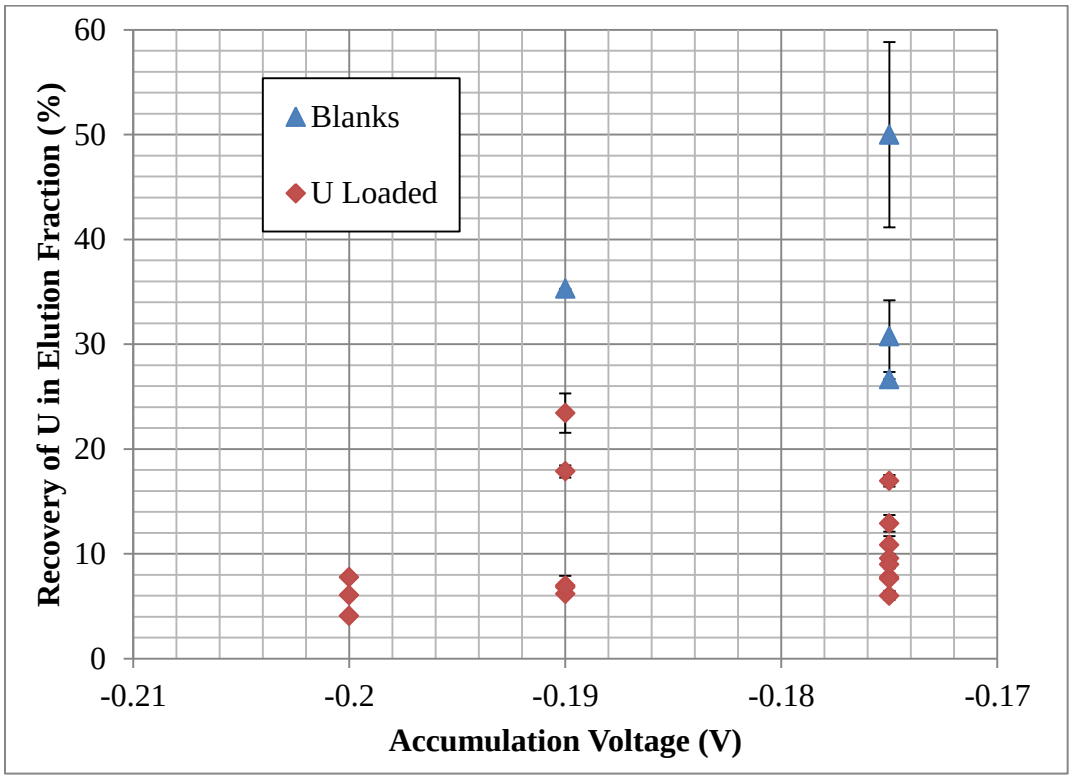

Figure 54: Synthetic Urine Separation Recoveries vs. Accumulation Voltages

Table 5: Standard Deviations for the Final Geometry Synthetic Urine Separations

Sample Set	Standard Deviation (%R)
All	12.1
Blanks	10.2
U-Loaded	5.2

There are several major observations to take from the synthetic urine samples. The first is that the -0.19 V accumulation voltage performed the best of the various accumulations voltages indicated by the literature and hydrodynamic cyclic voltammetry scans. Secondly, these separations were much more consistent than the previous geometry and there were no null separations. This is a vast improvement, but the

separations process is still variable. This particular system using synthetic urine has variance across the various trials and would require a tracer spike in order to ascertain the separation efficiencies when used in practical application. The third observation involves the blank samples. The blank samples which contained an order of magnitude less uranium than the standard uranium samples had much better performance. This could point to a low saturation point or a need for increased working electrode surface area for increased electrodeposition of the uranium atoms during accumulation. The system described in the literature performed better than this system; however, the synthetic urine samples are a much more complex matrix than the benchmarks and are not expected to perform as well as simpler matrices. It is important to note, the system described by publications of the group at PNNL did not test complex matrix solutions. Additionally, the offset of the glassy carbon electrode as compared to the centered approach used here may have an advantage in active surface area, but an offset electrode was not available for comparison.

Isotope Independence

Since the electrochemical properties of uranium being exploited in this separations process are independent of isotope, the uranium separated should have the same isotopic ratios as the loaded sample. Sample DL56-6 is used to demonstrate this isotopic independence. This particular sample was separated with a recovery of 17.9 percent. The Remainder (unprocessed sample), the Flow Through (raffinate), and Elution samples counts from the ICP-MS were used to check the enrichment of the detected uranium. The remainder serves as a control to quantify the contents of an

unmolested sample. The results of this are shown in Table 6. The data shows that all samples contained natural uranium. The uncertainties are large due to the trace amount being analyzed on the mass spectrometer, but no appreciable isotope preference is seen during accumulation.

Table 6: Isotopic Results from Sample DL56-6

Sample	U-238 (cps)	U-235(cps)	Percent U-235	Uncertainty (%)
Remainder	7784.3	57.9	0.74	±0.10
Flow Through	81926	599.6	0.73	±0.03
Elution	18165.4	133.6	0.73	±0.07

Qualitative Comparisons

The qualitative comparisons are a visual analysis of the intermediate dried phase of the experimental procedure combined with the analyzed recovery percentage. The overall goal of the qualitative comparison is to show the matrix reduction accomplished by processing the samples through the electrochemical separations process. Two synthetic urine samples (one uranium loaded and one blank) were chosen from the better performing separation experiments. The images were taken after the samples dried down overnight and crystalized, but before digestion in acid for volume normalization. The first sample is DL54-8 and was separated with a percent recovery of 23.4 percent. The second sample is BL2-2 and was separated with a percent recovery of 50.0 percent.

In examining the DL54-8 standard images, the size of each dried residue stands out. The vial in each image is one inch in diameter. The Flow Through sample is much larger, despite having a similar volume to the elution sample. The before blank sample

had the largest volume before dry down. The remainder sample is typically very small (5-10 µL) and diluted with clean HNO_3 used to rinse the sample vial and collect any remaining fluid. These images are shown in Figure 55.

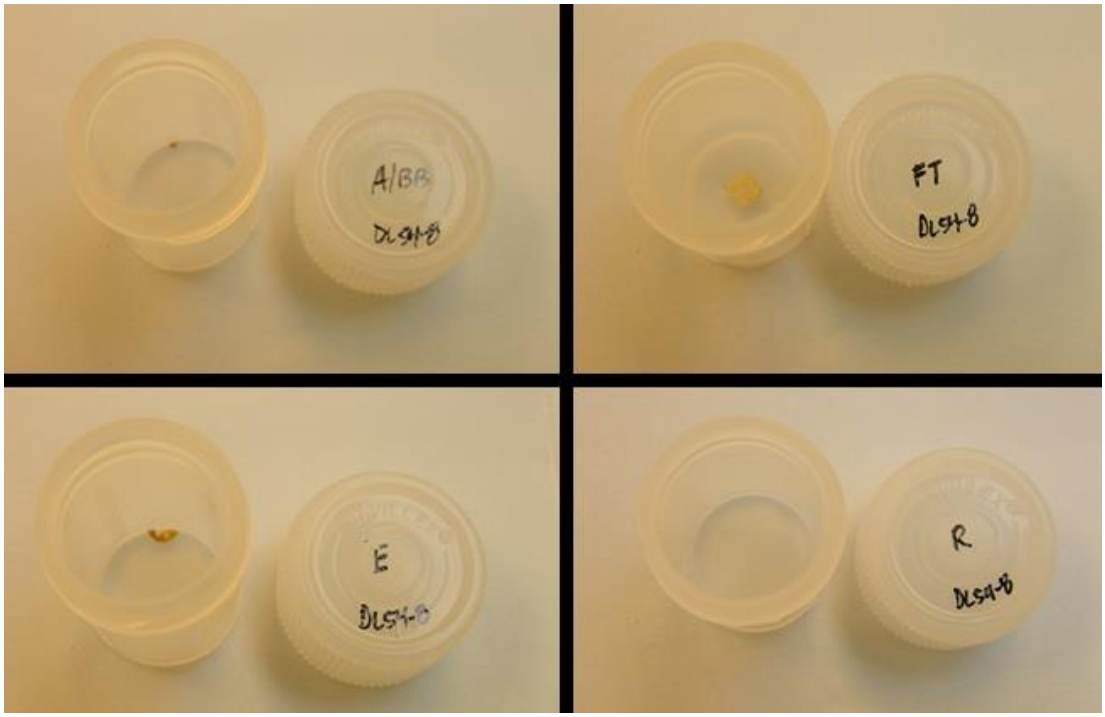

Figure 55: Synthetic Urine Sample DL54-8 Images After Dry Down (Clockwise from Top Left: Anodization/Before Blank, Flow Through, Remainder, and Elution)

The same synthetic sample is shown again in Figure 56. These images are microscope images. Each image is at least 25x magnification (Flow Through image) and up to 40x magnification (Remainder image). The structure of the different phases varies greatly. The yellow salt residues in the flow through image are not present in the others. Further, the remainder image has a similar coloring and structure to the flow through which is expected. The Elution sample clearly contains some salt in addition to

the separated uranium; however, it is clearly much less than the flow through sample which is the desired matrix elimination and reduction. After several discussions with members of both the LANL Staff and Texas A&M University faculty, the conclusion that the Elution sample is mostly likely uranyl permanganate was reached.

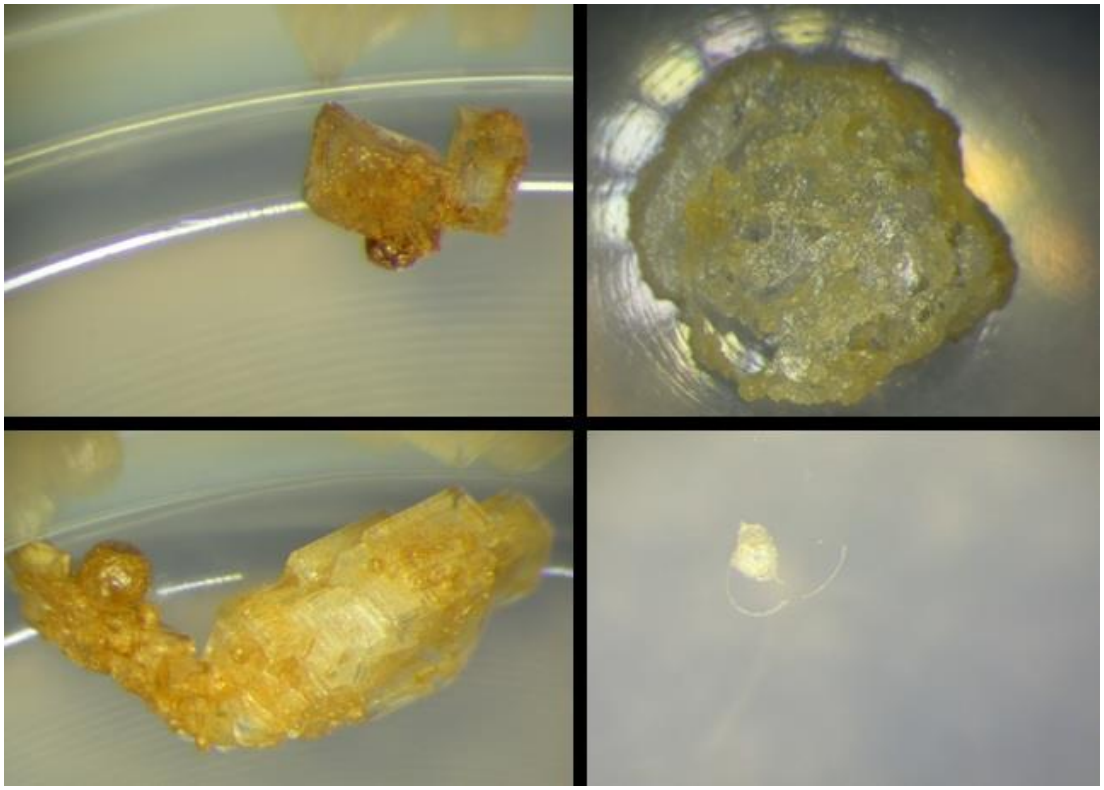

Figure 56: Synthetic Urine Sample DL54-8 Microscope Images After Dry Down (Clockwise from Top Left: Anodization/Before Blank, Flow Through, Remainder, and Elution)

The BL2-2 sample has similar images for comparison. The initial full size images are shown in Figure 57. Similar trends in the size and composition are seen in these images. The flow through image has a brighter yellow hue as opposed to the previous sample. The elution residue is brown and could indicate the presence of an

oxide compound. This elution sample contains 8 picograms of uranium while the previous elution sample (DL54-8) contains 26 picograms of uranium. The relative size of each reflects that difference.

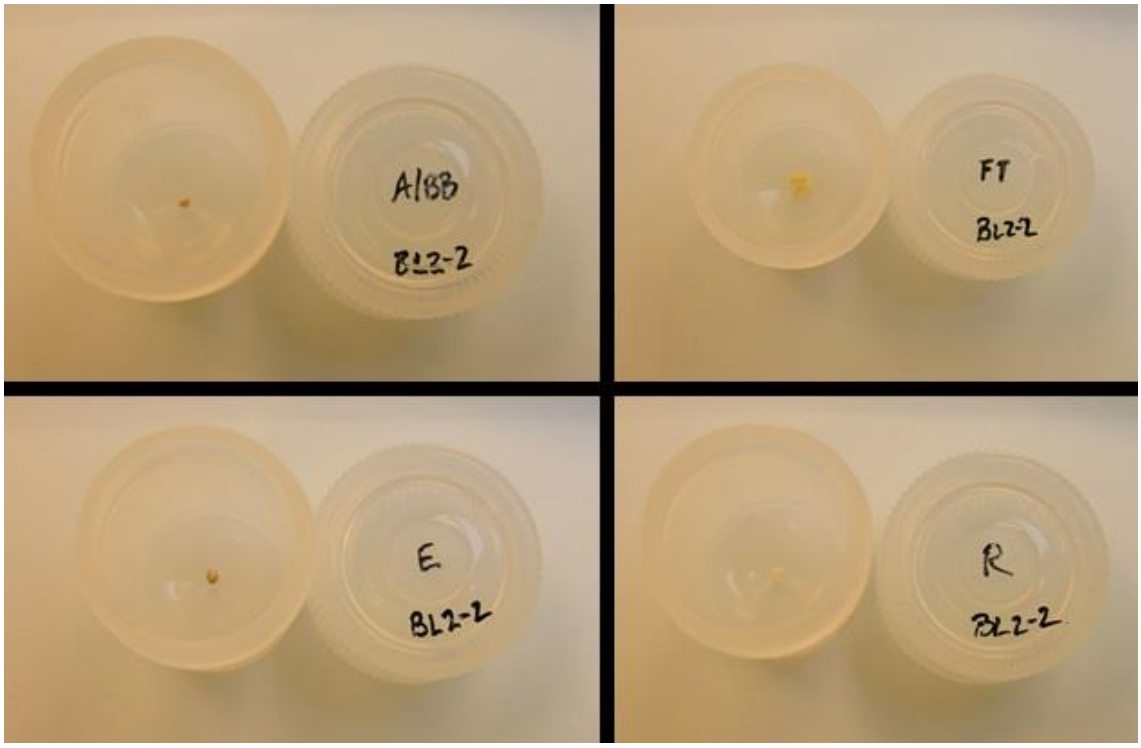

Figure 57: Synthetic Urine Sample BL2-2 Images After Dry Down (Clockwise from Top Left: Anodization/Before Blank, Flow Through, Remainder, and Elution)

The corresponding microscope images are contained in Figure 58. The structural differences are much more apparent in this sample than the previous sample. The flow through and remainder samples are very similar in both color and structure. The elution phase still exhibits some salt matrix crystals. Nevertheless, this sample had the same amount of uranium in both the flow through and elution phases. As a result, significant

matrix reduction is clear. By reducing the salt being measured, interferences and contaminants can be removed from the analysis process.

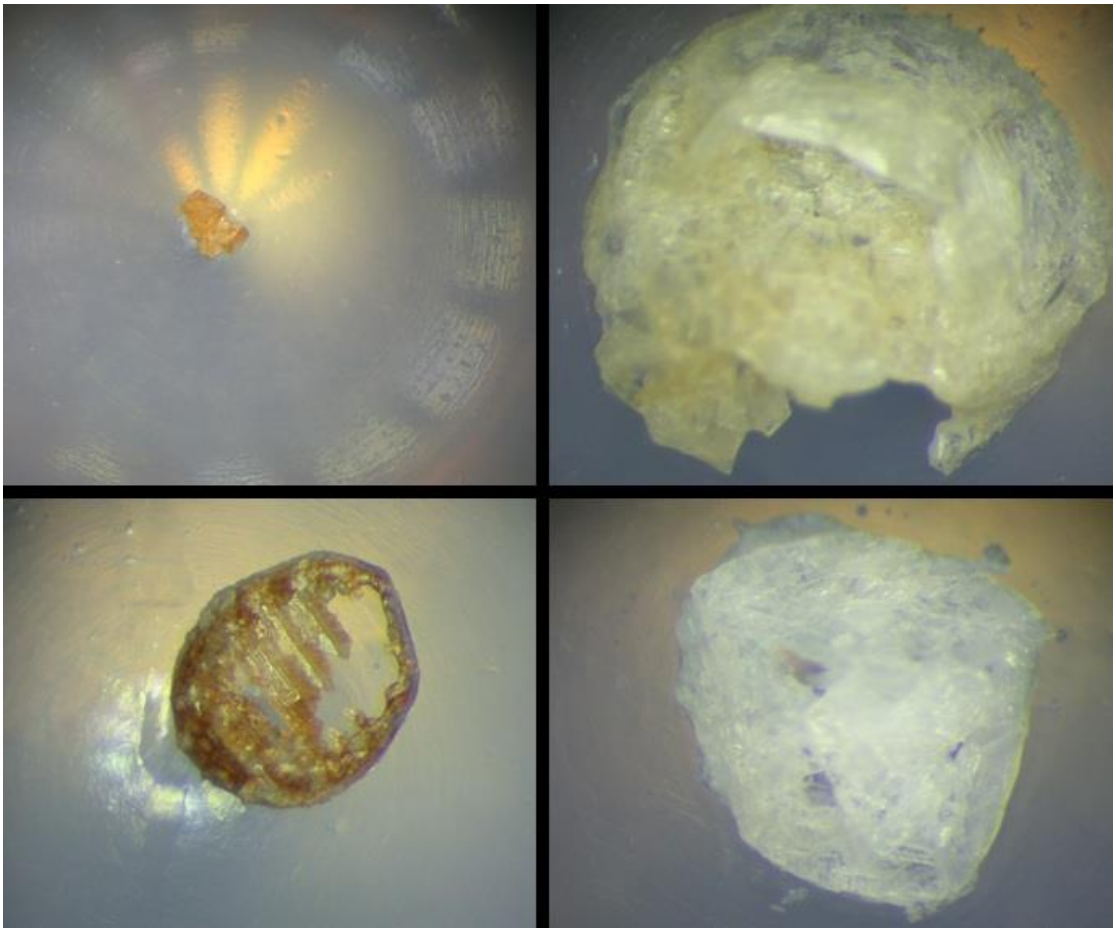

Figure 58: Synthetic Urine Sample BL2-2 Microscope Images After Dry Down (Clockwise from Top Left: Anodization/Before Blank, Flow Through, Remainder, and Elution)

The most important visual indicators are size and color. Typically, if no residue visible, then no uranium will be present in the sample. The size of the residue did not yield exact uranium content. But in general, larger residues indicated higher uranium content. The colors are consistent across samples. Exotic sample hues typically meant

an exterior material had contaminated the sample. In one such instance, the dried samples had a neon green hue. This was later determined to be a copper chloride compound from an electrical clip connection accidently exposed to the nitric acid during separations. The qualitative comparisons yield some additional knowledge to the performance of the system before final destructive analysis on the ICP-MS instrument.

CHAPTER V

BIOKINETIC MODELING

As first introduced in Chapter I, biokinetic modeling of exposures began early in the nuclear age. The current state of the art in biokinetic modeling is reported and maintained by the International Commission on Radiation Protection. Every few years, the ICRP will release a few updates and changes to the models. In general, the sixteen compartmental model from ICRP 23 remains the standard. One such update was in 1971 when the models were altered for children and infants. But the model for adults (those 20 years of age and older) essentially remained the same. Significant work has been put into verifying the models with both experimental and empirical data. Similarly, understanding the uncertainties within the models has received attention. This uncertainty relates to the source of data, the biological system, and data collection difficulties.[55] Regardless, the ICRP model is the best available model and was used in this report.

The model requires some initial information in order to calculate the expected excretion ratios, specifically the type of exposure. There are a variety of ways to occupationally introduce uranium including inhalation, ingestion, or injection. Each of these methods can have variations depending on particle size and chemical form. One of the most important pieces of information regarding the uptake and retention of uranium by the body is the chemical form. The chemical form relates to the solubility of the material in the body. As shown in Figure 59, the three rates of inhalation uptake and

retention (Fast, Moderate, and Slow) differ greatly. Similarly, differences in the ingestion uptake and retention are strictly related to the chemical composition of the uranium when ingested.

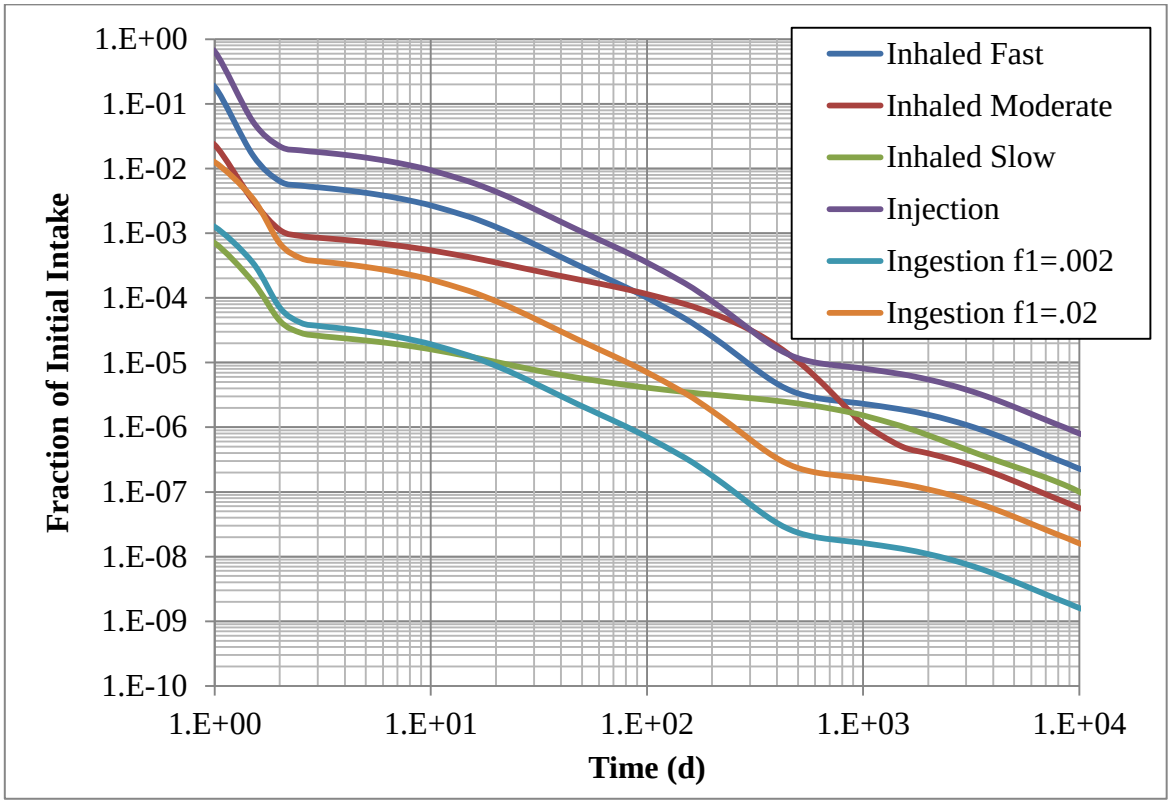

Figure 59: Urinary Excretion of Uranium as a Function of Time

Since this work is primarily concerned with the uptake, retention, and elimination of uranium after acute occupational exposures, it is important to consider the various isotopes of uranium. In a typical civilian program, a worker will only be exposed to uranium with enrichment much less than 20 percent ^{235}U, and most typically natural uranium. Meanwhile, a worker involved in a military program or naval propulsion

project could potentially be exposed to higher enrichments of uranium. Through the modeling codes, it was shown that the fractional retention and excretion of ^{234}U, ^{235}U, and ^{238}U, the major uranium isotopes, is identical. This is a predicted result since the three isotopes have nearly identical chemical properties. Thus, the excretion of uranium is isotope independent.

Further complicating the modeling problem is that the natural background of uranium in the body from uptake related to environmental conditions can be quite varied.[13] Drinking water is one of the major contributors to a background signature. In addition, the concentration and exposure to uranium via drinking water and food products is highly regionally dependent and can differ greatly between towns as close as 30 miles apart.[56] There have been several efforts to compensate and track the background exposure to uranium using data from UNSCEAR and controlled drinking water supplies.[40, 57] Overall, the models are only a general guide and are imperfect, but they are a nice stepping stone and should continue to improve over the next few decades as more data becomes available.

Forward Model Code

In selecting a forward model to be used for this work, several factors needed to be considered. Ideally, a code that has a high acceptance rate in the health physics community would be desired especially with thorough benchmarking. One such code is the Dose and Risk Calculation software (DCAL) developed by the Biosystems Modeling team at Oak Ridge National Laboratory. DCAL is an open source freely available code which has been used and validated extensively through its development and use. The

program has several modules which calculate various parameters used in biokinetic and dose modeling. This particular code can be difficult to run and is not always compatible with the newest computers. The user manual is inadequate as well. DCAL is based on the International Commission on Radiological Protection publications, specifically ICRP 67 through ICRP 72.[49]

The capabilities of DCAL are much larger than needed in this work. The first step in utilizing DCAL is to run the module ACTACAL which calculates the time-dependent activity of a specified radionuclide and its daughters as well as concentrations in a large number of biological compartments. The biokinetic models built into DCAL include occupational exposure (ICRP 68) and exposure to the public (ICRP 72). This work is concerned with exposures to individuals exposed while working with materials and thus used the occupational exposure model. More advanced use of this code allows for the absorption coefficients of a particular exposure to be modified. However, to avoid difficulties the standard fast, moderate, and slow absorption coefficients were used.

It is important to note that several assumptions embedded into this model; the most important of which is that organ masses for adults are estimated from ICRP 23. Also, the model assumes 20 years of age constitutes an adult; however, there are some radionuclides that bond with the skeleton differently for individuals nominally aged 20 and 25 years.[51] These assumptions are able to be changed when running the program; however, changing these variables has a small impact on the resulting excretion curves but can be adjusted on a case by case basis if necessary.

In Figure 59, the output for ^{238}U content in urine after an exposure is shown. The six primary methods for introducing uranium into the body are shown as independent curves. It is of note that the types of absorption by inhalation (fast, moderate, and slow) have significantly different curves. The three inhalation curves are shown in Figure 60. This is significant because it should allow for determination between the types based on a comparison of computed half-lives or slopes related to the excretion profile. The two ingestion lines and the fast inhalation line appear to mirror one another. This could provide complications when determining which type of exposure is suspected. But it is important to note that any exposure is likely to have a major component and minor components. The excretion profiles are tri-modal and should reflect three major decay portions. From the literature, the initial uranium purge (first day) will be fairly large and unreliable for accurate assessment in relation to this work.[48]

Sample Data

With the forward predictive model examined and in place, a sample case must be selected in order to test an inverse solution to these problems. It is impractical to find an exposure to personally test to obtain excretion data. There are several unclassified studies on large acute exposures. In selecting a data set several factors should be considered including breadth of data, availability of raw data, quality of data, length of the exposure follow up regime, and availability of information regarding the exposure outside of urinalysis. If data graphs conflicted with numbers in a report, that entire data set was removed from consideration.

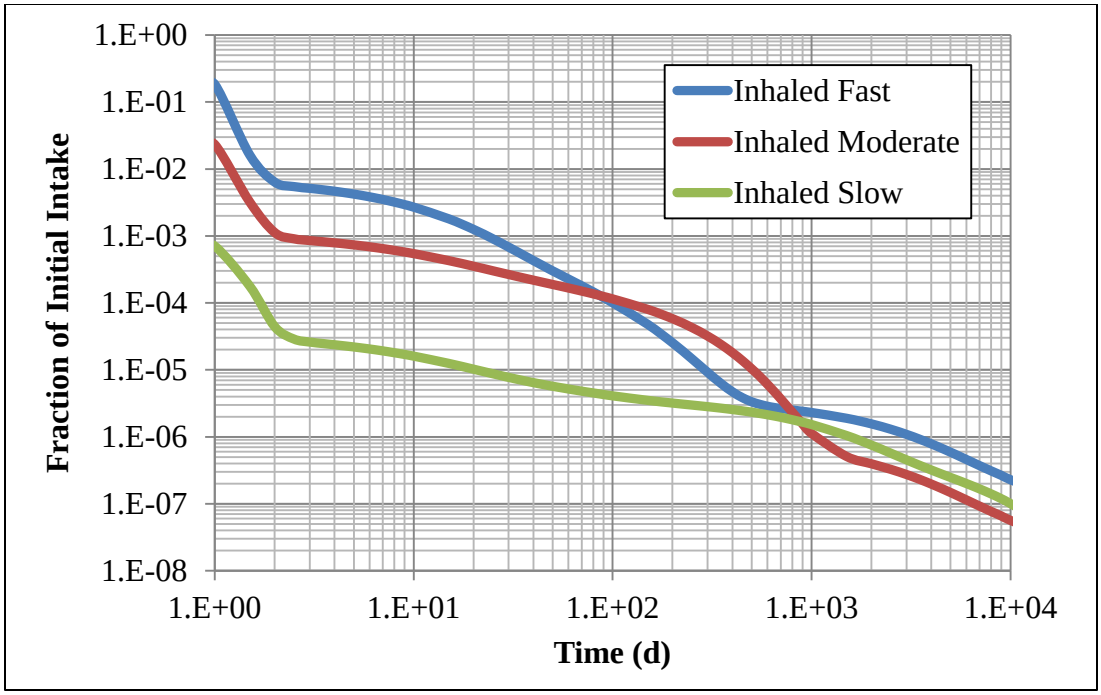

Figure 60: Normalized Inhalation of U Excretion Profiles (F, M, S)

The data set selected was from an exposure in 1962 at the Y-12 plant in Oak Ridge, TN as part of work through the Union Carbide Corporation.[41] A machinist was exposed to approximately 90 percent enriched ^{235}U while deburring a uranium metal piece. The worker inhaled a fume containing U_3O_8. Upon discovering the exposure through routine weekly urinalysis, an intensive monitoring regimen began to track the uranium excretion by the worker. This particular worker was monitored for over three years until his urinary uranium excretion returned to background levels. The data regression curve from this exposure is shown in Figure 61 and the raw interpolated data is contained in Appendix F. Unfortunately, the exact raw data was unavailable, but the data was recreated using interpolation of data points on a high resolution copy of the graph contained in the literature.[41] Undoubtedly, some additional variance will be

introduced into the dataset as a result. However, the general trend of the data should be preserved and be appropriate for this work. This data was not mass spectrometry data, but it was taken using electrodepostion and proportional counting in accordance with the Y-12 bioassay program at the time.

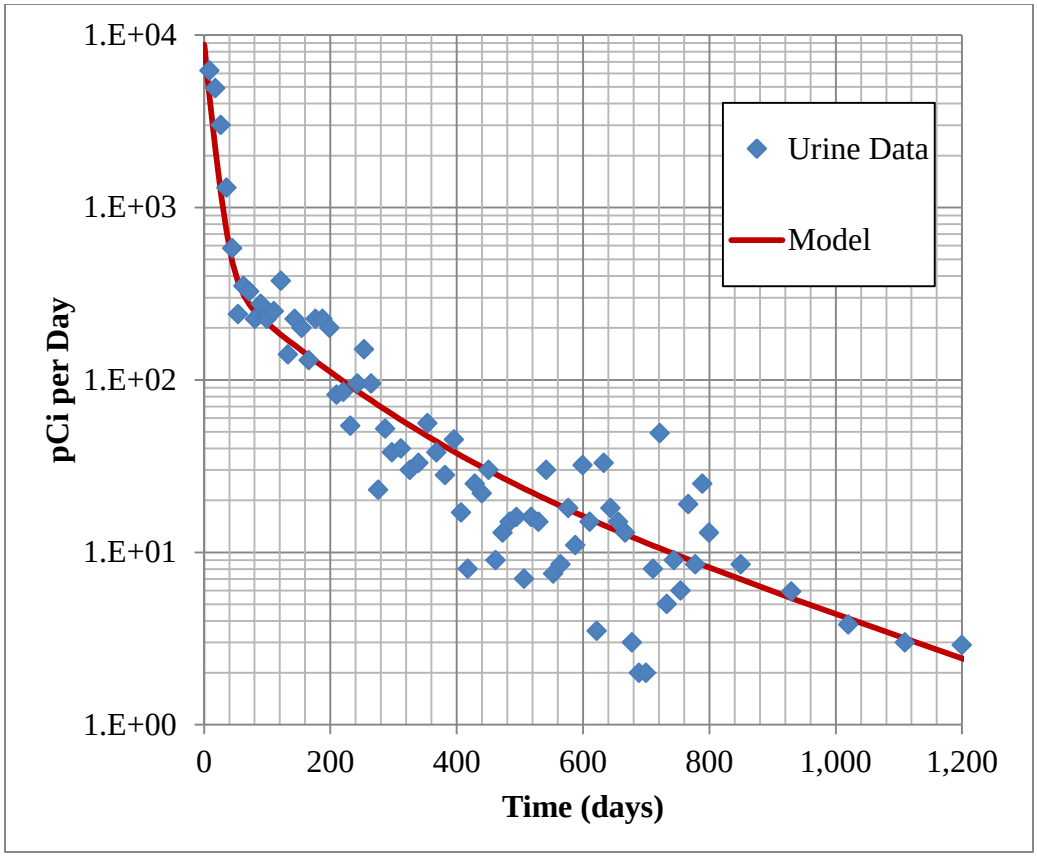

Figure 61: Uranium Content of Urine for an Exposed Worker at Y-12[41]

The data was fit using both a power curve and an exponential sum. The exponential sum curve was much more accurate in reflecting the data collected. The regression R^2 value for the exponential sum was over 0.99 compared to 0.90 for the power curve fitting. There is significant noise in the data after the 100 day mark. Since

Figure 61 has a logarithmic scale, the magnitude of these variances is not immediately apparent. The source of this variance is most likely from uranium background complexities previously discussed as well as potential difficulties in measuring such trace amounts of uranium. If an entire day's uranium excretion were able to be electrodeposited for the measurement (after 200 days), the total uranium would be on the order of micrograms. However, even the most efficient modern sampling techniques do not allow for complete uranium recovery in a 24 hour sample. The paper containing the data for this particular case did not include an error analysis for the alpha spectroscopy measurements of the urinalysis. Further the form of the data in the Scott and West study is not of the same form as the output from DCAL code. It was appropriately normalized such that it will be available for comparison to the forward model.

Comparison

With a dataset in hand, the data needed to be compared with the forward model as well as used to investigate inverse data recreation. Using a precedent originally developed by some health physicists in Germany, a set of regression algorithms for each exposure pathway for comparison to be created using a tri-modal regression algorithm from data created using an appropriate forward model code based on ICRP publications.[58] This should put the model and sample data on equal footing. From previous work and analysis, it was determined that a least squares multimodal nonlinear exponential sum regression would best represent the models and data. These regressions were done using an iterative least squares method in both SIGMAPLOT® and

MATLAB®. The regression formula for the program is a seven parameter exponential sum represented by

$$f(t) = y_0 + ae^{-bt} + ce^{-dt} + ge^{-ht}$$

where y_0 is the y-intercept, a, c, and g are amplitudes, and b, d, and h are fractional decay constants. The regressions were done using a reciprocal y^2 weighting and typically resulted in a minimum of 25 iterations to satisfy an imposed 1 x 10^{-15} tolerance (from the database of Urinary Excretion Profiles) and an R^2 value above 0.99. The results of the calculated regression parameters for the six introduction models are listed in Table 7.

Table 7: Regression Model for Biokinetic Excretions

Method of Exposure	Regression Parameters						
	y_0	a	b	c	d	g	h
Inhale (fast)	8.41E-08	5.77E-03	8.63E-02	4.06E-04	1.39E-02	3.07E-06	3.41E-04
Inhale (mod)	1.96E-08	7.26E-04	6.46E-02	2.00E-04	5.95E-03	6.28E-07	3.02E-04
Inhale (slow)	4.76E-08	2.36E-05	9.87E-02	4.95E-06	1.33E-02	3.02E-06	6.27E-04
Injection	2.95E-07	2.02E-02	8.63E-02	1.43E-03	1.39E-02	1.08E-05	3.41E-04
Ingest f1=0.002	5.90E-10	4.14E-05	8.65E-02	2.87E-06	1.39E-02	2.15E-08	3.41E-04
Ingest f1=0.02	5.90E-09	4.14E-04	8.65E-02	2.87E-05	1.39E-02	2.15E-07	3.41E-04

It is notable that when performing the regression the first three days of modeling data were excluded. This was done since it is highly unlikely that there will be an opportunity to test an individual so quickly after exposure. Also, the model predicts a quick excretion of a significant fraction of the uranium which was taken up by the body, thus the regression statistics would have been compromised for larger times if these data points had been considered. Typically up to the first ten days after exposure can be

disregarded as previously noted. After Day Three the curves appear to be in the second mode and Days Four through Ten were included for a higher degree of accuracy. Also of note is that the regression models have a tail around 10,000 days. This is due to the in accuracy of the model; however, based on the biological half-lives of uranium, excretion levels after 27 years should be well below background levels. Thus, this effect is not expected to have any significant effect on the overall viability of the proposed system. Typically 1000 days (3 years) is the accepted time interval for which exposures are monitored. A visual comparison of the regression (markers) and the DCAL model (solid lines) can be seen in Figure 62. This is the same graph as contained in Figure 59, but with added regression points to show the quality of the regression fitting algorithm.

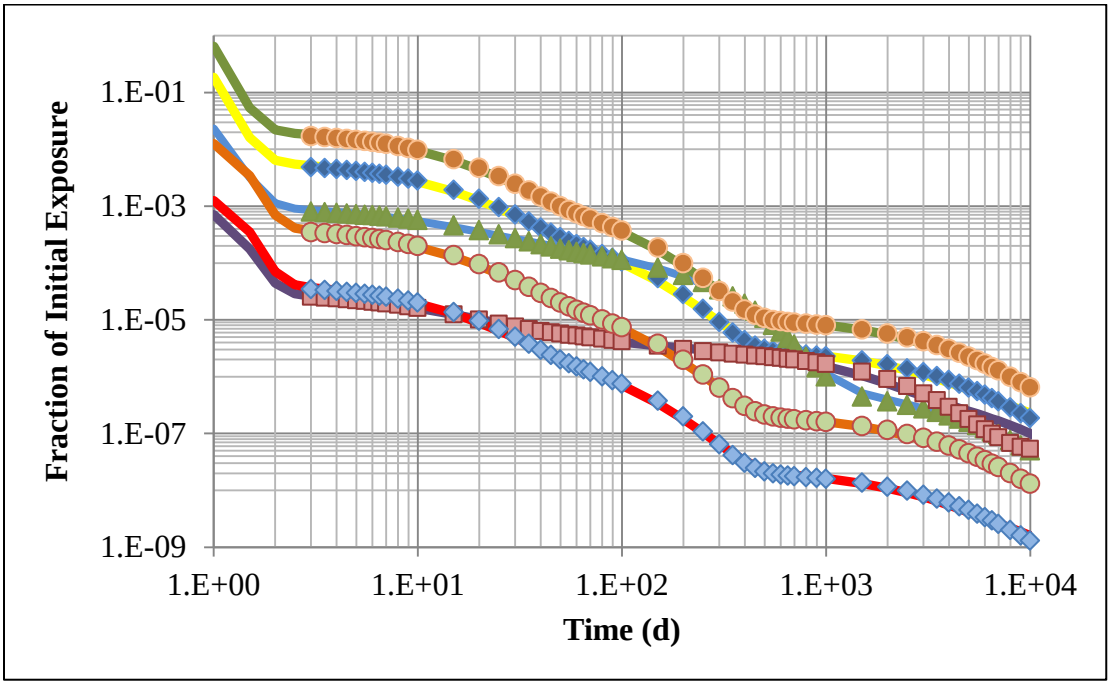

Figure 62: Biokinetic Model Regression Fits

Example Case

In evaluating the feasibility of the proposed inverse analysis, a randomly selected set of data points were taken from sample dataset. After some brief experimentation with various data selections taken from the sample dataset, it was determined that at least ten data points would be needed in order to track an individual's exposure. Thus using a random number generator, a sample of ten points was taken in order to compare to the aforementioned nonlinear models and regressions. Ideally, the points should be well spaced. A minimum of a week's separation is adequate. This data set had testing regime around one week intervals. The selected data set is shown in Table 8.

Table 8: Ten Randomly Selected Data Points

Time (d)	pCi
81	225
90	275
177	225
232	54
530	15
553	7.5
633	33
700	2
744	9
1020	3.8

Using the same nonlinear regression technique and regression equation used in numerically quantifying the DCAL models, the ten point sample was analyzed. This yielded a curve which is shown in Figure 63. The original regression model by Scott and West, after normalization, is overlaid with the ten point regression as well as the three major types of inhalation biokinetics as described by the DCAL model. From a

visual inspection of the figure, the 75 to 200 day range in both the original regression and ten point regressions fit nicely with the moderate inhalation case. Figure 64 shows a magnification of the area of interest from the results. However, the full sample regression performed by Scott and West most closely resembles the fast inhalation case in the 50 days immediately following exposure, but then appears to closely mirror the moderate inhalation case after 100 days. This supports the theory that each chemical has a specific absorption coefficient that might not match up exactly to each of the generalized fast, moderate, and slow cases. If the absorption coefficients become better known in the next few decades, this type of approach could be even more useful in determining the chemical form during exposure.

From this example, it is reasonable to conclude that the inhalation was a combination of fast and moderate exposures. With increased data, the type of exposure becomes clearer. The excretion is dominated early on by whatever portion of the exposure was of the fast absorption variety, but since the longer term excretion data changes to be dominated by a moderate absorption profile, this fits with the analysis done for this exposure case by health physics personnel at the Y-12 plant and alternate U_3O_8 exposures.[59] It also suggests that the inhalation exposure material was heterogeneous in composition with regard to either particle size, chemical form, or both.

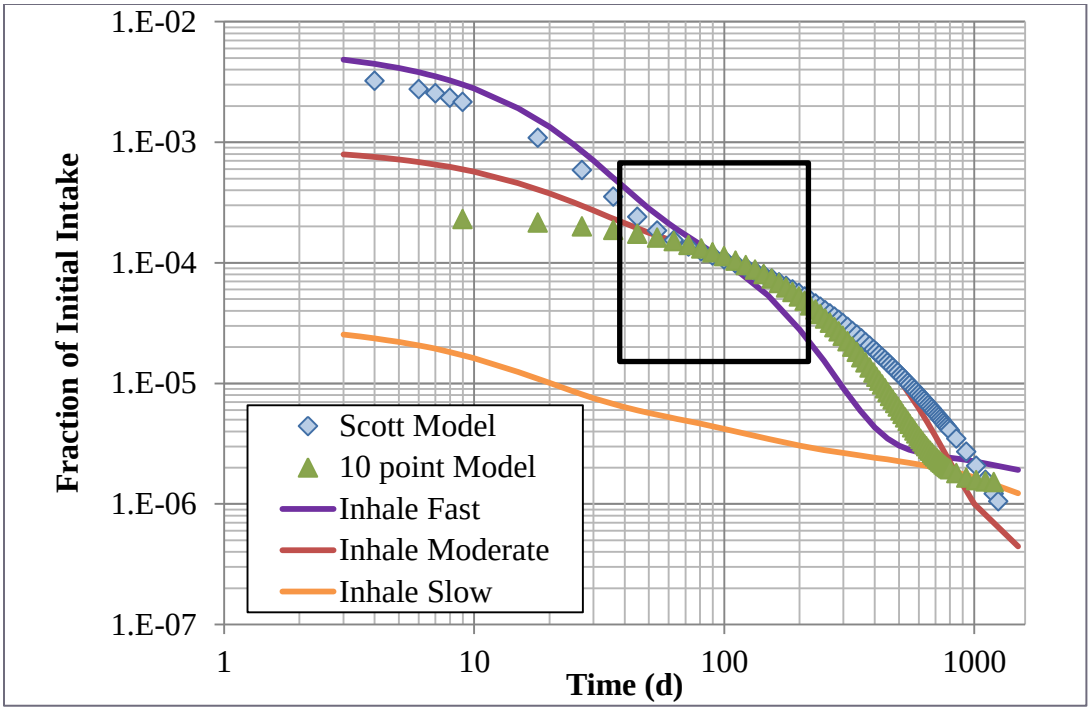

Figure 63: Comparison of Sample Case to Inhalation Models (box indicates magnification shown in Figure 64)

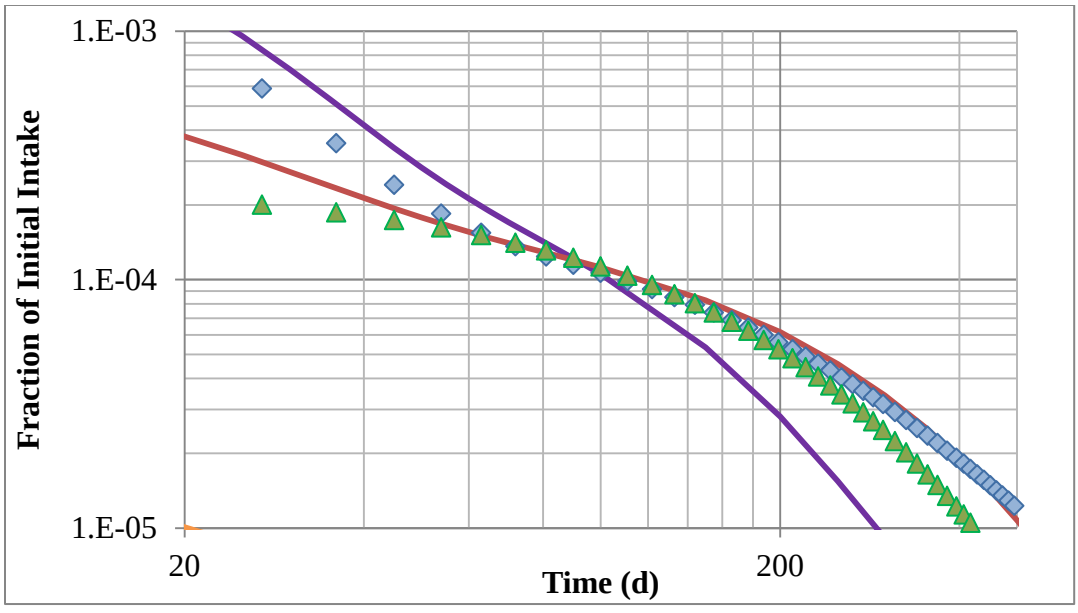

Figure 64: Magnification of the Sample Case Comparison

In keeping with the scenario of ten measurement analysis, the entire 1200 day measurement data would not be available for analysis. So this must be disregarded in drawing conclusions on the functionality of the system. The procedure calls for the ten point sample regression to be compared to the database of models provided by the forward model DCAL. In realistic analysis, the first data point in the set would be set as time equal to zero. For this example, that would translate the data point taken 81 days after exposure to time zero. This is how the analysis was run.

Comparing the datasets becomes complicated because the models and the regressed data might not match up for comparison. This is the case for this set. To solve this, the regression equation is adapted to become

$$f(t+\Delta t) = y_0 + ae^{-b(t+\Delta t)} + ce^{-d(t+\Delta t)} + ge^{-h(t+\Delta t)}$$

where Δt is some unknown time step from the time of exposure to the first measurement. This time step will be bound by the testing protocols. For example, a monthly bioassay program would be bound by a time step of 30 days and a quarterly bioassay program would be bound by a time step of 90 days. The assumption is that a bioassay sample would have been taken before that time step and registered without an exposure. This particular instance will be bound by a quarterly bioassay condition. With the values translated on the t-axis to be malleable for comparison, normalization must be done for the exposure values. Since the values of the models are more accurate several weeks post-exposure, a series of comparison points spaced ten days apart starting at 50 days and ending at 700 days were chosen to test the fits of the various models. Each was normalized to the first value at fifty days. Now to find which model best fit the

regression of the data, each model was in turn compared to the original 10 point data set using a Chi Squared Optimization. Thus the best fitting model will have a time step within the boundary condition and the smallest χ^2 value. The uncertainty in the measurement data was estimated to be five percent based on the random noise of the data as well as the alpha spectrometry sampling methodology described in the reporting of the exposure by Scott and West.

After completing this analysis, both the Fast and Moderate Inhalation classifications yielded plausible results. The Fast Inhalation classification resulted in a time estimate of 69.7 ± 7 days. The Moderate Inhalation classification resulted in a time estimate of 71.1 ± 7 days. The Moderate Inhalation classification resulted in a smaller χ^2 than the Fast Inhalation classification. Thus the Moderate Inhalation classification is the best fit between the two classifications. The Slow Inhalation classification resulted in an unreasonable answer give the boundary conditions of the bioassay sample regime. In reality, most exposures are a combination of adsorption types. Since both the Moderate and Fast Inhalations classifications yield plausible result, the most accurate assessment of the exposure would be an exposure with both Fast and Moderate components. Since, the actual desired value is 81 days according the random ten point sample, there is some inaccuracy. But this is an inexact science and the boundary conditions are instituted to keep incorporate additional knowledge. The uncertainty in the time frame estimation is from the calculation of the uncertainty in the y-intercept of the regression for each particular classification model. The time step results are shown in Table 9 and the

graphical representation of the fits are shown in Figure 65 (with Δt set to the corresponding values from Table 9).

Table 9: Time Step Calculation Results

Model	Δt (d)	χ^2
Fast	69.7	3.74×10^3
Moderate	71.1	2.72×10^3
Slow	4.8×10^9	6.99×10^6

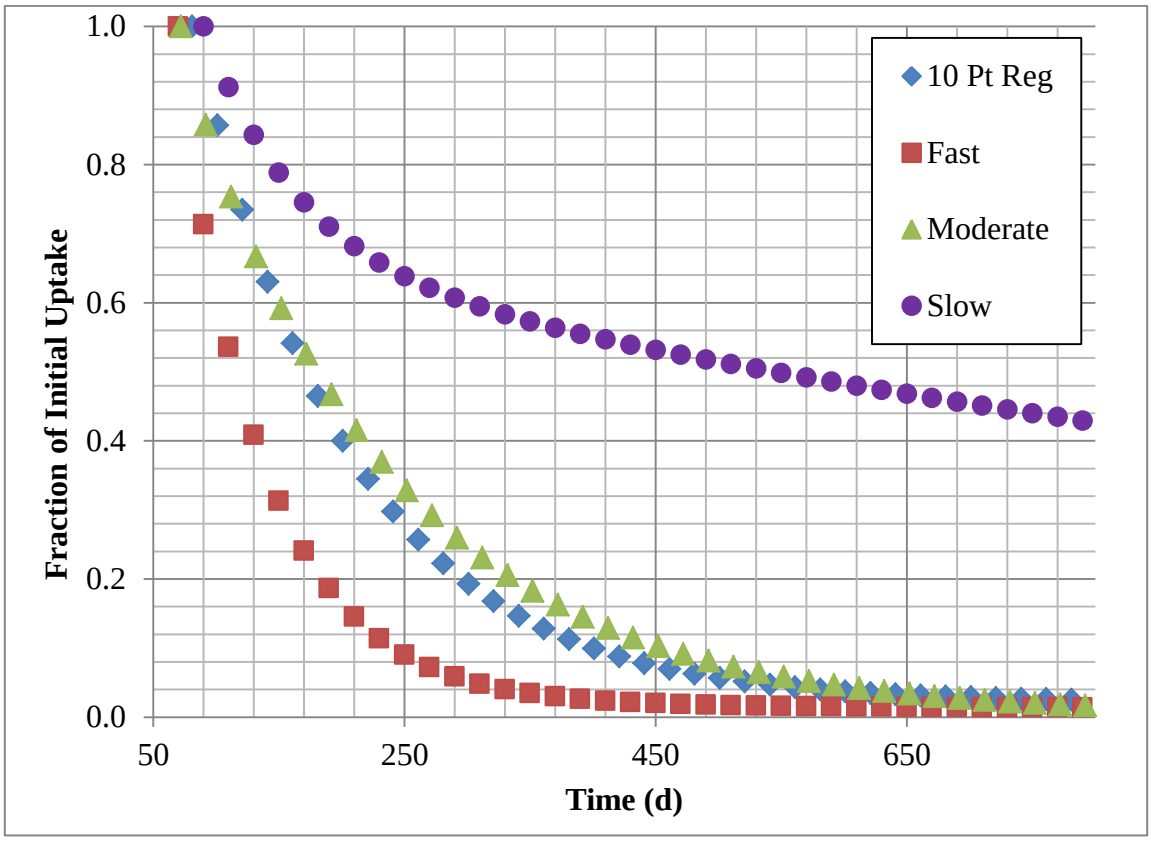

Figure 65: Model Comparison to 10 point Regression

Using the moderate model database and time step to predict amount of initial excretion under-predicts by a factor of five. However, this is an expected under-

prediction as was shown in previous graphs of the entire data set in concert with the models. This particular work is not interested in calculating the original dose, but rather is interested in estimating the time frame of that exposure. More sophisticated health physics measurements in conjunction with urinary excretion profiles are used to determine the initial dose. Furthermore, the goal is to use as little data as possible to get a reasonable answer for the time frame of exposure rather than estimate the amount of material inhaled and absorbed. The moderate dataset, ten-point dataset, and ten point regression are overlaid on the entire Scott and West dataset in Figure 66.

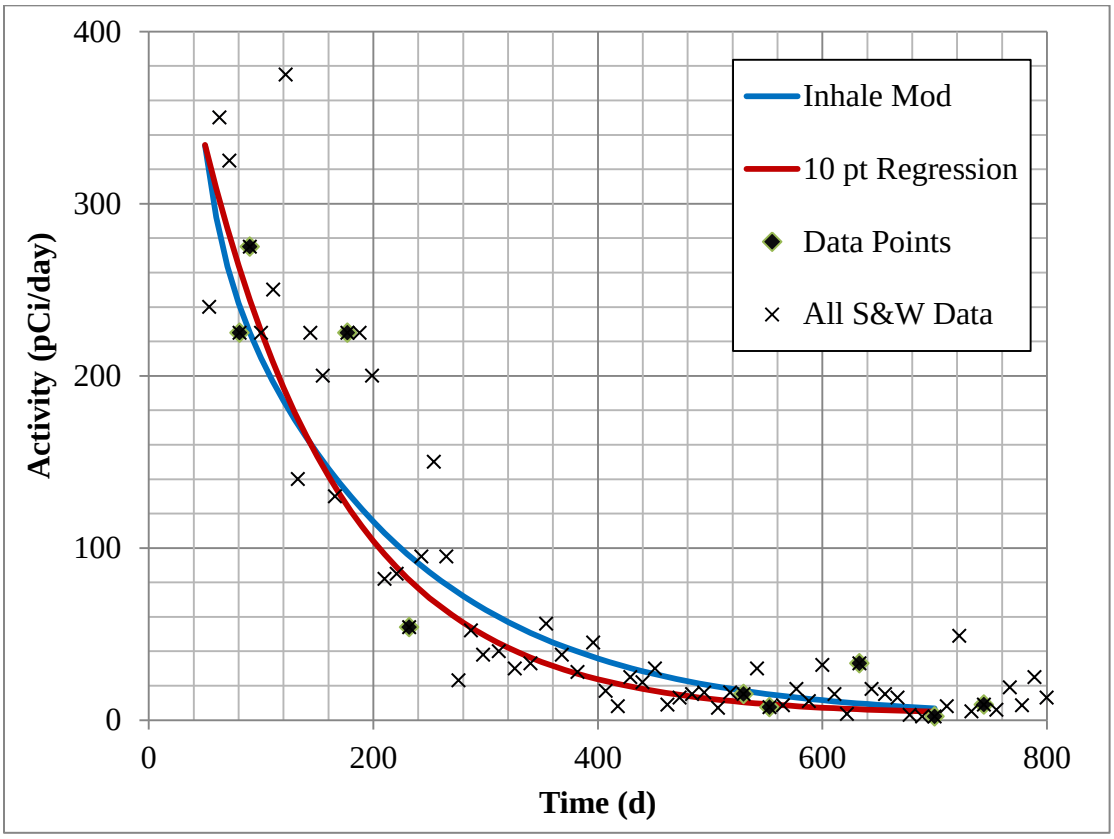

Figure 66: Final Model Fits and Data

In summary, using the biokinetic models put forth by the International Commission on Radiation Protection, a database of expected excretion profiles for uranium can be established. Using this database and a regression of at least ten data points well-spaced (at least one week apart) can yield a reasonable approximation for the time frame of exposure. Furthermore, utilizing more than ten data points can only serve to improve the quality of the inverse estimations. By no means should ten data points be the ultimate protocol, but rather should be the initial launching point into such an investigation of an individual incident to incorporate all potential data available.

CHAPTER VI

CONCLUSIONS AND RECOMMENDATIONS

A system for the analysis of urine bioassay samples for the purpose of inversely investigating an unknown exposure has been developed. This technique involves the use of a thin flow electrochemical cell in conjunction with an anodized glassy carbon electrode to selectively separate uranium out of solution for later analysis on an inductively coupled plasma mass spectrometer. Urinalysis samples are processed in batches and can be done successively. When instrument and facility use is not impeded by space sharing, an individual sample set can be analyzed in less than 24 hours. Successive uranium urinalysis bioassay sample results can be used to investigate the time frame and type of exposure. This analysis uses an exposure database and regression analysis to best fit urinalysis uranium excretion data to expected profiles using commercially available mathematics software. The analysis shows that ten data points with approximately 7 days between each point is sufficient to provide an acceptable level of certainty. The system was benchmarked using a random sampling of urinary excretion samples from a known case at the Y-12 plant in the 1960's.

The electrochemical system was characterized using U.S. Department of Energy synthetic urine quality assurance standards from and inter-laboratory exercise in April of 2012. The biological urine matrix has some unique challenges, and the synthetic urine standards were designed to mimic the most difficult urine complications. Over seventy sample sets were run in the characterization of the custom built thin flow circuit. The

separation apparatus was able to consistently separate uranium from the synthetic urine solutions with a consistent recovery between ten and fifteen percent and up to fifty percent. Furthermore, the system requires a fraction of the material needed in current bioassay systems. While state of the art practice uses at least 1 mL per sample, this electrochemical separations method needs only 0.1 mL. Furthermore, the major salt interferences are largely reduced from the sample allowing better ICP-MS analysis with decreased plasma loading and memory effects from the organic interferences contained within the urine samples. The method is isotope independent and maintains the enrichment of any excreted material. This allows for the material to be compared to operational logbooks at facilities using multiple enrichments in the nuclear fuel cycle.

This methodology is recommended for spot estimation in support of a traditional bioassay program. The Nuclear Regulatory Commission threshold monitoring requirement (15 µg/L) for bioassay program is five orders of magnitude higher than the system developed here. As a result, it is not recommended for primary or bulk urinalysis within a bioassay program. The best use is for individual unknown exposures and follow-up bioassay samples. The system requires a deft and experienced hand to ensure smooth and consistent operation. But in compliment to another system, this methodology should provide an excellent tool in following up on exposures to help prevent any further occupational exposures.

The inverse analysis of a uranium excretion analysis is capable of determining the type of absorption: Inhalation (fast, moderate, or slow), Injection, or Ingestion. Typically any inhalation exposure will have components of both fast, moderate, and

slow absorption, but the inverse system identifies which of the absorptions dominate the exposure. This information in concert with situational data should be able to confirm the material or method of exposure. The methodology is also capable of estimating the time frame of an exposure within an error margin of one week. However, the method is only as good as the available data. With increased data points, the performance increases to a point. Modeling biological systems is a complex problem that has a large uncertainty from the extraordinarily large number of independent variables from background sources to biological excretion variance. Independently, the method cannot recreate the exact scenario, but it can be a valuable asset when investigating exposures to protect the health and safety of nuclear workers.

Continued work on the electrochemical system could improve its usefulness. Several geometry recommendations, including a larger surface area electrode and offset position, could prove to increase both throughput and sensitivity. The same system has been used to separate other higher actinides from solution and should be tested for separation of those actinides from urine. Ideally, this could be the first tool validated for plutonium and uranium bioassay analysis through two identical systems in series.

There are several potential future expansions of this work. This system could be investigated for successive separations of plutonium, uranium, neptunium, and americium either in series or in parallel configurations. Since one of the goals is to reduce analysis time, a similar system could be coupled with an ICP-MS instrument to provide even quicker analysis of samples. The preprocessing procedures for bioassay are being compared to new microwave digestion procedures to further reduce overall

analysis time by reducing the time needed to break down organic constituents of the urine matrix. Coupling microwave digestions with anodized glassy carbon electrode preconcentration could provide a very rapid analysis when investigating biological samples. However, the most interesting expansion of this work would be an in depth study related to the anodization procedure and the related higher actinide affinity. Understanding the active oxygen groups on the surface of the electrode after anodization is a large research endeavor. This overall project could be broken into smaller sections researching the adsorption mechanisms, the efficiency of anodization, adsorption saturation, and anodization fractions between the expected functional groups. The applications for the anodized glassy carbon separations process are wide and varied.

REFERENCES

1. Nobelprize.org. *"Marie Curie - Biography"*. [cited 2013 Feb. 14]; Available from: http://www.nobelprize.org/nobel_prizes/physics/laureates/1903/marie-curie-bio.html.

2. World Nuclear Association. *WNA Nuclear Century Outlook*. 2013 [cited 2013 Feb. 14]; Available from: http://www.world-nuclear.org/outlook/clean_energy_need.html.

3. Nuclear Energy Institute. *Nuclear Statistics*. 2013 [cited 2013 Feb. 14]; Available from: http://www.nei.org/resourcesandstats/nuclear_statistics.

4. International Atomic Energy Agency. *Nuclear Fuel Cycle & Waste Technology*. 2013 [cited 2013 Feb 15th]. Available from: http://www.iaea.org/OurWork/ST/NE/NEFW/home.html

5. Nuclear Regulatory Commision., *Bioassay at Uranium Mills*,.Nuclear Regulatory Research. 1998: Washington, DC.

6. Taylor, G.A., *Evolution of Internal Dosimetry at the Savannah River Site*, Westinghouse Savannah River Company. (WSRC-MS-2000-00290). 2000: Aiken, SC.

7. Scott, C.M. and West, L.M., *Sixteen Years of Uranium Personnel Monitoring Experience in Retrospect.* Health Physics, 1979. **36**(6): p. 665-69.

8. Bogard, J.S., *Review of Uranium Bioassay Techniques*, Oak Ridge National Laboratory. 1996: Oak Ridge, TN.

9. Taylor, G.A., *The Evolution of Internal Dosimetry Bioassay Methods at the Savannah River Site*, 2000: Savannah River Site.

10. Karpas, Z., *Uranium Bioassay - Beyond Urinalysis.* Health Physics, 2001. **81**(October): p. 4.

11. Prasad, M. V. R., Surya Narayana, D. S., Jeevanran, R. K., and Sundararajan, A. R. *Review of Literature on Bioassay Methods For Estimating Radionuclides in Urine*, Indira Gandhi Centere for Atomic Research, Editor 1991: Kalpakkam, India.

12. McCurdy, D., Lin, Z., Inn, K. G. W., Bell III, R., Wagner, S., Efurd, D. W., Steiner, R., Duffy, C., Hamilton, T. F., Brown, T. A., and Marchetti, A. A. *Ultra-*

sensitive Mass Spectrometric and Other Advanced Methods Applied to Biological Samples; Second Interlaboratory Comparison Study for the Analysis of 239Pu in Synthetic Urine at the µBq (~100 aCi) Level by Mass Spectrometry. Journal of Radioanalytical and Nuclear Chemistry, 2004. **263**(2): p. 447-455.

13. Little, T., Miller, G., Guilmette, R. and Bertelli, L. *Uranium Dose Assessment: A Bayesian Approach to the Problem of Dietary Background.* Radiation Protection and Dosimetry, 2007. **127**(1-4): p. 333-338.

14. Kinman, W., LaMont, S., Steiner, R. *A Rapid Isotope Dilution Inductively Coupled Plasma Mass Spectrometry Procedure for Uranium Bioassay.* J. Radioanalytical Nuclear Chemistry, 2009. **282**: p. 1027-1030.

15. Kumar, R., Yadav, J.R., Rao, D., Chand, L. *Determination of Uranium Isotopes in Urine Samples from Radation Workers using U-232 Tracer, Anion Exchange Resin, and Alpha Spectrometry.* J. Radioanalytical Nuclear Chemistry, 2008. **279**: p. 787-790.

16. Attrep Jr., M., Efurd, D. W., Midkiff, W. S., and Covey, J. R. *Practical Radiometric and Mass Spectrometric Analytical Measurements of the Actindes*, L.A.N. Laboratory, Editor 1993: Los Alamos, NM.

17. Eckerman, K. F. , Kerr, G. D., *Y-12 Uranium Exposure Study*, Oak Ridge National Laboratory, Editor 1999: Oak Ridge, TX.

18. Putnam, D.F., *Composition and Concentrative Properties of Human Urine*, 1971: Huntington Beach, CA.

19. Lam, N. K., Kalvoda, R., and Kopanica, M. *Determination of Uranium by Adsorptive Stripping Voltammetry.* Analytica Chimica Acta, 1983. **154**: p. 79-86.

20. Wang, J., Wang, J., Lu, J. and Olsen, K. *Adsorptive Stripping Voltammetry of Trace Uranium: Critical Comparison of Various Chelating Agents.* Analytica Chimica Acta, 1994. **292**: p. 91-97.

21. Pretty, J. R., Duckworth, D. C., and Van Berkel, G. J. *Anodic Stripping Voltammetry Coupled On-Line with Inductively Coupled Plasma Mass Spectrometry: Optimization of a Thin-Layer Flow Cell System for Analyte Signal Enhancement.* Analytical Chemistry, 1997. **69**(17): p. 3544-3551.

22. Pretty, J. R., Duckworth, D. C., and Van Berkel, G. J. *Electrochemical Sample Pretreatment Coupled On-Line with ICP-MS: Analysis of Uranium Using an Anodically Conditioned Glassy Carbon Working Electrode.* Analytical Chemistry, 1998. **70**(6): p. 1141-1148.

23. Pretty, J. R., Deng, H., Goeringer, D. E., and Van Berkel, G. J. *Electrochemically Modulated Preconcentreation and Matrix Elimination for Organic Analytes Coupled On-Line with electrospray Mass Spectrometry.* Analytical Chemistry, 2000. **72**(9): p. 2066-2074.

24. Schwantes, J.M., *Utility of Mechanistic Models for Directing Advanced-Separations Research and Development Activities: Electrochemically Modulated Separation Example*, U.S. Department of Energy, Editor 2009: Pacific Northwest National Laboratory. (Report Number PNNL-18434)

25. Engstrom, R., *Electrochemical Pretreatment of Glassy Carbon Electrodes.* Analytical Chemistry, 1982. **54**: p. 2310-2314.

26. Clark, Jr, W. J., Park, S. H., Bostick, D. A., Duckworth, D. C., and Van Berkel, G. J. *Electrochemically Modulated Spearation, Concentration, and Detection of Plutonium and Uranium Using an Anodized Glassy Carbon Electrode and Inductively Coupled Plasma Mass Spectrometry.* Analytical Chemistry, 2006. **78**(24): p. 8535-8543.

27. McCreery, R.L., *Carbon Electrodes: Structural Effects on Electron Transfer Kinetics*, in *Electroanalytical Chemistry*, A. Bard, Editor. 1991. p. 221-373.

28. Duckworth, D. C., Liezers, M., Lehn, S. A., and Douglas, M. *Electrochemically-Modulated Separation and Mass Spectrometric Analysis of Actinides in Difficult Matrices*, in *Proceedings of the 8th International Conference on Facility Operations-Safeguards Interface March 30-April 4, 2008*, American Nuclear Society, IL, Editor 2009: Portland, OR.

29. Duckworth, D. C., Liezers, M., Lehn, S. A. *Electrochemically-Modulated Separation and Mass Spectrometric Analysis of Actinides in Difficult Matrices*, in *Workshop on Harsh- Environment Mass Spectrometry (HEMS)* 2007: Coco Beach, FL.

30. Duckworth, D. C., Van Berkel, G. J., and Riciuti, L. R. *Electrochemically-Modulated Separation and Concentration of Actinides Including Uranium and Plutonium*, 2005, Oak Ridge National Laboratory: Oak Ridge, TN. p. 8.

31. Liezers, M., Pratt, S. H., Hart, G. L., and Duckworth, D. C. *Electrochemically Modulated Separations for Rapid and Sensitive Isotopic Analysis.* J. Radioanalytical Nuclear Chemistry, 2013. **296**: p. 1037-1043.

32. Heineman, P.T., and Heineman, W. R. editors. *Laboratory Techniques in Electroanalytical Chemistry*. 2nd ed., rev. and expanded. ed. 1996, Marcel Dekker, Inc.: New York, NY. 986.

33. Bard, A. J., and Faulkner, L. R. *Electrochemical Methods: Fundamentals and Applications*. 2nd ed. 2001, Hoboken, NJ: Wiley & Sons, Inc.

34. Bioanalytical Systems, Inc., *Principles of EC Detection and Troubleshooting Guide*, in *Instruction Manual* 1994. Available from: http://www.basinc.com/mans/pecd.pdf

35. Pretty, J. R. and Van Berkel, G. J. *Electrochemical Sample Pretreatment Coupled On-line with Electrospray Mass Spectrometry for Enhanced Elemental Analysis.* Rapid Communications in Mass Spectrometry, 1998. **12**: p. 1644-1652.

36. Research Center for Deep Geological Environments *Atlas of Eh-pH Diagrams: Intercomparison of Thermodynamic Databases*, National Institute of Advanced Industrial Science and Technology, 2005: Naoto Takeno, Japan.

37. Burguera, M., Burguera, J. L., Rivas, D., Rondon, C., and Carrero, P. et. al, *On-line Electrochemical Preconcentration and Flame Atomic Adsorption Spectrometric Determination of Manganese in Urine samples.* Talanta, 2005. **June**: p. 56.

38. Duckworth, D.C., *Questions*, Personal Communication 2010.

39. Kuwabara, K. and Hoguchi, H. *Development of Rapid Urine Analysis Method for Uranium*. in *10th International Congress for International Radiation Protection Association*. 2000.

40. Giddings, M., *Uranium in Drinking Water*, World Health Organization. 2004. Available from: http://www.who.int/water_sanitation_health/dwq/chemicals/en/uranium.pdf

41. West, L. M.and Scott, C. M. *An Evaluation of U3O8 Exposure with an Estimate of Systemic Body Burden.* Health Physics, 1967. **13**: p. 21-26.

42. Schieferdecker, H., Dilger, H., Doerfel, H., Rudolph, W. and Anton, R. *Inhalation of U Aerosols from UO2 Fuel Element Fabrication.* Health Physics, 1985. **48**(1 (Jan)): p. 29-48.

43. Quastel, M. R., Taniguchi, H., Overton, T. R., and Abbatt, J. D. *Excretion and Retention by Humans of Chronically Inhaled Uranium Dioxide.* Health Physics, 1970. **18**: p. 233-244.

44. Dawson, S., *Navajo Uranium Workers and the Effects of Occupational Illness: A Case Study.* Human Organization, 1992. **51**(4): p. 389-397.

45. Roth, P., Werner, E., and Paretzke, H. G. *A Study of Uranium Excreted in Urine: An Assesment of Protective Measures Taken by the German Army KFOR Contingent*, GSF- National Research Center for the Environment and Health. 2001: Neuherberg, Germany.

46. International Commission of Radiological Protection. *Reference Man: Anatomical, Physiological, and Metabolic Characteristics*, 1975, Pergamon Press: Oxford, UK.

47. International Commission of Radiological Protection. *5. Uranium*, 1969, Pergamon Press: Oxford, UK.

48. Lippman, M., Ong, L. D. Y., and Harris, W. B. *The Significance of Urine Uranium Excretion Data*. American Industrial Hygiene Association Journal, 1964. **25**(Jan-Feb): p. 43-54.

49. Eckerman, K., *User's Guide to the DCAL System*, Oak Ridge National Laboratory. 2006: Oak Ridge, TN.

50. Leggett, R. W., Eckerman, K. F., and Williams, L. R. *An Elementary Method for Implementing Complex Biokinetic Models.* Health Physics, 1993. **64**(3): p. 260-271.

51. Wrenn, M. E. and Bertelli, L. *A Compliation of Abstracts of Published Materials Relating to the Estimation of Lung Burdens from Uranium in Urine Analysis*, Los Alamos National Laboratory. 1992: Los Alamos, NM.

52. International Commission of Radiological Protection. *Uranium (Z=92)*, 2010, Pergamon Press: Oxford, UK.

53. Duckworth, D.C., *AdSV Question*, Personal Commuication. 2012.

54. Bioanalytical Systems, Inc. *LCEC and EC Assessories*, in *Electrode Polishing and Care* 2001. Available from: http://www.basinc.com/mans/epc.pdf

55. Harrison, J. D., Fell, T. P., Pellow, P. G. D., Phipps, A. W., and Puncher, M. *Uncertainty Analysis of the ICRP Systemic Model for Uranium as Applied to Interpretation of Bioassay Data for Depleted Uranium*, Health Protection Agency. 2007: Oxfordshire, UK.

56. Muikku, M., Heikkinen, T., Puhakainen, M., Rahola, T, and Salonen, L. *Assessment of Occupational Exposure to Uranium by Indirect Methods Needs Information on Natural Background Variations.* Health Physics, 2007. **125**: p. 1-4.

57. United Nations. *Sources and Effects of Ionizing Radiation: 2000 Report to the General Assembly, with Scientific Annexes*, United Nations Scientific Committee on the Effects of Atomic Radiation. 2000: New York, NY.

58. Li, W. B., Roth, P., Wahl, W., Oeh, U., Hollriegl, V., and Paretzke, H. *Biokinetic Modeling of Uranium in Man After Injection and Ingestion.* Radiation Environment Biophysics, 2005. **44**: p. 29-40.

59. Hodgson, A., Hodgson, S. A., Stradling, G. N., Birchall, A., Fell, T., Henge-Napoli, M. H., and Ansoborlo, E. *Biokinetics of a Uranium Octoxide-Bearing Aerosol Formed in a New Laser Enrichment Process: Implications for Human Exposure.* Ann. Occup. Hyg., 1997. **41**(Supplement 1): p. 70-76.

APPENDIX A

LOS ALAMOS NATIONAL LABORATORY INTEGRATED WORK DOCUMENT

Los Alamos NATIONAL LABORATORY EST.1943

FILE COPY

Form 2100

IWD Part 1, Activity Specific Information

IWD#: IWD-RC45-0050 Revision#: 0			**Activity/Task Title** Electrochemical Separations
Work Document # ~~IWS-NTR-INR~~ 3C040A-4745-C-NR			**Planner/Preparer (Name/Z No./Date)** James Miller / 219009 / 10/17/2010
TA 48	**Building** 45	**Room** N102, E104B, E115	**Other Location(s)(TA) as required** N/A

Activity Description/Overview

This IWD covers the electrochemical separation of trace uranium (1dpm/mL) and plutonium from the acidic aqueous solutions to later be analyzed by mass spectrometry. The samples will be preprocessed in the manner which is employed for the bioassay program which can be found in IWD-RC45-0016 Rev. 2.0

List Names of Hazard Analysis (HA) Team (Attach sheet if necessary): Dave Podlesak, Will Kinman, James Miller, Rob Steiner, Pat Foy Date HA Performed: 12/02/10

The RLM approval on indicates IWM has been applied appropriately, work is authorized, workers are qualified, work will be performed in accordance with ESH&Q/Security and Safeguards (S&S) requirements and the IWD, and facility safety basis, aggregate hazards, and collocated hazards were appropriately included in the hazard analysis and acknowledges completion of a peer review.

RLM (Signature/Z#/Date) **Required:** [signature] / 094411 / 12-16-10

The FOD approval indicates work is appropriate to be conducted in this facility (the activity is within the Authorization Basis [AB] and the work is appropriate for the facility), and facility safety basis, aggregate hazards, and collocated hazards will be managed.

Work activities in multiple FOD jurisdictions, e.g., additional facility safety envelopes, require FOD or Representative approval, where applicable.

FODs or FOD Representatives (Signature/Z#/Date/TA) **Required:** [signature] 114272 12/8/10 TA-48

SME(s) Review (Signature/Z#/Date) **If Required:** [signature] 121089 12/7/10 [signature] 092469 RPI 12/14/10

Peer Review (Signature/Z#/Date) **If Required:** [signature] 117667 12/14/10

Hazard Determination by Hazard Grading Table ☐ Low-Hazard ☒ Moderate-Hazard ☐ High-hazard/Complex ☐ Standing IWD	Expiration Date: 12-15-12 **RLM and FOD or FOD Representative** reapproval is required. **Annual Review Completed** (RLM Initial/Date): _____ Name of **Primary PIC** (Print): Rob Steiner Name of **Alternate PIC**: Wil Kinman Name of **Alternate PIC**: _____	Classification review completed, if required. _____ **Reviewer** Signature/Z#/Date

IWD#: IWD-RC45-0050		Revision#: 0	Activity/Task Title Electrochemical Separations
TA 48	Building 45	Room N102, E104B, E115	Other Location(s)(TA) as required N/A

Work Tasks/Steps Identify work steps/tasks in sequence when such sequencing contributes to safety, security, and/or environmental protection.	Hazards, Concerns, and Potential Accidents/Incidents Identify both activity and work-area hazards for each task/step.	Controls, Preventive Measures, and Bounding Conditions Specify preventive measures, controls for each hazard [e.g., lockout/tagout points, specific PPE, Tamper Indicating Device TIDs), alarms, safes, recycle, waste minimization]	Reference Documents List permits, operating manuals, security plans, and other reference procedures.	Training List training and qualification requirements.
All Tasks	CHEMICAL HAZARDS: Low hazard level due to lower concentration of reagents and reduced volume of samples. Spill and Splash hazard concerns *There is a potiential for exposure to ionizing radiation and/or radiological contamination from handling samples. Very low level Plutonium and Uranium activity levels	*This is very low level radation work. Similarly to other work done in RC-45, TLD's are required for all personnel. PPE: *Safety glasses with side shields *Latex gloves or equivalent when handling samples or reagents. Changing gloves when there is known chemcial contact *Laboratory Coat required when working with reagents. *Shorts and open toed shoes not allowed. *Face Shield required when handling greater than 1 L of acid Engineering Controls: *This work will only be done using UL listed or ESO approved equipment *Follow instructions in operating manuals for commercial equipment (potentiostat, Thin flow cell, parastaltic pump, six port peek valve) *Operations to be performed in Chemical hood (the acid components). If the air handling system is not working, then work can not be performed.	P101-6 Personal Protective Equipment P101-14 Chemical Management P-121 Radiation Protection: P101-16 Local Exhaust Ventilation and HEPA Filtration Systems	TP #5875: MCFO TA-48, RC-1 Complex Facility Access TP # 6351: C-INC General Worker Lab Policies TP # 6957: IWM Worker Training Requirements TP # 6778: TA-48 RC-45 Access TP # 115: Radiological Worker II TP # 10341: Ventilation: Fume Hoods TP #4261 General Chemical Worker TP #7015 C-DO General Chemical Wkr TP #2297 Corrosives Hazards Training
Security	There are no security concerns related to this activity.			Access Requirements (site specific training: see all tasks)
Electrode Prep: Polishing: SiC papers, Alumina Slurries, and Sonication using ultrapure water and methanol Polarization: potientiostat digitally controlled voltage oscillations in	*There is a potential for minor skin abrasions during the polishing procedure. The electrode will be polished using succesively finer SiC papers.	Engineering Controls: *Work is to be performed on the bench top or in fume hood *Sonicator is to be used per manufacturer's directions	P101-13 Electrical Safety Program	TP #2914: General Workers: Electrical Hazards TP # 2899: R&D Electrical Workers

IWD#: IWD-RC45-0050		Revision#: 0	Activity/Task Title Electrochemical Separations
TA 48	Building 45	Room N102, E104B, E115	Other Location(s)(TA) as required N/A

conjuction with weak base (0.5 M NaOH) Anodization: Cyclic voltage oscillations using digitally controlled potentiostat in conjuction with weak acid (0.5 M HNO3)	*NOTE: Any injury (Cuts or Abrasions) compromising the integrity of the skin must be reported to RLM and RCT's immediately.* *Chemical Hazards: potential exposure to weak acids. Spill and splash hazard. Electrical Hazards: Electrode Prep done at less than 10 V and less than 1 amp	PPE: Same for all tasks as listed above Administrative Controls: Current and Voltage associated with electrode prep does not pose an electrical shock hazard Whenever assembling or disassembling the flow cell electrode apparatus, verification that electrical currents are not flowing is obtained by removing electrical power from the system (Unplug)		non-energized
EMS Separation: Injection Accumulation Rinse Release	Chemical Hazards: Low Hazard due to lower concentrations of reagents and reduced volume of solutions. Spill and splash hazard potential.	Engineering Controls: *Work is to be performed on the bench top or in fume hood when a hood is necessary D=2.14.2010 *All samples and reagents bottles not being used are to be closed *Sample and reagent transfer is to be done remotely using pumps and valves PPE: Same for all tasks listed above		Same as for All Tasks (above)
Waste Generation: Acid Solutions: store in bottles, transport to RLW sink Unused Chemicals: store for later use	*There is a potential for explosion and/or fire due to energetic reactions between incompatible chemicals *Adverse health effects or respiratory injury could result from chronic and/or acute exposure to toxins such as strong acid vapors, or any inhalation or skin contact with acids. Eye and skin damage may result from contact with strong acids and bases – eg hydrochloric or nitric acid *Improper disposal could result in a release to the environment	Procedural: *Maintain unobstructed access to showers and eyewash stations *Keep combustible and flammable materials away from heat sources. Ensure flammable materials are stored in flammables cabinet. Store acids in acid cabinet. *Utilize MSDS/other information to access the hazard type, level, and mitigation for a given chemical *Contact WMC for information on proper labeling and disposal of waste *Segregate incompatible chemicals and store waste in appropriate SAA *Waste will be bottled from each step and then disposed of in the appropriate waste stream. Most of the waste will be produced during the electrode polishing step. All solutions come out of the EMS separation step will be considered samples for determining the effectiveness of the EMS seperation.	As in above tasks, plus the following: *applicable policy documents: -P409 Waste Management P930-1 Waste Acceptance Waste Profile #: 37842, 30458, 30457,& 35231	TP #256: RCRA Hazardous/Mixed Waste Worker Trng. TP #11228 STO Waste Operations

***Insert Rows above** for additional Tasks/Steps or attach pages to clearly communicate ES&H/S&S hazards and associated controls.*

Los Alamos NATIONAL LABORATORY EST.1943

Form 2102

IWD Part 2
FOD Requirements and Approval for Entry and Area Hazards and Controls

Tenant Activity Form

IWD No./Work Request No: _____ Revision #: _____

FOD must determine the facility entry and coordination requirements and identify the ESH/S&S hazards and controls associated with the activity location.

FOD	TA	Bldg.	Room	Other Location
6	48	45	D102, E104B, E15	
FOD Designated Facility Point-of-Contact	Name Gary Hagermann	Phone 7-6036	Pager 4-9100	Email ghagermann@lanl.gov

Entry and Coordination Requirements (*Check one or more of the following*):

☐ No Entry/Coordination Requirements	☐ FOD designated facility point-of-contact must sign IWD Part 3		
☒ POTD/POTW	☐ Check in at Start of Work	☒ Work-Area Training Required	☐ Security Clearance Requirements
☒ Work must be Scheduled	☐ Check in Daily	☐ Escort Required	☐ Other Security Requirements
☒ Co-located Hazards/Concerns	☐ Check out at End of Work	☐ Quality Issues	
☒ Review under AB/Safety Basis/USQ	☐ Check out Daily	☐ Other Bounding Conditions _____	

Instructions: In the block below, provide facility or work-area information needed by the workers on this activity. (Things to consider include specific work-area hazards and controls, potential conflicts with co-located activities, or any facility restrictions on the activity.) Identify relevant reference documents and any training required.

Facility/Work-Area Information Relevant to this Activity

Plan of the Week: : All facility work must go through the FMO-STO Plan of the Week (POTW). The POTW meeting is conducted weekly (TA-48, RC-1 Conf Rm, Thurs@ 3pm). All work must be scheduled and authorized on the FMO-STO Plan of the Week (POTW). Submit all work online through the POTW Request System (http://www.mst.lanl.gov/dbsystems/pow/frmEntryPOTW.html) prior to attending the meeting.

Co-located Hazards/Concerns: TA-48-1 is a low hazard radiological facility with RCAs (Radiologically Controlled Areas) located throughout the facility. Obey all postings and entry/exit monitoring requirements. Contact local HSR-1 RCTs (4-4648) if any questions/issues arise. Specific laboratory hazards are listed on hazard communication signs posted at each laboratory entry.

Review under AB/Safety Basis/USQ: Required for Facility modifications and new Programmatic work. Contact the Operations Manager prior to the initial walkdown of work scope for new activities. Quantities of radioactive materials are strictly controlled in RC-1. To initiate new experimental activities or bring barcodeable radioactive materials into RC-1, prior approval must be granted by the RC-1 Working Group/"Gatekeeper".

Work-Area Training Required: The following training plans are required to perform work in TA48-1: #5875-TA-48 Complex, #6113-all those who receive handle, store or process radioactive material.

Other Bounding Conditions: Environmental Impacts - A NEPA screen must be completed on all new or modified programmatic and facility work. All regulated waste streams require prior approval and documentation before generation, contact the area Waste Management Coordinator for assistance (996-1477). Historical Building-Ecology Group Historic Bldg approval (5-8961) is required for building modifications that:1) change the exterior appearance of the building; 2) add to or remove parts of the building; 3) remove, relocate, or install scientific/technical equipment (small, portable equipment is excluded); or 4) alter the overall function/floorplan of experimental/technical space.

Other Security Requirements: No 2-way pagers, cameras, or PDAs behind the perimeter fence at TA-48. All personally owned electronic devices (cell phones, cameras, PDAs, laptops, and 2-way pagers) are STRICTLY PROHIBITED within the perimeter fence at TA-48. Other security requirements will be posted for specific areas.

Reference Documents: FSP-C-OPS-4801, PRO-C-DO-007, PRO-C-DO-008, LIR402-510-01, C-INC-POL-1000 or POL-C-SIC-001, C-INC-POL-1001 or POL-C-SIC-002, POL-C-DO-006, POL-C-DO-007, POL-C-DO-009, IMP 300.2 SR-0268-PRO-ALL-NOTIF/INCI

Training Requirements: For site specific training contact the MC-FOD Training Office at 5-9430.

FOD Approval

I have verified that the hazards identified above adequately identify the area hazards and that the IWM process has been applied appropriately.

FOD or Representative (Signature/Z #/Date) **Approval Required** 114272 12/8/10

Date Approval Expires:

Form 2103

Los Alamos NATIONAL LABORATORY EST.1943

IWD Part 3, Validation and Work Release

By signing below, I verify this activity is compatible with current facility configuration and operating conditions.

FOD designated Ops Mgr or other facility point-of-contact for work area

Signature/Z#/Date **(If required by FOD)**: _____

Note: For Standing IWD, release may be given concurrently with signatures on Part 2.

By signing below, I have verified the following:

- I have verified authorization by ensuring approval signatures of the RLM and FOD.
- I have jointly conducted a validation walkdown with workers to confirm the IWD can be performed as written, required initial conditions and other prerequisites are in-place.
- The assigned workers are authorized and are qualified to perform the work in a safe, secure, and environmentally responsible manner.
- I have conducted the pre-job briefing, and all workers have been briefed.
- I have ensured coordination with any required FOD work area representatives (*e.g., area work coordinators*).

Primary PIC (Signature/Z#/Date) **Required**: [signature] / 121399 / 1/13/11

Alternate PIC Signatures **acknowledges** PIC authority is assumed for the first time *(Note: Alternate PICs are required to sign only once, but formal handoff includes conferring with previous PIC to obtain all required information associated with the handoff).*

Alternate PIC (Signature/Z#/Date) **Required**: [signature] / 226215 / 13JAN11

Alternate PIC (Signature/Z#/Date) **Required**: _____

Pre-Job Brief Content

- What are the critical steps or phases of this activity?
- How can we make a mistake at that point?
- What is the worst thing that can go wrong?
- What controls, preventive measures, and bounding conditions are needed?
- What work permits are required and how will we meet their requirements?
- What are the handoffs and coordination requirements among workers and multiple PICs?
- Are there hold-points including those that require sign-offs?
- What are the stop work responsibilities and expectations (e.g. for unanticipated conditions or hazards)?
- How would we respond to alarms and emergencies?
- Are there lessons learned from previous similar work?
- Is other information needed to perform this activity in a safe, secure, and environmentally responsible manner?
- Does everyone agree to the work tasks/steps, hazards, and controls and commit to follow them?

Pre-Job Brief Attendance Roster

By signing below **as required**, I agree to the following:

- I agree to follow the work steps and implement the controls as written as applicable to my work assignments.
- I agree to stop work when conditions or hazards change or when I encounter unexpected conditions during the execution of work, or when work cannot be performed as written, or instructions become unclear during execution.
- I confirm that I am authorized, qualified, and fit to perform the work.

Worker (Signature/Z#/Date) [signature] 226215 13JAN 11	**Worker** (Signature/Z#/Date)
Worker (Signature/Z#/Date) [signature] / 121399 / 1/13/11	**Worker** (Signature/Z#/Date)
Worker (Signature/Z#/Date) [signature] / 219009 / 1/13/11	**Worker** (Signature/Z#/Date)
Worker (Signature/Z#/Date)	**Worker** (Signature/Z#/Date)

Form 2103 (7/10) (P300)

Los Alamos NATIONAL LABORATORY EST. 1943

Form 2104

IWD Part 4, Post Job Review

IWD #: _____ Revision #: _____

A post-job review with the workers and PIC should include the following:

- Verify that the activity is complete and make notifications in accordance with FOD requirements;
- Ensure that follow-through actions (*e.g. clean-up, recycle, waste disposal, equipment removal, and secure storage*) are completed;
- Identify inefficiencies, problems during the activity, coordination issues, unanticipated conditions, and near misses; and
- Develop recommendations for improvement.

Lessons learned; safety, security, and environmental issues; coordination issues; and unexpected conditions.
Suggested improvements to enter into the JHA Tool, Foot Prints, or other integrated work control data bases supported by Lessons Learned.
Other recommendations for improvements to performing this activity. State the positive attributes of this activity.

Completion Statement

By signing below, I have verified that the activity scope, final worksite ESH&Q/S&S restoration, and cleanup are complete, and I have ensured proper notifications and turnover in accordance with FOD requirements.
PIC (Signature/Z #/Date) **Required:**

Form 2104 (7/10) (P300) Page ___ of ___

Subject: Hazard Analysis Meeting for IWD
From: "James C. Miller" <jcmiller@lanl.gov>
Date: Fri, 3 Dec 2010 11:15:33 -0700
To: "'Danielle F Roybal'" <danir7@lanl.gov>, <cjb@lanl.gov>

Carol and Danielle,

We held the IWD Hazard analysis meeting for my IWD (IWD-RC45-0050) on Dec 2, 2010 at 8.30 AM. The people present for the formal HA meeting were Dave Podelsak, Will Kinman, and Myself. I previously had discussions with Rob Steiner and Pat Foy. Both of them were unavailable for the official HA meeting.

At the meeting we discussed the procedure for polishing the electrode as well as the sample accumulation on the electrode. We discussed the strength of the acids and reagents to be used during the procedure. We also discussed the sampling method as well as waste disposal of the small amount of waste generated.

I previously discussed the electrical safety measures with both Rob and Pat. The voltages and currents used are well beneath the minimum for ESO concern (less than 2 volts and less than 10 amps). And we are using only certified electronic equipment. We also added the provision to unplug any equipment while assembling or disassembling.

Please let me know if you need any more details of the HA done for this particular IWD. Thank you.

James

--
James C. Miller
Nuclear and Radiochemistry (C-NR)
Los Alamos National Laboratory
Email: jcmiller@lanl.gov
Phone: (505) 606-2015

APPENDIX B

CAD DRAWINGS OF FLOWCELL

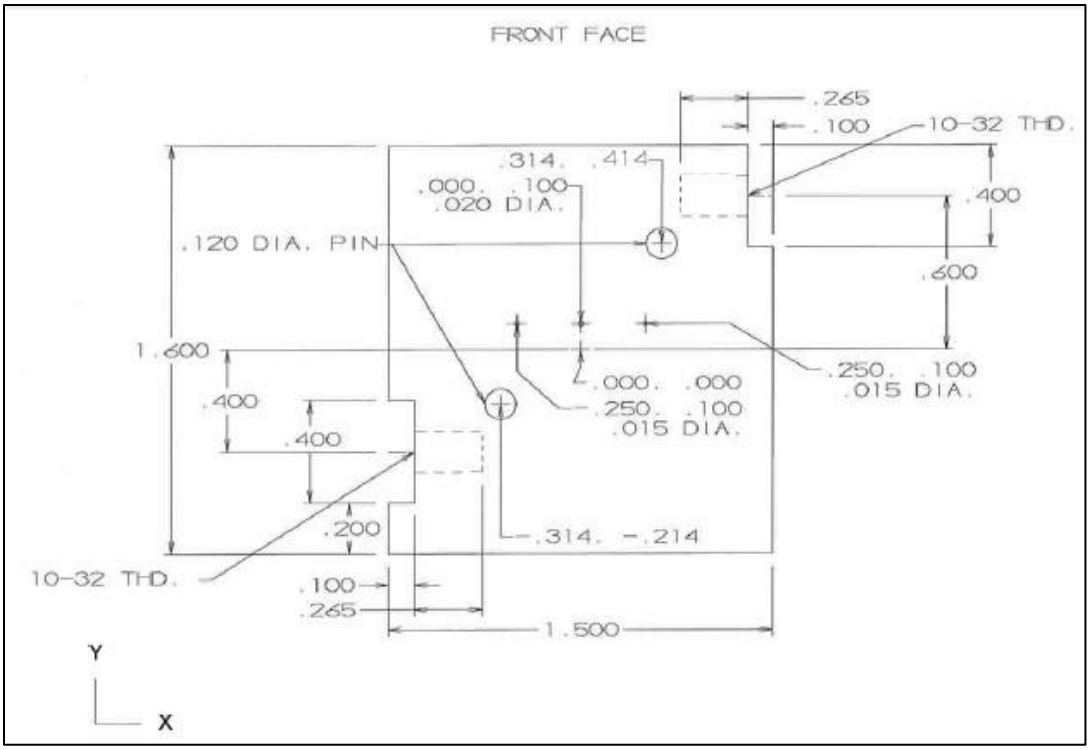
FRONT FACE
.265
.100
10-32 THD.
.314, .414
.000, .100
.020 DIA.
.400
.120 DIA. PIN
.600
1.600
.250, .100
.015 DIA.
.000, .000
.250, .100
.015 DIA.
.400
.400
.200
.314, -.214
10-32 THD.
.100
.265
1.500
Y
X

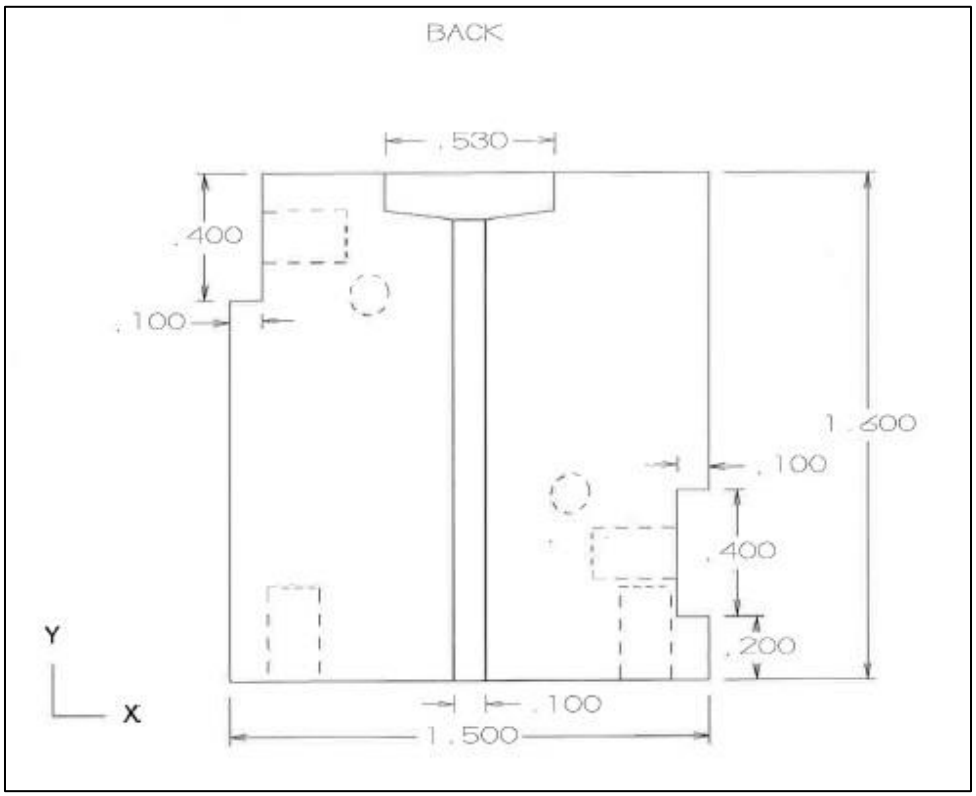
BACK
.530
.400
.100
1.600
.100
.400
.200
Y
X
.100
1.500

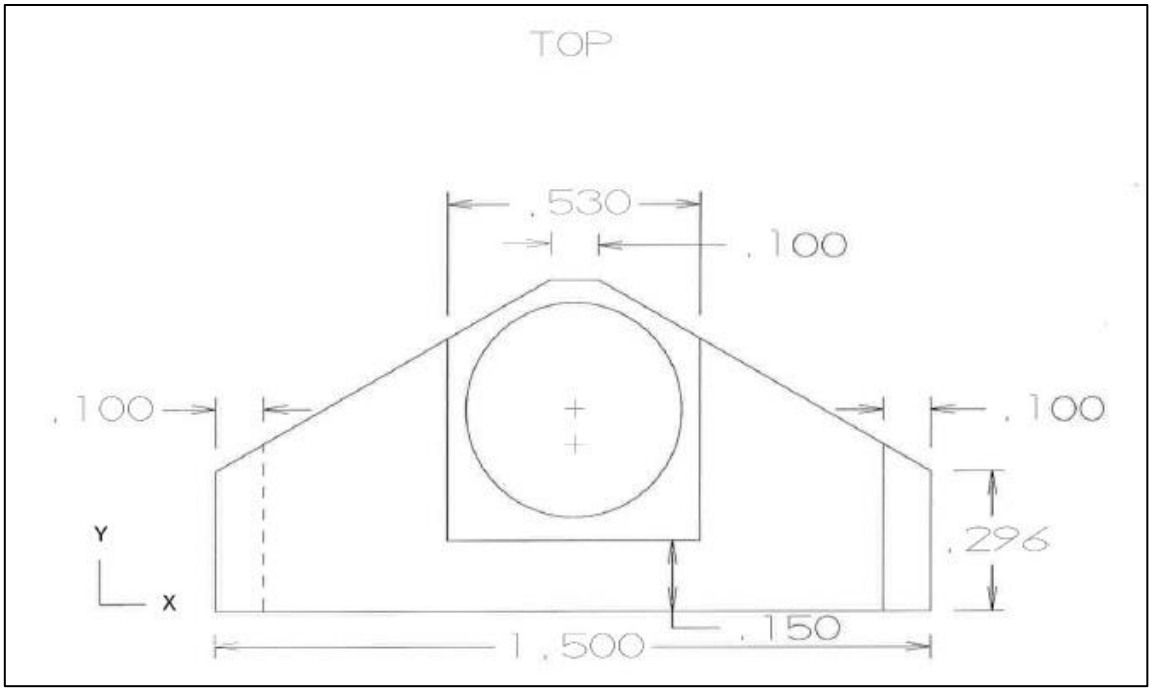
TOP
.530
.100
.100
.100
.296
Y
X
.150
1.500

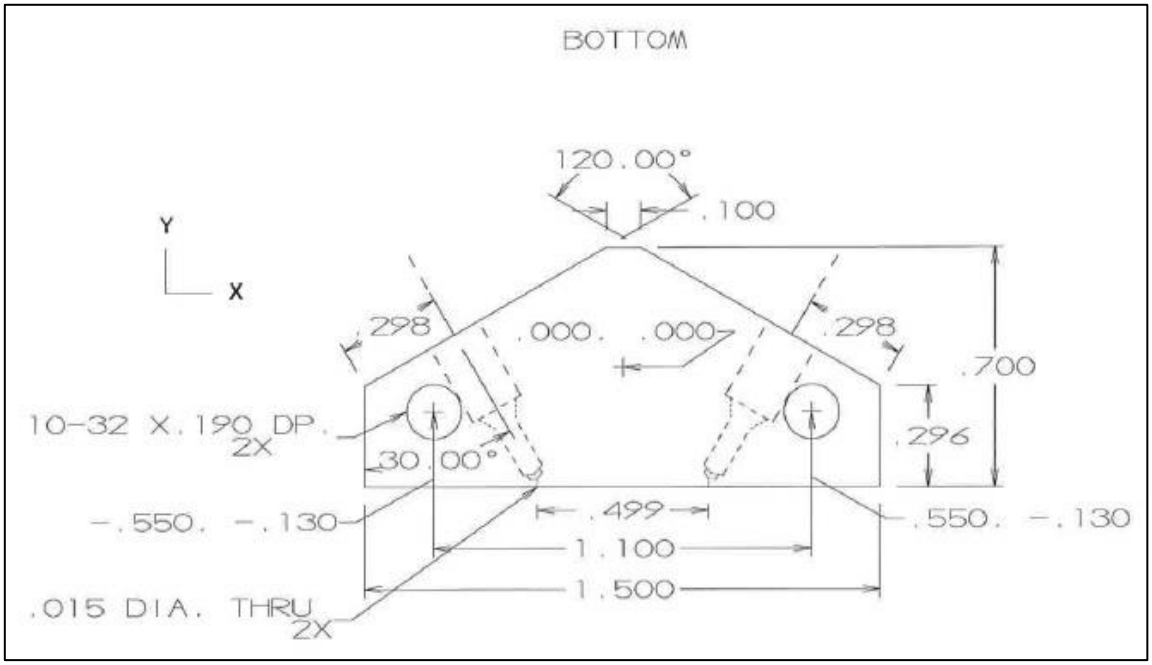
BOTTOM
120.00°
.100
Y
X
.298
.000
.000
.298
.700
10-32 X.190 DP.
2X
30.00°
.296
-.550.
-.130
.499
.550.
-.130
1.100
1.500
.015 DIA. THRU
2X

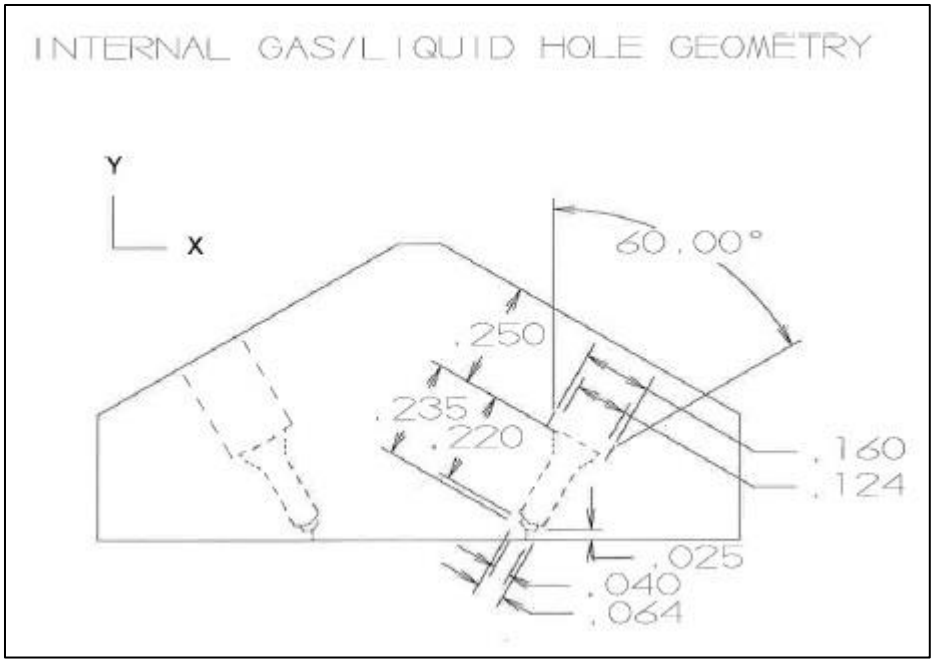
INTERNAL GAS/LIQUID HOLE GEOMETRY
Y
X
60.00°
.250
.235
.220
.160
.124
.025
.040
.064

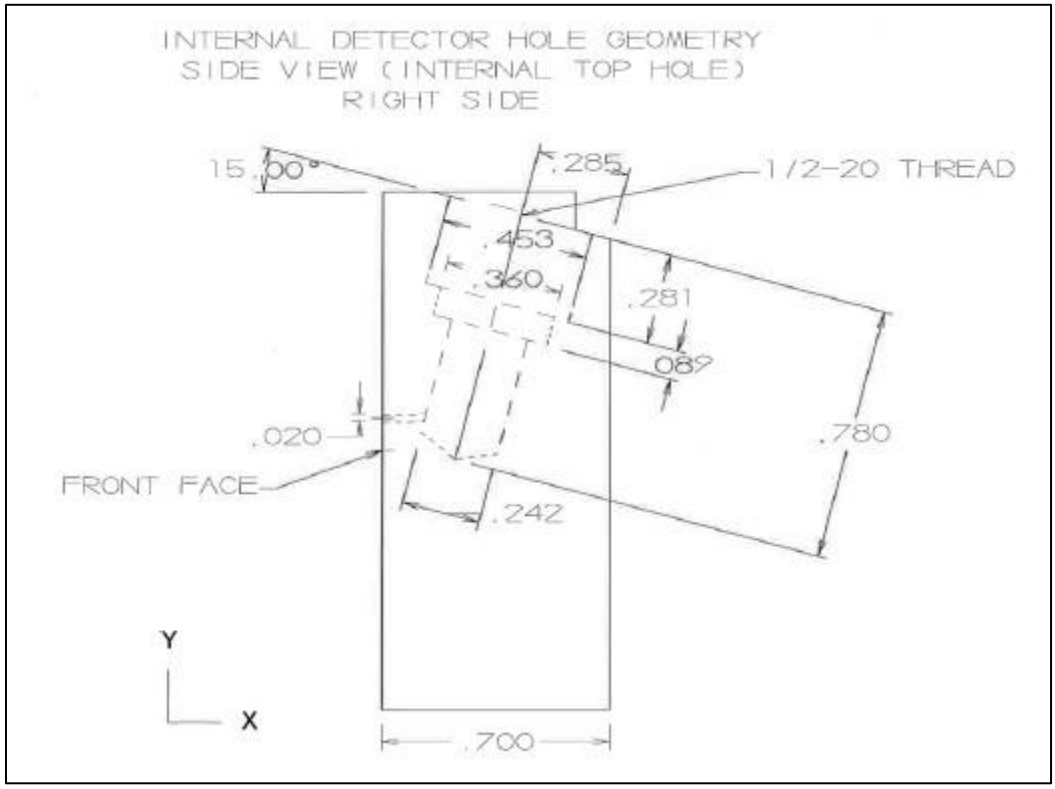
INTERNAL DETECTOR HOLE GEOMETRY
SIDE VIEW (INTERNAL TOP HOLE)
RIGHT SIDE
15.00°
.285
1/2-20 THREAD
.453
.360
.281
.089
.020
FRONT FACE
.780
.242
Y
X
.700

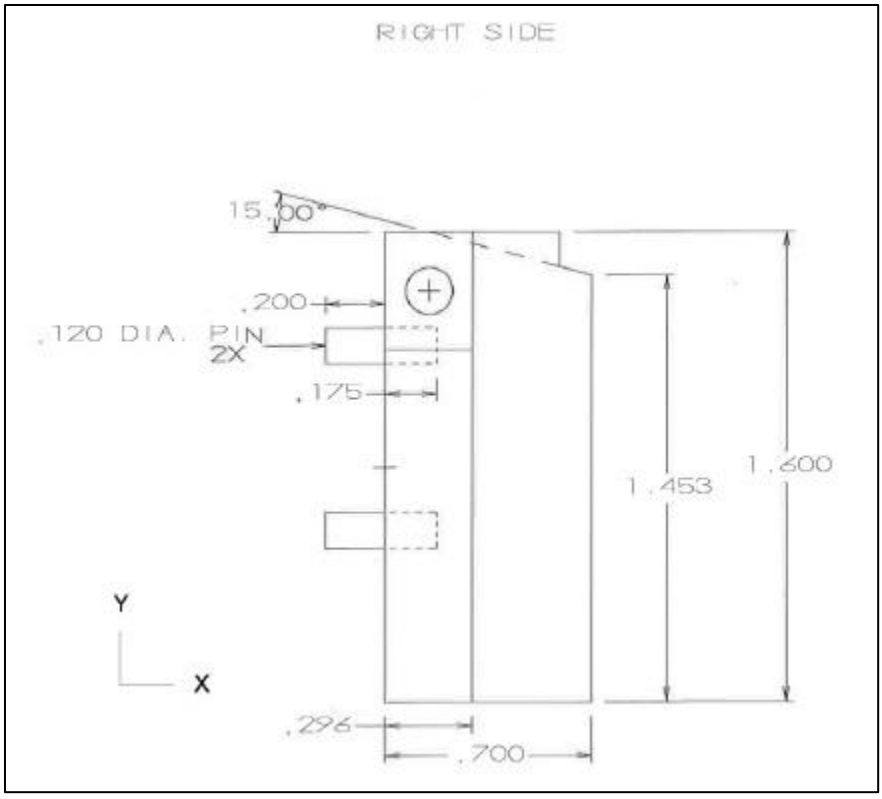
RIGHT SIDE
15.00°
.200
.120 DIA. PIN
2X
.175
1.600
1.453
Y
X
.296
.700

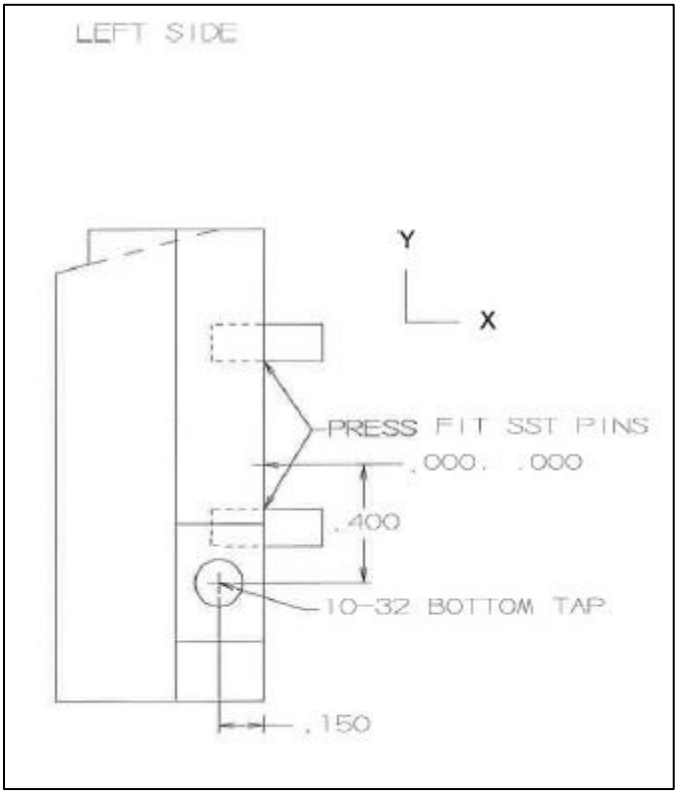
LEFT SIDE
Y
X
PRESS FIT SST PINS
.000 .000
.400
10-32 BOTTOM TAP
.150

APPENDIX C

SYNTHETIC URINE PACKING SHEET AND CONTENTS

DOELAP IN VITRO SAMPLE INFORMATION FOR LABORATORIES

The reporting deadline is **Wednesday April 18, 2012, 12:00 (Noon) MST**. DOELAP will send an e-mail with instructions for reporting results at least 2 weeks prior to the reporting deadline. A performance evaluation report will be issued within 60 days after the closing date for reporting results.

INSTRUCTIONS FOR LABORATORIES

NOTE: Collusion, either between participants or between individual participants and DOELAP, is contrary to professional scientific conduct and serves only to nullify the benefits of proficiency testing. By reporting radiobioassay DOELAP results, you attest to the fact that the reported analytical results were generated by your facility and are not a result of collusion with any other analytical body. Any participant found guilty of collusion will be in breach of conduct and will have their application for radiobioassay DOELAP accreditation immediately terminated and may face other for cause adverse actions.

1. Please send an e-mail to marletgm@id.doe.gov confirming receipt of the performance evaluation (PE) samples. Also include the name of the person at your laboratory responsible for submitting DOELAP results, their e-mail address, and phone number.

2. The service laboratory shall use the counting procedure and counting times normally employed for analysis of that radionuclide in worker measurements or contract. Any deviations from the routine measurement protocol shall be documented in the report to the performance testing laboratory.

3. Please use the sample identification numbers when submitting data or correspondence. The number of performance testing samples you receive is dependent on the request made by your laboratory in the application package.

4. The analytical results should be reported with associated uncertainties in units of pCi per sample for the synthetic fecal (SF) samples and units of pCi/L for the synthetic urine (SU) samples. The SU samples for the analysis of elemental uranium (EL suffix) should be reported in units of ug/L. The experimental results should be reported as determined at the time of measurement and should not be decay corrected. DOELAP will perform the decay correction based on the reported time of measurement. The experimental uncertainties should be expressed at one standard deviation.

5. Eleven samples are included in a set of performance evaluation standards. Five samples are blanks and six samples are spiked with known activities of NIST

traceable radionuclides. Please analyze the samples for the radionuclides requested by your laboratory in the application package. If your analytical determination of uranium is based on KPA, mass spectrometry or other non-radiochemical counting methods, a separate set of urine samples will be included.

Sample identification numbers are coded to indicate matrix and categories of testing:

SU: Synthetic Urine **EL: Elemental Uranium** **BK: Blank**

SF: Synthetic Fecal **MR: Mixed Radionuclide**

SU--MR: Synthetic Urine Matrix may contain ^{90}Sr, $^{228/232}$Th, ^{230}Th, $^{238/234}$U, ^{235}U, ^{238}Pu, $^{239/240}$Pu, ^{241}Am, ^{137}Cs, and ^{60}Co (also ^{237}Np if requested).

SU--EL: Synthetic Urine containing ^{238}U, ^{234}U, and ^{235}U to be determined by non-radiochemical counting methods.

SU--BK: Synthetic Urine containing no added radionuclides.

SF--MR: Synthetic Fecal Matrix may contain ^{90}Sr, $^{228/232}$Th, ^{230}Th, $^{238/234}$U, ^{235}U, ^{238}Pu, $^{239/240}$Pu, ^{241}Am, ^{137}Cs, and ^{60}Co (also ^{237}Np if requested).

SF--BK: Synthetic Fecal containing no added radionuclides.

SAMPLE PREPARATION

6. **Synthetic Fecal Samples:**
The entire fecal sample must be taken for analysis. Analytical results should not be reported for the blank samples; however the blank sample results should be subtracted from the PE samples.

Note: Fecal samples have been mixed, but are not homogenous enough to be subdivided before complete dissolution.

7. **Synthetic Urine Samples:**
Radiological Analyses – MR Suffix: (prepare 1.0 L total sample volume)
Eleven jars each contain about 34 grams of salts for mixed radionuclide analyses. Each salt sample must be diluted to 1000 mL with 2% nitric acid prior to analyses. Five of the jars contain blank urine salts. The remaining six samples contain known activities of NIST traceable radionuclides within the testing range defined in DOE-STD-1112-98. Analytical results should not be reported for the blank samples; however the blank sample results should be subtracted from results obtained for the PE samples. Please report a minimum of five results from the six samples.

Elemental Uranium Analyses – EL Suffix: (prepare 0.5 L total sample volume) Eleven jars each contain about 17 grams of salts for elemental uranium analyses. Each salt sample must be diluted to 500 milliliters (mL) with 2% nitric acid. **Do NOT dilute to 1000 mL as described above for radiological analyses.** Five of the jars are blank urine samples. Analytical results should not be reported for the blank samples; however the blank sample results should be subtracted from results obtained for the PE samples. The remaining six samples contain known activities of NIST traceable radionuclides within the testing range defined in DOE-STD-1112-98. Please report a minimum of five results from the six samples.

Note: The entire sample should be taken for analysis. The urine salts provided are not homogenous enough to be subdivided before dissolution.

REPORTING RESULTS

8. Please report the analytical results and associated uncertainties, expressed at one standard deviation, in the following units:

    a. **Synthetic Fecal Samples (SF) - pCi/sample.**

    b. **Synthetic Urine Samples (SU) Mixed Radionuclide (MR) suffix - pCi/L**

    c. **Synthetic Urine Samples (SU) Elemental Uranium (EL) suffix - ug/L**

9. Detailed instructions for reporting results will be provided in an e-mail approximately two weeks before the reporting deadline.

Each sample contains a total activity of less than the 49 CFR 173.436 DOT regulation limits.

The artificial fecal material is not a RCRA hazardous waste. It is the responsibility of the participant laboratory to be aware of the analytical procedures performed on the sample and how those procedures may or may not affect the regulatory status of any resulting waste.

If you have any questions regarding the sample(s), please contact Guy Marlette at 208-526-2532 (marletgm@id.doe.gov).

MINIMUM TESTING LEVEL (MTL)
FOR INDIRECT RADIOBIOASSAY PERFORMANCE TESTING

MEASUREMENT CATEGORY		RADIONUCLIDE[a]	MTL [b] (Per L or per sample)
I.	BETA activity: average energy <100 keV	Hydrogen-3 Carbon-14 Sulfur-35 Radium-228	2 kBq (54 nCi) 2 kBq (54 nCi) 20 Bq (0.54 nCi) 0.9 Bq (24 pCi)
II	BETA activity: Average energy = or >100 keV	Phosphorus-32 Strontium-89/-90 or Strontium-90	4 Bq (0.11 nCi) 4 Bq (0.11 nCi)
III	ALPHA activity: Isotopic analysis	Thorium-228/-230 or Thorium-232 Uranium-234/-235 or Uranium-238 Neptunium-237 Plutonium-238 or Plutonium-239/240 Americium-241	0.02 Bq (0.54 pCi) 0.02 Bq (0.54 pCi) 0.01 Bq (0.27 pCi) 0.01 Bq (0.27 pCi) 0.01 Bq (0.27 pCi)
IV	Elements (mass/volume)	Uranium	1 ug
V	GAMMA (photon) activity	Cesium-137 Cobalt-60 Iodine-125	2 Bq (54 pCi) 2 Bq (54 pCi) 0.4 kBq (11 nCi)

[a] Indirect bioassay service laboratory may elect to be tested for a specific radionuclide or elect to be tested for the category. The testing laboratory will select the test radionuclide if a category is requested.

[b] The upper bound of the testing range shall not exceed 20 times the stated MTL.

Department of Energy - Idaho Field Office
DOELAP Radiobioassay Team
Sample (Fecal) Information and Receiver Notice

The information presented in this notice concerning quality control samples contained in this package is intended for use in the final disposal of excess sample material and to aid the disposal of analytical waste. The sample material provided is artificial fecal matter consisting of the following components:

COMPONENT	g/SAMPLE
Calcium Hydroxide ($Ca(OH)_2$)	0.97
Ferric Ammonium Sulfate (NH_4FeSO_4)	0.04
Magnesium Carbonate ($MgCO_3$)	0.61
Potassium Carbonate (K_2CO_3)	0.83
Ammonium Dihydrogen Phosphate (H_6NO_4P)	2.10
Sodium Sulfate (Na_2SO_4)	0.37
Ammonium Chloride (NH_4Cl)	0.04
Zinc Sulfide (ZnS)	0.01
Stannous Sulfide (SnS)	0.03
Leucine ($C_6H_{13}NO_2$)	7.10
Lysine ($C_6H_{14}N_2O_2$)	5.10
Methionine ($C_5H_{11}NO_2S$)	0.80
Threonine ($C_4H_9NO_3$)	2.00
Palmitic Acid ($C_{16}H_{32}O_2$)	3.00
Stearic Acid ($C_{18}H_{36}O_2$)	2.00
Cellulose $(C_6H_{10}O_5)_n$	4.00
Gelatin	5.00
Oleic Acid ($C_{18}H_{34}O_2$)	1.00
Peanut Oil	1.50
Water (distilled hot) (H_2O)	65 mL

Department of Energy - Idaho Field Office
DOELAP Radiobioassay Team
Receiver Notice and Sample (Urine) Information

The information presented in this notice concerning quality control samples contained in this package is intended for use in the final disposal of excess sample material and to aid the disposal of analytical waste. The sample material provided is synthetic urine salts consisting of the following components:

COMPONENT	g/L
Urea (CH_4N_2O)	16.00
Sodium chloride (NaCl)	2.32
Potassium chloride (KCL)	3.43
Creatinine ($C_4H_7N_3O$)	1.10
Sodium sulfate ($Na_2SO_4 \cdot H_2O$)	4.31
Hippuric acid ($C_9H_9NO_3$)	0.63
Ammonium chloride (NH_4Cl)	1.06
Citric acid ($C_6H_80_7$)	0.54
Magnesium sulfate ($MgSO_4$)	0.46
Sodium phosphate, monobasic ($NaH_2PO_4 \cdot H_2O$)	2.73
Calcium chloride ($CaCl_2 \cdot 2H_2O$)	0.63
Oxalic acid ($C_2H_2O_4$)	0.02
Lactic acid ($C_3H_6O_3$)	0.09
Glucose ($C_6H_{12}O_6$)	0.48
Sodium silicate ($Na_2SiO_3 \cdot 9H_2O$)	0.07
Pepsin	0.03
(H_2O for H-3 analysis only)	(966.00)

Each sample contains a total activity of less than the 49 CFR 173.436 DOT regulation limits.

The artificial urine material is not a RCRA hazardous waste. It is the responsibility of the participant laboratory to be aware of the analytical procedures performed on the sample and how those procedures may or may not affect the regulatory status of any resulting waste.

If you have any questions regarding the sample(s), please contact Guy Marlette at 208-526-2532 (marletgm@id.doe.gov).

END OF INSTRUCTIONS

APPENDIX D

OLD GEOMETRY DATA CHART

Old Geometry (ng U unless otherwise noted)													
c/s	Sample	V	FR	FT	± FT	E	± E	R	± R	% R	± %R	Load	% D
c	71112	-0.15	60	0.1	0.001	0.011	0	0	0	9.91	0.10	0.11	101.82
c	80112	-0.2	60	0.085	0.002	0.013	0	0	0	13.27	0.31	0.091	109.89
c	80212	-0.2	75	0.166	0.004	0.02	0	0	0	10.75	0.26	0.214	88.79
c	81312	-0.2	60	0.222	0.002	0.019	0	0	0	7.88	0.07	0.257	94.55
c	081312D	-0.2	30	0.243	0.004	0	0	0	0	0.00	0.00	0.259	95.37
c	081312T2	-0.2	20	0.153	0.002	0.068	0.001	0	0	30.77	0.42	0.26	86.15
c	81412	-0.2	30	0.205	0.003	0.03	0	0	0	12.77	0.19	0.258	92.25
c	a	-0.2	10	0.172	0.019	0.017	0.002	0	0	8.99	1.00	0.242	86.78
c	A4*	0	0	0.111	0.006					0.00	0.00	0.119	98.32
c	b	-0.2	10	0.159	0.015	0.01	0.001	0.001	0	5.92	0.56	0.242	76.86
c	C**	-0.2	5	0.071	0.01	0.013	0.001	0.023	0.001	15.48	2.18	0.111	106.31
c	D**	-0.2	7.5	0.065	0.003	0.011	0	0.02	0	14.47	0.67	0.118	83.90
c	E	-0.2	10	0.065	0.005	0.004	0	0.007	0	5.80	0.45	0.11	73.64
c	F	-0.2	15	0.081	0.004	0.009	0.001	0.007	0.001	10.00	0.50	0.11	92.73
c	G	-0.17	5	0.072	0.004	0.018	0.001	0.007	0.001	20.00	1.12	0.113	90.27
c	H	-0.17	7.5	0.082	0.008	0.004	0	0.012	0.001	4.65	0.45	0.113	93.81
c	I	-0.17	10	0.093	0.003	0.004	0.001	0.008	0.001	4.12	0.15	0.117	93.16
c	Number1	-0.15	80	0.8985		0.008		0		0.88	0.00	1.009	89.84
c	Number2	-0.15	80	0.6675		0.0091		0		1.34	0.00	1.028	65.82
c	S1	-0.15	100	3.98		0.001		0		0.03	0.00	5	79.62
c	S2	-0.15	100	4.5		0.002		0		0.04	0.00	5	90.04
s	BL1-1	-0.25	5	0.011	0.003	0.001	0.001	0.001	0	8.33	2.29	0.013	130.77
s	DL51-1	-0.3	7.5	0.099	0.005	0.005	0	0.003	0	4.81	0.24	0.125	89.60
s	DL51-2	-0.3	5	0.095	0.007	0.011	0.001	0.003	0	10.38	0.77	0.126	92.86

s	DL51-3	-0.3	10	0.078	0.002	0.004	0	0.002	0	4.88	0.13	0.126	68.25
s	DL51-4	-0.3	7.5	0.092	0.018	0.007	0.001	0.01	0.001	7.07	1.39	0.122	104.92
s	DL51-5	-0.2	5	0.091	0.006	0.002	0	0.007	0.001	2.15	0.14	0.132	80.30
s	DL51-5	-0.2	5	0.067	0.004	0.002	0	0.006	0.001	2.90	0.17	0.132	59.85
s	DL51-6	-0.2	5	0.085	0.008	0.001	0	0.004	0.002	1.16	0.11	0.128	76.56
s	DL51-6	-0.2	5	0.079	0.003	0.001	0	0.004	0.001	1.25	0.05	0.128	67.97
s	DL51-7*	0	5	0.097	0.007					0.00	0.00	0.127	81.89
s	DL51-7*	0	5	0.095	0.006					0.00	0.00	0.127	79.53
s	DL51-8	-0.2	5	0.092	0.006	0.002	0.001	0.003	0.001	2.13	0.15	0.125	83.20
s	DL51-8	-0.2	5	0.092	0.007	0.002	0	0.003	0.001	2.13	0.16	0.125	83.20
s	DL52-5**	-0.235	5	0.084	0.014	0.001	0	0.006	0.001	1.18	0.20	0.129	81.40
s	DL52-6**	-0.25	5	0.099	0.016	0.002	0.001	0.004	0.001	1.98	0.32	0.127	96.06
s	DL52-7**	-0.25	5	0.106	0.008	0.001	0.001	0.003	0.002	0.93	0.08	0.125	95.20
s	DL52-8**	-0.25	5	0.114	0.007	0.002	0.001	0	0.001	1.72	0.11	0.126	98.41
s	DL54-1	-0.25	5	0.088	0.002	0.01	0.001	0.002	0.001	10.20	0.25	0.125	82.40
s	DL54-2***	-0.25	5	0.089	0.003	0.007	0.001	0.001	0.001	7.29	0.26	0.124	81.45
s	DL54-3***	-0.25	5	0.106	0.008	0.005	0	0.001	0.001	4.50	0.34	0.124	96.77
s	DL54-4*	0	5	0.1	0.006						0.00	0.123	86.18

*Control Sample (Flowed Through Apparatus)

**2nd ICP-MS run

***Big Before Blanks

APPENDIX E

NEW GEOMETRY DATA CHART

New Geometry (ng U unless otherwise indicated)												
Sample	V	FR	FT	± FT	E	± E	R	± R	% R	± %R	Load	% D
BL1-2	-0.175	5	0.011	0	0.004	0	0	0	26.67	0.00	0.0135	111.11
BL2-2	-0.175	5	0.008	0.001	0.008	0.001	0.002	0	50.00	8.84	0.014	142.86
BL2-3	-0.175	5	0.009	0.001	0.004	0	0	0	30.77	3.42	0.013	107.69
BL2-1	-0.19	5	0.011	0	0.006	0	0	0	35.29	0.00	0.014	121.43
DL54-5	-0.175	5	0.107	0.002	0.013	0.001	0.006	0	10.83	0.86	0.129	100.00
DL54-6	-0.175	5	0.081	0.005	0.012	0	0.006	0	12.90	0.80	0.126	82.54
DL56-9	-0.175	5	0.085	0.002	0.009	0	0.011	0	9.57	0.23	0.13	82.31
DL56-10	-0.175	5	0.093	0.003	0.019	0	0.012	0	16.96	0.55	0.13	97.69
DL56-1	-0.175	5	0.095	0.004	0.008	0	0.01	0.001	7.77	0.33	0.133	87.97
DL56-2*	-0.175	5	0.085	0.004	0.007	0.001	0.012	0.001	7.61	1.14	0.131	83.21
DL56-3*	-0.175	5	0.071	0.003	0.007	0	0.02	0.001	8.97	0.38	0.128	78.91
DL53-6	-0.175	5	0.094	0.006	0.006	0	0.011	0	6.00	0.38	0.127	92.13
DL54-7	-0.19	5	0.107	0.006	0.008	0.001	0.009	0.001	6.96	0.95	0.125	104.80
DL54-8	-0.19	5	0.085	0.002	0.026	0.002	0.001	0	23.42	1.88	0.116	100.00
DL56-6*	-0.19	5	0.092	0.003	0.02	0	0.008	0	17.86	0.58	0.125	98.40
DL56-7	-0.19	5	0.091	0.001	0.006	0	0.01	0.001	6.19	0.07	0.126	85.71
DL56-8	-0.19	5	0.082	0.002	0.006	0	0.009	0	6.82	0.17	0.124	79.84
DL53-5	-0.2	5	0.093	0.003	0.006	0	0.009	0	6.06	0.20	0.127	87.40
DL53-7	-0.215	5	0.08	0.006	0.005	0	0.01	0.001	5.88	0.44	0.127	79.53
DL53-8	-0.215	5	0.097	0.005	0.004	0.001	0.006	0	3.96	1.01	0.125	90.40
J	-0.2	5	0.094	0.003	0.004	0	0.003	0	4.08	0.13	0.116	89.66
K	-0.2	5	0.095	0.002	0.008	0	0.005	0	7.77	0.16	0.124	88.71
BL1-3*	-0.175	5										
BL1-4*	-0.175	5										

DL56-4*	-0.175	5			
DL56-5*	-0.175	5			

* Discarded by WK before additional of first analysis

APPENDIX F

SCOTT AND WEST DATA TABLE[41]

Time(d)	pCi/Day	Time(d)	pCi/Day	Time(d)	pCi/Day
9	6200	276	23	588	11
18	4900	287	52	600	32
27	3000	298	38	611	15
36	1300	312	40	622	3.5
45	580	326	30	633	33
54	240	340	33	644	18
63	350	354	56	656	15
72	325	368	38	667	13
81	225	382	28	678	3
90	275	396	45	689	2
100	225	407	17	700	2
111	250	418	8	711	8
122	375	429	25	722	49
133	140	440	22	733	5
144	225	451	30	744	9
155	200	462	9	755	6
166	130	473	13	767	19
177	225	484	15	778	8.5
188	225	495	16	789	25
199	200	507	7	800	13
210	82	518	16	850	8.5
221	85	530	15	930	5.9
232	54	542	30	1020	3.8
243	95	553	7.5	1110	3
254	150	565	8.5	1200	2.9
265	95	577	18		